Linking PAR polarity proteins to cell fate regulation: analysis of MEX-5 localization in *Caenorhabditis elegans* embryos

Jennifer R. Tenlen

A dissertation
submitted in partial fulfillment of the
requirements for the degree of

Doctor of Philosophy

University of Washington
2007

Program Authorized to Offer Degree:
Molecular and Cellular Biology

INFORMATION TO USERS

The quality of this reproduction is dependent upon the quality of the copy submitted. Broken or indistinct print, colored or poor quality illustrations and photographs, print bleed-through, substandard margins, and improper alignment can adversely affect reproduction.

In the unlikely event that the author did not send a complete manuscript and there are missing pages, these will be noted. Also, if unauthorized copyright material had to be removed, a note will indicate the deletion.

ProQuest Information and Learning Company
300 North Zeeb Road
P.O. Box 1346
Ann Arbor, MI 48106-1346

University of Washington
Graduate School

This is to certify that I have examined this copy of a doctoral dissertation by

Jennifer R. Tenlen

and have found that it is complete and satisfactory in all respects,
and that any and all revisions required by the final
examining committee have been made.

Chair of the Supervisory Committee:

James R. Priess

Reading Committee:

Robert E. Braun

James R. Priess

Linda G. Wordeman

Date: April 26, 2007

In presenting this dissertation in partial fulfillment of the requirements for the doctoral degree at the University of Washington, I agree that the Library shall make its copies freely available for inspection. I further agree that extensive copying of the dissertation is allowable only for scholarly purposes, consistent with "fair use" as prescribed in the U.S. Copyright Law. Requests for copying or reproduction of this dissertation may be referred to ProQuest Information and Learning, 300 North Zeeb Road, Ann Arbor, MI 48106-1346, 1-800-521-0600, to whom the author has granted "the right to reproduce and sell (a) copies of the manuscript in microform and/or (b) printed copies of the manuscript made from microform."

Signature Jennifer R. Tinlen

Date May 16, 2007

University of Washington

Abstract

Linking PAR polarity proteins to cell fate regulation: analysis of MEX-5 localization in *Caenorhabditis elegans* embryos

Jennifer R. Tenlen
Chair of the Supervisory Committee:
Affiliate Professor James R. Priess
Department of Biology

Specification of somatic and germline lineages in the nematode *Caenorhabditis elegans* requires the establishment of anterior-posterior polarity in early embryos. Polarization begins by a sperm-induced cue in 1-cell embryos that cortically localizes PAR polarity proteins, including the Ser/Thr kinases PAR-1 and PAR-4/LKB1. Capping at the anterior pole of non-muscle myosin and several PAR proteins leads to asymmetric localization of proteins such as MEX-5 and MEX-6. MEX-5,-6 are closely-related CCCH zinc finger proteins required for germline specification that are anteriorly localized in 1-cell embryos. While no direct targets of the PAR proteins have been described in *C. elegans*, MEX-5,-6 are proposed to function as key intermediaries in the transduction of polarity cues from PAR proteins to downstream cell fate regulators. To understand how MEX-5 asymmetry is established, I constructed a series of fusion proteins containing Green Fluorescent Protein (GFP) fused to all or part of the MEX-5 protein; these fusion proteins allowed me to monitor asymmetry in living embryos. Deletion analysis of GFP:MEX-5 identified a single residue, Ser458, that is necessary for anterior localization of GFP:MEX-5 in 1-cell embryos. MEX-5 is phosphorylated at Ser458 in vivo, and this phosphorylation occurs at the onset of MEX-5 expression in the gonad. In a screen of 41 Ser/Thr kinases, I found that only PAR-1 and PAR-4 are necessary for MEX-5 phosphorylation. PAR-1 kinase activity is required for the initial phosphorylation of MEX-5, as a kinase-dead allele of *par-1* abolished all staining with anti-MEX-5(pSer458) in oocytes and embryos. PAR-4 kinase activity is required to maintain MEX-5

phosphorylation in mature oocytes; anti-MEX-5(pSer458) staining decreased progressively in *par-4* mutant oocytes, and was present only at low levels in 1-cell embryos. While phosphorylation of MEX-5 is necessary for its asymmetry in 1-cell embryos, it is not sufficient; in *par-1* alleles with mutations outside the kinase domain, MEX-5 was phosphorylated but remained symmetric. In summary, my research has described multiple roles for the PAR-1 and PAR-4 kinases in MEX-5 phosphorylation and localization. These results provide the first evidence of a role for the PAR kinases in setting up embryonic asymmetries prior to fertilization.

Table of Contents

List of Figures

List of Tables

Acknowledgements

First and foremost, I thank my family, who have always been my personal cheerleaders. I would not have made it this far without their love and encouragement.

My adviser, Jim Priess, deserves special thanks and appreciation for his patience and support, and especially for teaching me the art of storytelling. Jim is a consummate biologist with a keen eye for details, a firm grasp of logic, and a deep understanding of the history of *C. elegans* research. I could not have asked for a better lab in which to do my graduate training.

I appreciate the support and advice from my supervisory committee: Bob Braun, Susan Parkhurst, Jim Priess, Linda Wordeman, and Ted Young. In particular, I thank my reading committee: Bob Braun, Jim Priess and Linda Wordeman.

I am indebted to the Developmental Biology Training Grant program, in particular to program director Lynn Riddiford, for financial support and numerous training opportunities during my graduate studies.

My labmates, past and present, have made the Priess lab a great place to work. In particular, I learned much from discussions with Rafal Ciosk, Jeremy Nance, Barbara Page and Jennifer Schisa. My fellow graduate student, Alexandre Neves, has been a sounding board, has gently (and repeatedly) reminded me of the importance of taking a break, and has been a great source of comic relief over the years. I appreciate the support of other members of the lab, including Mike DePalma, Kathryn English, Arne IJpma, Erin Jezuit, Nitobe London, Jeff Molk, Siew-Loon Ooi, Jeff Rasmussen, Ujwal Sheth and Uta Wolke.

Michele Karantsavelos and MaryEllin Robinson in the Molecular and Cellular Biology program provided a sympathetic ear when needed, and made navigating through all of the paperwork, funding changes and program requirements as easy and seamless as possible.

My research was assisted greatly by contributions from several individuals. Jeremy Nance adapted the microparticle bombardment protocol for our lab. He and Jennifer Schisa provided several vectors used to create the GFP:MEX-5 constructs. Rafal Ciosk developed the protocols for protein extractions and immunoprecipitation. Nitobe London and Kathryn English provided valuable technical assistance throughout the course of this project. Uta Wolke kindly provided the diagram of the gonad used in Figure 1A. Ed Munro (Center for Cell Dynamics, Friday Harbor Laboratories) provided his expertise in microscopy and use of their microscope facilities. The Scientific Imaging staff at Fred Hutchinson Cancer Research Center, in particular Julio Vasquez and Dave Macdonald, were very helpful. I thank Ken Kemphues (Cornell University) for generously providing strains, reagents and advice regarding *par-1*and *par-4*, and Yuji Kohara (National Institute of Genetics, Mishima, Japan) for providing cDNAs. Some of the strains used in this study were obtained from the *Caenorhabditis* Genetics Center, which is supported by the NIH National Center for Research Resources. My research was supported in part by NIH Training Grant 5T32 HDO7183. Jim Priess is an Investigator with the Howard Hughes Medical Institute.

Dedication

To my grandmothers,
Dorothy King Sherbondy and Louise Mathiassen Tenlen.

Introduction

The survival of a species depends on the faithful transmission of genetic information from one generation to the next. Such transmission requires the proper formation of gametes from the adult germline. The germ cells which give rise to gametes must be totipotent – that is, able to regenerate entire organisms (Seydoux and Braun, 2006). As such, these germ cells must be protected from factors that promote somatic cell fates. This protection requires mechanisms to specify distinct germline and somatic lineages.

One mechanism by which organisms specify germ cell fate is through the polarization of oocytes and embryos by asymmetric distribution of maternally-provided factors. In *Drosophila* oocytes, polarization of the microtubule cytoskeletal network is critical to establish the anterior-posterior axis (van Eeden and St Johnston, 1999). For example, this polarization is necessary for the localization of maternally transcribed mRNAs, including *oskar*. Localization of *oskar* mRNA to the posterior end of the oocyte is required for the recruitment of proteins, including Vasa and Tudor, which are integral components of pole plasm (Ephrussi and Lehmann, 1992). After fertilization, this pole plasm is incorporated into several pole cells. These cells become primordial germ cells (PGCs) and subsequently form the germline of *Drosophila* embryos (Williamson and Lehmann, 1996). In the absence of *oskar* mRNA, no pole plasm is detected at the posterior pole, and there is no germline development (Ephrussi and Lehmann, 1992). Similar events are required to localize germline-specific maternal

RNAs in other organisms, including *Xenopus* oocytes (Saffman and Lasko, 1999; King et al., 2005).

The nematode *Caenorhabditis elegans* has emerged as an important model in understanding how cell polarization leads to the proper compartmentalization of cell fate regulators, and the specification of distinct somatic and germline lineages. Multiple tools are available for the study of *C. elegans*, including a fully-sequenced genome, the ability to study mutant phenotypes through forward and reverse genetics, and the ability to generate transgenic animals. The complete lineage has been described, facilitating the characterization of the molecular pathways that produce different tissues.

C. elegans germline is established early in embryo development

The *C. elegans* embryo undergoes a series of invariant, asymmetric cell divisions that result in the establishment of a unique germ cell lineage (Sulston et al., 1983). The one-cell embryo will produce all of the somatic and germ cell lineages, so it can be considered a totipotent cell (called P_0). During the first cell cycle, posterior displacement of the spindle poles results in asymmetric division, producing a larger anterior blastomere (AB) and a smaller posterior blastomere (P_1). During the second and subsequent cell cycles, AB divides symmetrically to form several somatic cell types, including neurons and the anterior pharynx. However, P_1 divides asymmetrically to produce a somatic daughter blastomere (EMS) and a germline daughter blastomere (P_2). The germline blastomere divides asymmetrically two more times, resulting in a single blastomere, P_4, being set aside for the germline.

These asymmetric divisions ensure that maternally-provided proteins are segregated to appropriate blastomeres. Somatic cell lineages are determined by the activities of several proteins in either the anterior or posterior somatic blastomeres. The transcription factor SKN-1 is expressed in posterior blastomeres starting at the 2-cell stage, and promotes the specification of intestinal and muscle cell fates in the somatic daughter of P_1 (Bowerman et al., 1992; Bowerman et al., 1993). The fact that SKN-1 is present in the posterior embryonic cells that produce the germline, as well as in posterior cells that produce the intestine and muscles, raises the question of how the germline precursors prevent SKN-1 activity; this question is addressed further below. Starting at the 4-cell stage, the transcription factor PAL-1, a homolog of the *Drosophila* Caudal protein, is similarly expressed in posterior blastomeres, and is necessary to specify muscle and other cell fates in the somatic descendants of P_2 (Hunter and Kenyon, 1996). Conversely, the KH domain protein MEX-3 is symmetrically expressed in 1-cell embryos, and is then segregated to the anterior blastomere AB and its descendants starting at the 2-cell stage (Draper et al., 1996; Hunter and Kenyon, 1996). MEX-3 may function to repress PAL-1 expression in anterior blastomeres since *mex-3* mutant embryos produce ectopic, PAL-1-dependent muscles in these blastomeres (Draper et al., 1996). The activity of the Notch-like receptor GLP-1 is also required in anterior blastomeres. GLP-1 protein is expressed in AB and its descendants starting at the 2-cell stage, and is necessary at the 4-cell stage to ensure that the anterior and posterior daughters of AB produce distinct lineages (Priess et al., 1987; Evans et al., 1994).

The specification and maintenance of germ cell fate requires the segregation of several factors to germ cell precursors. One of the earliest germ cell markers are P granules, cytoplasmic ribonucleoproteins transported to the posterior pole of 1-cell embryos following fertilization. At each cell division, these P granules are partitioned to germline blastomeres only (Strome and Wood, 1982; Strome and Wood, 1983). Multiple maternal mRNAs and proteins have been shown to associate with P granules in both the germline and in embryos (Pitt et al., 2000; Schisa et al., 2001). While no mutations have been identified that prevent P granule assembly, depletion of several P granule-associated proteins, including the RNA-binding protein PGL-1, and the RNA helicases GLH-1 and GLH-4, results in sterility (Gruidl et al., 1996; Kawasaki et al., 1998; Kuznicki et al., 2000). These observations, and the known association of P granules with RNAs and proteins important for early development suggest that P granules may have a role in the maintenance of germline integrity.

In addition to P granules, the expression of several other proteins, including PIE-1, MEX-1 and POS-1, is restricted to the germline blastomeres. PIE-1 is localized to the posterior pole in one-cell embryos, and is segregated to the germline blastomere at each cell division (Mello et al., 1996; Reese et al., 2000). It is expressed at low levels in the cytoplasm, but is enriched in germ cell nuclei and on P granules (Mello et al., 1996; Tenenhaus et al., 1998). PIE-1 is required to prevent germ cells from adopting a somatic cell fate by repressing transcription of some genes in the germline (Seydoux, 1996). In *pie-1* mutant embryos, the germline fails to develop, since blastomeres that would normally form the germline instead adopt the fate of their somatic sister blastomere (Mello et al., 1992). Like PIE-1, MEX-1 is also localized to the posterior

pole in one-cell embryos, and is segregated to the germline blastomere in subsequent divisions (Guedes and Priess, 1997). MEX-1 is expressed in the germline cytoplasm and on P granules, and is required for the correct localization of several proteins, including PIE-1 and P granules. In *mex-1* mutants, PIE-1 is ectopically expressed in multiple blastomeres (Guedes and Priess, 1997). Although SKN-1 and PAL-1 are expressed in posterior somatic and germline blastomeres, their activities are repressed in germline blastomeres by both PIE-1 and MEX-1. In *pie-1* or *mex-1* mutant embryos, SKN-1 activity is derepressed, and germline blastomeres adopt either intestinal [*pie-1(-)*] or muscle [*mex-1(-)*] cell fates (Mello et al., 1992). Unlike PIE-1 and MEX-1, POS-1 does not become enriched in the germline blastomere until the two-cell stage (Tabara et al., 1999). In *pos-1* mutant embryos, the germline blastomere P_3 divides symmetrically, resulting in the equal partitioning of PIE-1 and P granules to the daughter blastomeres (Tabara et al., 1999). POS-1 also represses translation of some somatic cell fate regulators in posterior blastomeres by binding the 3'UTR of mRNA (Tabara et al., 1999; Ogura et al., 2003). These observations demonstrate that the correct localization of germline determinants is required to not only preserve the integrity of the germline, but also to correctly localize other cell fate determinants in the early embryo.

Fertilization transforms unpolarized oocytes into polarized embryos

One common feature of each of the proteins discussed above is that they are translated from maternally-provided, class II mRNAs (Evans et al., 1994; Seydoux and Fire, 1994; Draper et al., 1996; Guedes and Priess, 1997; Tabara et al., 1999). Class II

mRNAs are distributed uniformly in oocytes and early 1-cell embryos (Seydoux and Fire, 1994). A key question in the understanding of cell fate specification is how the diverse patterns of protein expression result from similar distributions of maternal mRNAs. In recent years, it has become apparent that the patterns of protein expression observed for cell fate regulators depend on fertilization-induced events that establish the anterior-posterior axis of new embryos.

Fertilization initiates a series of events in early embryos that includes exit from meiosis, a reorganization of cortical and internal cytoplasm, and establishment of the anterior-posterior axis (Kemphues and Strome, 1997). Following fertilization, waves of cortical contraction of an actin-rich cytoskeletal network move anteriorly away from the site of sperm entry (Strome and Wood, 1983; Hird and White, 1993). As cortical cytoplasm reaches the anterior pole, internal cytoplasm is displaced from the anterior pole and flows posteriorly, carrying with it P granules and the oocyte pronucleus (Strome and Wood, 1983). Embryos with mutations in a gene encoding non-muscle myosin 2 (*nmy-2*) lack all cytoplasmic flow and fail to establish the anterior-posterior axis (Guo and Kemphues, 1996). Visualization of NMY-2:GFP fusion proteins in living embryos demonstrated that NMY-2:GFP is initially expressed uniformly around the cortex as part of a dynamic actomyosin network; at the appearance of the sperm pronucleus, NMY-2:GFP is destabilized in the posterior cortex, and flows toward the anterior during cortical contractions (Munro et al., 2004). This NMY-2-mediated cortical flow requires the activities of at least two other proteins, the RhoGTPase

RHO-1, and the RhoGEF ECT-2 (Jenkins et al., 2006; Motegi and Sugimoto, 2006; Schonegg and Hyman, 2006). These studies demonstrate that the actin cytoskeleton plays an integral role in setting up downstream polarity events in the early embryo.

Although the role of sperm in initiating cytoplasmic reorganization is well-understood, the identity of the specific sperm polarity cue remains controversial. The first evidence that the establishment of anterior-posterior polarity depends directly on a sperm-provided cue came from analysis of the site of sperm entry in oocytes during fertilization. In the majority of oocytes, sperm entered the oocyte at the presumptive posterior pole. However, in some oocytes, sperm entered at either the anterior pole or at lateral surfaces. In these cases, cytoplasmic flow was oriented toward the sperm pronucleus, and P granules accumulated near the site of sperm entry (Goldstein and Hird, 1996). These results suggested that oocytes have no intrinsic anterior-posterior polarity prior to fertilization, and demonstrated that sperm provided the initial polarity cue. The authors proposed that sperm-provided centrosomes were the critical element, nucleating astral microtubules and initiating a flow of cortical actin away from the sperm pronucleus (Goldstein and Hird, 1996). This model has been supported by several studies. First, oocytes fertilized with anucleate sperm establish an apparently normal anterior-posterior axis, including anterior cortical flow and posterior cytoplasmic flow, suggesting that sperm nuclear material is not necessary for embryo polarization (Sadler and Shakes, 2000). Physical disruption of sperm-provided centrosomes, or mutations in several centrosome-associated genes prevent the establishment of anterior-posterior polarity in 1-cell embryos (O'Connell et al., 2000; Hamill et al., 2002; Cowan and Hyman, 2004). It is still not clear whether the initial

polarity cue comes from the sperm-provided microtubule organizing center (MTOC) or from another centrosome-associated protein. In mutant embryos arrested in meiosis, no visible sperm asters form, and polarity appeared to be reversed. Abrogation of the meiotic spindle prevented all asymmetry, suggesting that the meiotic microtubules were sufficient to initiate polarity (Wallenfang and Seydoux, 2000). Disruption of aster sperm formation by depletion of the Aurora A kinase AIR-1 or the centrosomal protein SPD-2 also prevented polarity formation (O'Connell et al., 2000; Wallenfang and Seydoux, 2000). However, abrogation of microtubules by depletion of tubulin subunits individually or in combination with the microtubule inhibitor nocodazole did not prevent the establishment of anterior-posterior polarity in 1-cell embryos (Cowan and Hyman, 2004; Liu et al., 2004; Sonneville and Gonczy, 2004). These results suggest that a centrosome cue other than microtubules produces a local change in the cortex that initiates cortical contractions. One candidate for this cue is the GTPase-activating (GAP) protein, CYK-4, which is enriched in sperm. Depletion of sperm-provided *cyk-4* prevented the disassembly of the actomyosin cytoskeleton in the posterior and disrupted downstream polarity events (Jenkins et al., 2006). However, it is not known whether CYK-4 acts in parallel with the centrosome, or is part of a centrosome-associated pathway to initiate destabilization of the actomyosin network.

Specification of somatic and germline fates requires the PAR proteins

The reorganization of the cortical actin cytoskeleton is concurrent with a redistribution of PAR (*partitioning-defective)* polarity proteins, which specify the anterior and posterior domains of 1-cell embryos (Nance, 2005; Munro, 2006). A

complex of three proteins containing the PDZ-domain proteins PAR-3 and PAR-6, and the atypical protein kinase C, PKC-3, localizes to the anterior cortex shortly after fertilization (hereafter referred to as the anterior PAR complex) (Etemad-Moghadam et al., 1995; Tabuse et al., 1998; Hung and Kemphues, 1999). The anterior PAR complex is initially expressed throughout the cortex of the zygote, but cortical changes at the posterior pole then restrict this complex from the posterior cortex (Cuenca et al., 2003). This restriction allows the RING finger protein PAR-2 to localize to the posterior cortex to establish the posterior domain (Boyd et al., 1996; Cuenca et al., 2003). The anterior PAR complex and PAR-2 are mutually dependent on each other for their proper localization. In *par-3* mutants, PAR-2 is uniformly expressed in the cortex (Boyd et al., 1996). In *par-2* mutants, PAR-3 remains asymmetric, but its expression extends into the posterior cortex (Etemad-Moghadam et al., 1995). While NMY-2 is required for proper localization of the PAR proteins (Guo and Kemphues, 1996), the PAR proteins are also necessary to promote appropriate anterior cortical flow of the actomyosin cytoskeleton (Munro et al., 2004). Therefore, NMY-2 and the PAR proteins participate in a feedback loop to ensure the proper establishment of anterior and posterior domains in 1-cell embryos.

Both *par-2* and *par-3* are required to localize the Ser/Thr kinase PAR-1 to the posterior cortex. In *par-3* mutants, PAR-1 is expressed uniformly at the embryo cortex (Watts et al., 1996). In *par-2* mutants, PAR-1 does not localize to the posterior cortex, but instead is present at wild-type levels in the cytoplasm (Boyd et al., 1996). PAR-1 is most immediately required for the establishment of anterior-posterior polarity. In *par-1* mutants, cell division is symmetrical, resulting in the uniform distribution of P granules

in all blastomeres of the early embryo (Kemphues et al., 1988). Loss of *par-1* does not prevent posterior flow of P granules, but does prevent stabilization of P granules in the posterior (Cheeks et al., 2004). In addition, *par-1* mutants express low levels of germline determinants such as PIE-1 and MEX-1 (Tenenhaus et al., 1998). These observations suggest that PAR-1 may act in germ cell precursors to protect germline proteins from degradation. This function for PAR-1 may be conserved; in *Drosophila* oocytes, PAR-1 directly phosphorylates Oskar, resulting in its stabilization at the posterior cortex. Unphosphorylated Oskar is quickly degraded (Riechmann et al., 2002). However, the mechanism by which PAR-1 regulates the expression of germline proteins in 1-cell embryos is unknown.

The PAR proteins are remarkably conserved in many eukaryotes, including *Drosophila* and mammals. With the exception of PAR-2, homologues to each of the PAR proteins and PKC-3 have been found in other organisms. In *Drosophila*, the coordinate activity of several PARs, including Par-1, Par-3 (Bazooka) and Par-4 (LKB1), is required to establish correct anterior-posterior domains in oocytes (Cox et al., 1998; Riechmann et al., 2002; Vaccari and Ephrussi, 2002; Martin and St Johnston, 2003). In mouse oocytes, PAR-3, PAR-4 and PAR-6 appear to be localized to the animal pole and associate with meiotic spindles, possibly involved in polar-body extrusion (Vinot et al., 2004; Duncan et al., 2005; Szczepanska and Maleszewski, 2005). In both *Drosophila* neuroblasts and mammalian epithelial cells, the PAR-3/PAR-6/PKC-3 complex is required for cell-cell adhesion and apical-basal polarity (Suzuki et al., 2002; Betschinger et al., 2003).

MEX-5 and MEX-6 act downstream of the PAR proteins to regulate cell fate

Although the role of the PAR proteins in regulating cell polarity has become clearer, the downstream targets of these proteins in *C. elegans* are still largely unknown. To identify potential targets, genetic screens have searched for embryos with phenotypes similar to *par* mutant phenotypes. One such phenotype is an excess of muscle (Mex), which is due to ectopic activation of SKN-1 in anterior blastomeres (Bowerman et al., 1992; Schubert et al., 2000). Mutations in *mex-5* result in inviable embryos that produce excess muscle, and misexpress SKN-1 in anterior blastomeres (Schubert et al., 2000). In contrast, mutations in a closely-related gene, *mex-6*, produce viable embryos that grow into healthy adults. However, the phenotype of *mex-5;mex-6* double mutant embryos differs significantly from the phenotype of *mex-5* single mutant embryos. These double mutant embryos fail to produce multiple tissue types, including pharynx, intestine and germ cells. Multiple proteins, including SKN-1, PIE-1, MEX-1 and POS-1, are misexpressed in all blastomeres (Schubert et al., 2000). This early loss of asymmetry in *mex-5;mex-6* double-mutant embryos suggests that the proteins encoded by *mex-5* and *mex-6* have partially redundant functions in early development. MEX-5 and MEX-6 proteins share 70% identity and are members of a family of CCCH zinc finger proteins related to the mammalian Tis11/TTP family (Schubert et al., 2000). Outside of the CCCH domains, MEX-5,-6 have no known homologues in other organisms. The CCCH zinc fingers of Tis11/TTP proteins bind mRNA, and have been shown to target mRNAs for degradation (Carballo et al., 1998; Lai et al., 1999). Recently, MEX-5 and MEX-6 were both shown to bind AU-rich response elements in some maternal mRNAs, suggesting that this RNA-binding role for CCCH proteins is

conserved in MEX-5,-6 (Pagano et al., 2007). However, this RNA-binding role is unlikely to explain the establishment of germline asymmetry as germline mRNAs and proteins are uniformly distributed in early 1-cell embryos.

MEX-5 is initially detected in the bend of gonads, where germ cells enter oogenesis, and is expressed uniformly throughout the cytoplasm of oocytes (Figure 1A) (Schubert et al., 2000). Shortly after fertilization, MEX-5 becomes enriched at the anterior pole of 1-cell embryos. This anterior enrichment results in the partitioning of MEX-5 into the anterior blastomere AB at the first cell division. At the 4-cell stage, MEX-5 is initially expressed at high levels in the anterior blastomeres, with reduced expression in the posterior somatic blastomere EMS. However, in the late four-cell embryo, anterior expression disappears, while it increases in EMS and the germ cell precursor (Figure 1B). At each subsequent division of the germ cell precursor, MEX-5 is expressed asymmetrically in the two daughter cells, with higher expression in the somatic daughter. MEX-5 expression disappears rapidly in all other somatic blastomeres (Schubert et al., 2000). In addition to this cytoplasmic expression, MEX-5 is localized to the germline P granules and to posterior centrosomes. While antibodies against MEX-6 do not exist, embryos expressing GFP:MEX-6 fusion proteins have similar expression patterns as MEX-5 (Cuenca et al., 2003).

One striking feature of MEX-5 localization is that it reciprocates the expression of the germline proteins (Figure 1B). For example, in 1-cell embryos, the anterior MEX-5 gradient appears to mirror the posterior PIE-1 gradient. This reciprocity is preserved in subsequent divisions of the germ cell precursors, in which the somatic sister has high MEX-5 expression, while the germline sister has high PIE-1 expression

(Schubert et al., 2000). This localization pattern suggests that MEX-5 is required to restrict germline proteins to the posterior. This model is supported by several experiments. In *mex-5;mex-6* double mutant 1-cell embryos, PIE-1 and MEX-1 are expressed uniformly throughout the embryo. Neither *pie-1*, *mex-1* nor *pos-1* mutants show mislocalization of MEX-5 in 1-cell embryos. These results place *mex-5* genetically upstream of *pie-1*, *mex-1* and *pos-1*. Conversely, MEX-5 is symmetrically expressed in *par-1* or *par-3* mutants, placing *mex-5* genetically downstream of the *par* pathway (Schubert et al., 2000). In *par-1* and *par-3* single mutant, 1-cell embryos, PIE-1 is expressed at only low levels, suggesting repression by the high levels of MEX-5. If *par-1* embryos are depleted of both *mex-5* and *mex-6*, then PIE-1 is again expressed uniformly at high levels (Schubert et al., 2000). Repression of germline proteins by MEX-5 is also supported in experiments in which MEX-5 was overexpressed in *mex-5;mex-6* double-mutant embryos. In these double-mutant embryos, germline proteins, including MEX-1, were expressed at high levels in all cells due to the absence of MEX-5 and MEX-6. However, following heat-shock induction of MEX-5, cells with high levels of MEX-5 had low levels of MEX-1 (Schubert, 2000). These results suggest that MEX-5,-6 restrict germline proteins to the posterior by repressing their expression in the anterior. Although MEX-5,-6 are genetically downstream of the PAR proteins, analysis of *mex-5;mex-6* double mutant embryos revealed a potential role in promoting the posterior domain of 1-cell embryos (Cuenca et al., 2003). Thus, MEX-5,-6 may participate in a feedback loop with the PAR proteins to ensure proper establishment of anterior and posterior domains. However, the nature of this interaction between MEX-5,-6 and the PAR proteins is unknown.

Although MEX-5 and MEX-6 are essential for the posterior localization of germline proteins in 1-cell embryos, it is unknown whether they function directly in this asymmetry. In one screen to identify other genes necessary for the asymmetry of germline proteins, PIE-1 and POS-1 localization were shown to require the activity of a dual receptor tyrosine kinase, MBK-2. In *mbk-2* mutant embryos, both PIE-1 and POS-1 are expressed throughout the 1-cell embryo, although PIE-1 is still excluded from a small region at the anterior pole. MBK-2 is proposed to function in targeting germline proteins for degradation in the posterior (Pellettieri et al., 2003). MBK-2 does not affect MEX-5 asymmetry because MEX-5 accumulates normally in the anterior of *mbk-2* mutant 1-cell embryos (Pellettieri et al., 2003). Instead, the slight asymmetric expression of PIE-1 in *mbk-2* mutants suggests that MEX-5 and MBK-2 act in parallel pathways to restrict PIE-1 and other germline proteins from the anterior pole. However, it is not known how MEX-5 facilitates this restriction.

MEX-5 and MEX-6 localization is regulated by two independent mechanisms

The degradation of MEX-5 in somatic blastomeres after the second cell division is similar to the degradation seen with other CCCH proteins, including PIE-1 (Reese et al., 2000; DeRenzo et al., 2003). MEX-5 and PIE-1 contain two adjacent CCCH domains, ZF1 and ZF2. The ZF1 domain of PIE-1 is necessary for degradation of PIE-1 in somatic blastomeres after the two-cell stage, while the ZF2 domain of MEX-5 has the analogous function (Reese et al., 2000; DeRenzo et al., 2003). This ZF-mediated degradation of PIE-1 and MEX-5 requires the activity of the SOCS box protein ZIF-1, as *zif-1(RNAi)* embryos had high levels of PIE-1 and MEX-5 expression in all

blastomeres. ZIF-1 was shown to bind to the E3 ubiquitin ligase complex by in vitro assays, and may be required to target CCCH proteins for ubiquitination (DeRenzo et al., 2003).

ZIF-1-dependent degradation requires expression of MEX-5,-6, and protection from this degradation in germline blastomeres requires PAR-1. In *par-1* mutant embryos, CCCH proteins are degraded in all blastomeres. However, in *par-1;mex-5;mex-6* triple mutant embryos, CCCH proteins are stabilized in all blastomeres (DeRenzo et al., 2003). These results suggest a model by which MEX-5,-6 are necessary to activate ZIF-1-dependent degradation in somatic blastomeres. PAR-1 acts in the germline blastomere to protect germline proteins from degradation, possibly by exclusion of MEX-5 and MEX-6 (DeRenzo et al., 2003).

While the ZIF-1-E3 ubiquitin ligase complex is necessary for later MEX-5 asymmetry, it is not required for MEX-5 asymmetry in 1-cell embryos; localization of MEX-5 is normal in *zif-1(RNAi)* embryos (DeRenzo et al., 2003). These results suggest that two independent mechanisms regulate MEX-5,-6 localization. An early PAR-dependent mechanism localizes MEX-5,-6 to the anterior pole of the zygote. After the 2-cell stage, ubiquitin-mediated proteolysis progressively degrades MEX-5,-6 in the oldest somatic blastomeres, such that MEX-5,-6 is present primarily in the youngest somatic blastomere (the somatic daughter of each germline blastomere). Early localization of MEX-5,-6 is not regulated at the level of mRNA as both *mex-5* and *mex-6* mRNAs are distributed uniformly throughout the 1-cell embryo (Nematode Expression Pattern Database, http://nematode.lab.nig.ac.jp/db/). Several mechanisms may result in MEX-5 asymmetry in 1-cell embryos, although these mechanisms are not

mutually exclusive. MEX-5 may be transported to the anterior, either by anterior cortical flow, or by associating with other anteriorly-localized proteins. Alternatively, asymmetry may result from MEX-5 stabilization in the anterior, and degradation in the posterior. In a converse example, P granules that occasionally are mislocalized to anterior, somatic blastomeres are rapidly degraded, while posterior P granules appear stable (Hird et al., 1996; Cheeks et al., 2004). Enrichment of MEX-5 in anterior blastomeres may result from non-localized mRNA translation coupled with exclusion from, or degradation of MEX-5 protein in the posterior. A role for translation in embryonic MEX-5 expression appears likely, due to the upregulation of MEX-5 expression in the posterior blastomeres at the 4-cell stage (Schubert et al., 2000).

Although the mechanistic details are far from clear, the data discussed above have suggested a linear sequence of events for the role of MEX-5 in establishing germline asymmetry (Figure 2). In summary, fertilization of unpolarized oocytes initiates extensive reorganization of the actomyosin cytoskeleton and establishment of anterior and posterior domains by the PAR proteins. The specification of the anterior-posterior axis by the PAR proteins leads to MEX-5 asymmetry and, ultimately, germline asymmetry. The establishment of asymmetries is also dependent upon two feedback loops. First, several PAR proteins act to promote appropriate cortical dynamics during reorganization of the actomyosin cytoskeleton. Second, MEX-5,-6 act to promote the expansion of the posterior domain by the PAR proteins. These interactions ensure that anterior and posterior domains of 1-cell embryos are appropriately defined, and that downstream proteins, including the germline proteins, are properly sorted within the embryo. However, it is still not understood how PAR

polarity information is translated into the specification of somatic and germline lineages. My thesis work has focused on elucidating the mechanisms that establish MEX-5 asymmetry in 1-cell embryos. An understanding of these mechanisms may also shed light on how MEX-5 functions to exclude germline proteins from the anterior. More generally, these studies may help us to better understand how the symmetric distribution of multiple proteins in unpolarized oocytes is transformed into reciprocal protein expression domains in polarized embryos.

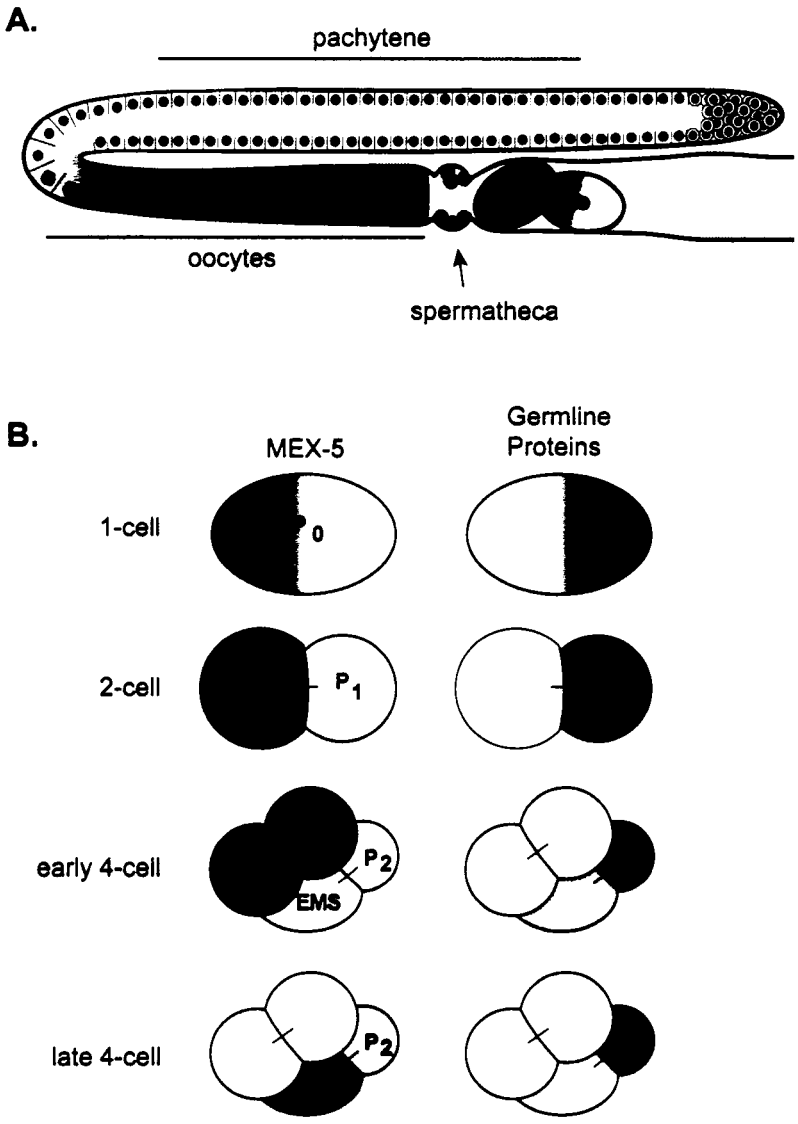

Figure 1. Localization of MEX-5 and germline proteins in early embryos. (A) Diagram of adult hermaphrodite gonad. In the distal arm (upper right), germ cells are arranged in a syncytium and arrest at the pachytene stage of meiotic prophase. Germ cells exit pachytene in the bend (left) and then mature into oocytes. Mature oocytes pass through the spermatheca to be fertilized. MEX-5 (red) is initially expressed in the bend of the gonad, and remains uniformly distributed until after fertilization. (B) MEX-5 (red) and germline proteins (green) localize to reciprocal domains in early embryos (see text for details).

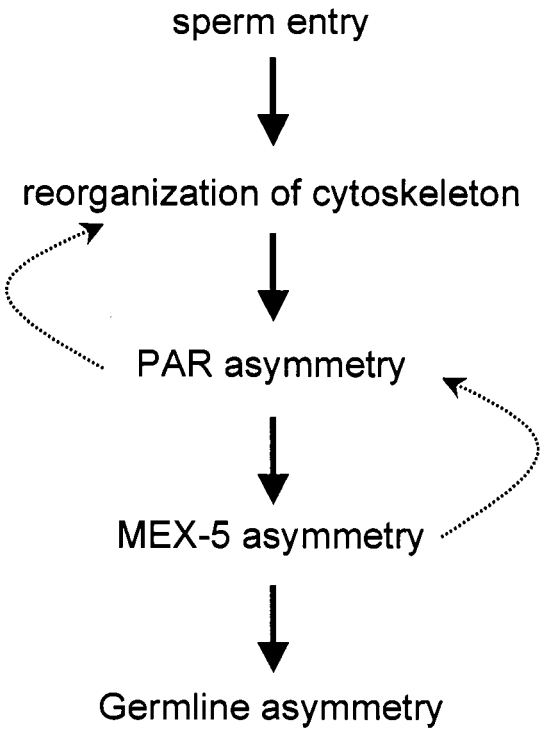

Figure 2. Model for setting up asymmetry of germline proteins in 1-cell embryos. Sperm entry into unpolarized oocytes initiates a reorganization of the cytoskeleton marked by capping of the anterior pole by non-muscle myosin. This anterior capping results in the establishment of anterior and posterior domains by the PAR proteins, leading to MEX-5 asymmetry. MEX-5 asymmetry in turn sets up germline asymmetry. While the establishment of these asymmetries appears to follow a linear cascade of events, the maintenance of asymmetry requires feedback loops between the PAR proteins and non-muscle myosin, and between MEX-5 and the PAR proteins (see text for details).

Materials and Methods

Nematode Strains and Maintenance

The wild-type *Caenorhabditis elegans* strain used in these studies was originally isolated from the N2 Bristol strain. All worms were cultured and maintained as previously described (Brenner, 1974). The following alleles were used: Chromosome II (LGII): *mex-6(pk440)* (Schubert et al., 2000); LGIII: *unc-119(ed3)* (Maduro and Pilgrim, 1995); LGIV: nT1, *fem-1(hc17ts)* (Nelson et al., 1978), *him-8(e1489)*, *unc-30(e191)*, *mex-5(zu199)* (Schubert et al., 2000); LGV: *par-1(b274)*, *par-1(e2012)*, *par-1(it51)*, *par-1(it60)* (Guo and Kemphues, 1995), *par-1(zu310)* (Schubert, 2000), *par-4(it33)*, *par-4(it47ts)*, *par-4(it75)* (Watts et al., 2000). Unless noted otherwise, alleles are described by Hodgkin (Hodgkin, 1997). Transgenes created for this study are listed in Table 1.

Plasmid Construction

Standard techniques were used to manipulate and amplify DNA. All site-directed mutagenesis was performed using the QuikChange Site-Directed Mutagenesis kit (Stratagene). All PCR reactions were performed using the Expand High Fidelity PCR kit (Roche). For preparation of genomic DNA from wild-type animals, worms were rinsed off plates, washed several times in 1X M9 buffer, and added drop-wise to liquid nitrogen. Frozen pellets were incubated in 1 volume of lysis buffer [0.1 M Tris, pH 7.5; 0.05 M EDTA, pH 7.4, 0.5% SDS, 0.5 mg/ml proteinase K] at 65°C for 45 minutes. The supernatant was extracted with phenol/chloroform, and the genomic DNA

precipitated in 0.1 volume 3 M sodium acetate and 2.5 volumes ethanol. The DNA pellet was washed in 70% ethanol and resuspended in 100 μl Tris-EDTA buffer.

Constructs containing the *pie-1* promoter and 3'UTR were modified from a *pie-1*:GFP expression vector (Strome et al., 2001). Site-directed mutagenesis was used to remove one of two *NotI* sites in the multiple-cloning site. The *unc-119(+)* genomic fragment (Maduro and Pilgrim, 1995) was inserted into the modified plasmid at the single *NotI* site; this construct was named pJS109. The full-length *mex-5* coding sequence was PCR amplified from the cDNA clone yk851b04, which was obtained from Yuji Kohara (National Institute of Genetics, Mishima, Japan). Primer sequences for amplification were 5'-GAGATCACTAGTATGAGCTCGGCGTCAGTC-3' and 5'-GAGATCACTAGTCTAAAGGTTCAGCTCTTG-3', which incorporated *SpeI* sites (underlined). The *mex-5* PCR product was cloned into the unique *SpeI* site of pBluescript II(KS+) (pBS; Stratagene) to facilitate manipulation and cloning of the *mex-5* sequence; this construct was named pJN148. Deletions of amino-terminal and carboxyl-terminal MEX-5 sequences were generated by PCR amplification of selected sequences from pJN148 and cloned into pJS109 at the *SpeI* site (see Table 2 for primer sequences). All amino-acid substitutions were made by site-directed mutagenesis (see Table 3 for primer sequences). The MEX-5 coding sequence was then excised from pJN148 by *SpeI* digest and cloned into pJS109 at the *SpeI* site.

Constructs containing the *mex-5* promoter and 3'UTR were created using pBS as the backbone (Figure 3). The *gfp:mex-5* sequence, including the *mex-5* stop codon, was PCR-amplified from pJT02 using the primers 5'-ATCAAGCTTATCGATACCGTCGACC-3' and 5'-

TTTCGTGTGGTAACATACAACTTAGGATCCACTAGTCTAATAGTGTC-3'. The *mex-5* 3'UTR was PCR-amplified from genomic DNA starting immediately after the stop codon and extending for 648 base pairs. The primers used for this amplification were 5'-GTTGTATGTTACCACACGAAATTGC-3' and 5'-GAAGACTACCTCGGAGTTCTCAG-3'. The 3'UTR was joined to the *gfp:mex-5* sequence by fusion PCR (Hobert, 2002), using primers that included *KpnI* sites (underlined): 5'-TTCGAGGTACCATGAGTAAAGGAGAAGAACTTT-3' and 5'-GGACAGGTACCAAGATTCTCTATCATTCAGTGAAC-3'. The final *gfp:mex-5:mex-5(3'UTR)* product was cloned into the *KpnI* site of pBS to give construct pJT82.2. A 4.4-kb fragment of the *mex-5* promoter was PCR-amplified from genomic DNA using the primers 5'-CTTACAAAGAAGGCCCTCAAAGGCGG-3' and 5'-TGCAAGGCCCTTCTCTGTCTGAAACATTCAATTGATTATCG-3', including *Eco0109I* sites (underlined). The promoter was cloned into the *Eco0109I* site of pJT82.2, just upstream of the *gfp* ORF. The *unc-119(+)* genomic sequence was cloned into a unique *NotI* site immediately upstream of the *mex-5* promoter; this final construct was named pJT82.5.

Full-length *par-1* cDNA was prepared from total RNA by RT-PCR. RNA was extracted from wild-type worms as described (Portman, 2006) except that frozen worm pellets were lysed in tubes containing 3 volumes of glass beads (450-600 microns, Sigma) and 3 volumes TRIZOL (Invitrogen). The SuperScript II Reverse Transcriptase kit (Invitrogen) was used to amplify *par-1* cDNA. First-strand cDNA synthesis was performed using oligo$(dT)_{12-18}$ (supplied with the kit). The first-strand cDNA product was used as a template for PCR amplification of *par-1*, using the primers 5'-

CAACAATGAGCTCGGCGTCAG-3' and 5'-GAGGCGGTTAGAGAGAGAGAGTG-3'. The *par-1* PCR product was then re-amplified using the primers 5'-GAGATCACTAGTATGAGCTCGGCGTCAGTC-3' and 5'-GAGATCACTAGTCTAAAGGTTCAGCTCTTG-3', which introduced *SpeI* restriction sites at the 5' end (underlined). Three isoforms of *par-1* were amplified. The longest of these included exons 1-7 and exons 9-16, based on the predicted structure in WormBase (H39E23.1, www.wormbase.org). This isoform had four nucleotide substitutions that resulted in missense mutations, in comparison with the genomic sequence (WormBase). These mutations were corrected by site-directed mutagenesis, and the cDNA was cloned into the *SpeI* site of both the *mex-5:GFP* (construct pJT90) and *pie-1:GFP* (construct pJT91) expression vectors.

Full-length *par-4* cDNA was prepared by fusion PCR. Exons 1 – 6 of *par-4* were amplified by PCR and fused in frame to the *par-4* partial cDNA pDM1.2, which encodes exons 7 – 11 (a gift from K. Kemphues). The final fusion PCR product was then amplified using the primers 5'- GAGATCACTAGTATGGATGCTCCGTCGAC-3' and 5'- GAGATCACTAGTCTAAGCACTATCGGTAC-3', which introduced *SpeI* restriction sites (underlined). The full-length *par-4* cDNA was cloned into the *SpeI* site of both the *pie-1:GFP* (construct pJT93) and *mex-5:GFP* (construct pJT94) expression vectors.

The *nmy-2:PA-GFP* expression vector, in which photoactivateable GFP is under the control of the *nmy-2* promoter and 3'UTR, was provided by Uta Wolke. The MEX-5 open reading frame was cloned into the vector at the *AscI-SbfI* restriction sites.

Worm Transformations

Transgenic strains were created by microparticle bombardment of *unc-119* animals with the constructs described above (Praitis et al., 2001). All transgenic strains were maintained at 23°C. Both *pie-1:GFP:MEX-5:pie-1(3'UTR)* and *mex-5:GFP:MEX-5:mex-5(3'UTR)* fusion proteins were able to rescue the *mex-5(zu199)* mutant phenotype, indicating that these transgenes are functional.

Sequence Analysis

Putative MEX-5 paralogs in *Caenorhabditis briggsae* (gene CB12031) and *C. remanei* (cr01.sctg31.wum.31.1) were identified in WormBase release WS150 (ws150.wormbase.org). Sequence alignments were performed using ClustalW (www.ch.embnet.org/software/ClustalW.html). Predictions of potential serine and threonine phosphorylation sites were made by the Netphos 2.0 Server using algorithms based on a neural network model (Blom et al., 1999) (www.cbs.dtu.dk/services/NetPhos/). Residues that produced a score of 0.500 or higher were predicted to have a high probability of phosphorylation.

RNA interference

RNA interference by feeding was performed as previously described (Timmons and Fire, 1998; Kamath et al., 2001). Bacterial clones corresponding to the gene of interest were isolated from a library of genes cloned into the L4440 vector, which includes inverted T7 polymerase sites (Kamath et al., 2003). Bacteria were grown in Luria broth supplemented with carbenicillin (50 mg/ml) and tetracycline (10 mg/ml) to mid-log phase, then incubated in 0.4 mM IPTG for 3 hours at 37°C to induce

transcription of double-stranded RNA. 300 μl of induced culture were seeded onto modified NGM agar plates, supplemented with 1 mM IPTG, 50 μg/ml carbenicillin and 10 μg/ml tetracycline. For kinase RNAi experiments, approximately 50 worms at the first larval (L1) stage were placed onto seeded plates and allowed to feed for 48 hours at 25°C. After 48 hours, adults were removed from plates and prepared for immunostaining with antibodies against MEX-5 and MEX-5(pS458) (see below). 24 hours after removal of the adults, plates were scored to determine the percentage of viable progeny. In cases where no lethality or obvious phenotypic defects were observed, progeny of RNAi-treated parents were raised on RNAi feeding plates and examined by immunostaining. In cases where RNAi resulted in a sterile phenotype in treated animals, the experiment was repeated by placing worms on plates at the L4 stage to allow for development of the germline. Treated animals were examined by immunostaining 36 – 40 hours after initiation of feeding. For proteasome RNAi experiments, approximately 25 L4 animals expressing GFP:MEX-5 were placed on feeding plates and allowed to feed for 48 hours at 25°C. After 48 hours, adults were removed from plates, placed in a drop of 1X M9 and mounted on agar pads (2% agarose in water) for live GFP microscopy. In cases where no lethality or obvious phenotypic defects were observed, the progeny of RNAi-treated parents were raised on fresh RNAi feeding plates.

Bacterial clones specific to *mbk-2* (F49E11.1), *mek-2* (Y54E10BL.6), and *plk-2* (Y71F9B.7) failed to grow from the RNAi feeding library. Clones containing cDNAs for *mbk-2* (yk1696b04) and *plk-2* (yk1546g02) were obtained from Yuji Kohara (National Institute of Genetics, Mishima, Japan). The cDNAs for both *mbk-2* and *plk-2*

were amplified by PCR using the vector-specific primers 5'-GCTATCTAGACTTCTGCTCTAAAAGCTGCG-3' (including an *XbaI* site, underlined) and 5'-GCTACTCGAGTGTGGGAGGTTTTTTCTCTA-3' (including an *XhoI* site, underlined). For *mek-2*, a 480-bp sequence corresponding to exons 1-3 was amplified from genomic DNA by nested PCR. The first round of PCR used primers 5'-ATGTCGAGCGGAAAACGGCGTAATCCG-3' and 5'-GCCGAATCCGAGAATCCTGCG-3'. The second round of PCR used primers 5'-CAGCTATCTAGACGGAAAACGGCGTAATC-3' (including an *XbaI* site, underlined) and 5'- GTCGATCTCGAGCCAATAAACTATTACC-3' (including an *XhoI* site, underlined). PCR products were cloned into the *XbaI-XhoI* site of L4440, and the constructs were transformed into *E. coli* strain HT115 (Timmons and Fire, 1998). Bacterial clones were subsequently handled as described above.

Antisera and Immunofluorescence

The anti-MEX-5(pS458) antiserum was generated by immunizing rabbits with a peptide phosphorylated at Ser458 [WTpSEENLGLRGHY]. The antiserum was precleared with the non-phosphorylated peptide, and affinity-purified using the phosphorylated peptide (Bethyl Laboratories, TX). ELISA testing demonstrated that the affinity-purified, phosphorylated antiserum reacted with >98-fold higher affinity for the corresponding phosphorylated peptide than for the non-phosphorylated peptide.

For immunostaining, adult hermaphrodites were cut in 0.5X PBS on a cover slip to extrude gonads and embryos, then inverted onto a poly-L-lysine-coated slide (Cel-line, #10-2066). Slides were placed on dry ice for five minutes. Cover slips were

removed and slides placed in ice-cold methanol for 5 minutes. A formaldehyde fix solution [2% paraformaldehyde; 48 mM PIPES; 25 mM HEPES, pH 6.9; 10 mM EGTA, pH 7.5; 2 mM $MgCl_2$] was applied to each slide for 10 minutes. Slides were washed in 1X Tris + 0.1% Tween twice for 5 minutes each. The following primary antisera were used: anti-MEX-5(pS458) (1:1000, this study); anti-MEX-5 [1:50, (Schubert et al., 2000)], anti-GFP (1:2000, Abcam ab6556), anti-PIE-1 [1:20; (Tenenhaus et al., 1998)], and mAb 3NB12 (Priess and Thomson, 1987). Slides stained with anti-MEX-5(pS458), anti-GFP or mAb 3NB12 antisera were incubated at room temperature for two hours. Slides stained with anti-MEX-5 or anti-PIE-1 antibodies were incubated at 4°C overnight. Slides were washed twice in 1X Tris + 0.1% Tween as before, then incubated in secondary antibody for 1 hour at room temperature. Secondary antibodies used were Cy3 anti-mouse IgG Fγ (1:250, Jackson Immunologicals) and Alex488 anti-rabbit IgG (H+L) (1:1000, Molecular Probes). Slides were washed twice as before, then washed in 1X PBS for one minute. Slides were incubated for five minutes in 1X PBS with DAPI (1 μg/ml) (Sigma) to visualize DNA. After rinsing slides in 1X PBS for one minute, mounting media [90% glycerol, 20 mM Tris, pH 8.0; 23 mg/ml DABCO (Sigma)] was applied.

All images were obtained using a Zeiss Axioplan microscrope equipped with Nomarski DIC, polarization and epifluorescence optics and the following objective lenses: Plan NEOFLUAR 40x 1.3 oil, Plan APOCHROMAT 63x 1.4 oil and Plan NEOFLUAR 100x 1.3 oil Pol objectives. Images were acquired using a CCD camera (Photometrics CoolSnap, Roper Scientific) and CoolSnap software (v.1.2.0; Roper Scientific). Images were manipulated using Photoshop (v. 8.0; Adobe Systems, Inc.).

Pixel intensities in fluorescence images were measured using ImageJ software (v. 1.34s, Wayne Rasband, National Institutes of Health).

Protein extracts and Western blot hybridization

Wild-type or transgenic animals were synchronized at the L1 stage and grown on 25 plates containing peptone-enriched media [2.5% w/v agar (Sigma), 2.0% w/v peptone (Fisher), 0.12% w/v NaCl, 0.25 mM potassium phosphate buffer, 1 mM $MgSO_4$, 1 μg/ml cholesterol] seeded with *E. coli* strain NA22. Young adults were treated with sodium hypochlorite solution [1 volume 5 M KOH, 2.5 volumes sodium hypochlorite solution (Sigma), 16.5 volumes dH_20] to collect embryos. Embryos were washed twice in 1X M9, and embryo pellets were flash-frozen in liquid nitrogen before freezing at -80°C. Protein extracts were prepared from embryo pellets using a protocol modified from Zachariae et al. (Zachariae et al., 1998) (R. Ciosk, personal communication). Embryos were lysed in four volumes of elution buffer [50 mM HEPES, pH 6.9; 70 mM potassium acetate, 5 mM magnesium acetate, 10% Triton-X-100, 1 mM DTT, 10% glycerol, 20 mM β-glycerophosphate, 1 mM PMSF, 0.16 mg/ml Complete-EDTA Free Protease Inhibitors (Roche)]. Lysates were added to tubes containing 1 ml of glass beads (450-600 micron, Sigma), vortexed for 3 minutes, then incubated on ice for 30 seconds. Vortexing and incubation steps were repeated seven times. Lysates were centrifuged at 2000 rpm for 1 minute at 4°C and supernatants were removed to a new tube. The supernatant was centrifuged at 2000 pm for 3 minutes at 4°C, and the cleared supernatant was transferred to a new tube. An equal volume of elution buffer was added to the pellet fraction and centrifuged at 5000 rpm for 2

minutes at 4°C. The supernatant was combined with the previous supernatant to obtain the crude whole embryo extract. Protein concentrations were determined by the Bradford method using the Bio-Rad Protein Assay reagent (Bio-Rad).

Protein extracts were combined with LDS sample loading buffer (Invitrogen) and reducing agent (Invitrogen) and incubated at 70°C for 10 minutes. Extracts were separated by electrophoresis under reducing conditions using NuPAGE Novex 4-12% Bis-Tris pre-cast gels (Invitrogen), following manufacturer's instructions. Anti-oxidant (Invitrogen) was added to running and transfer buffers. After electrophoresis, separated proteins were transferred to PVDF membrane (Millipore). Membranes were probed with anti-MEX-5 (1:75), anti-MEX-5(pS458) (1:10,000), or anti-GFP (1:1000, Roche). Secondary antibodies used were ECL anti-mouse IgG HRP linked whole antibody or ECL anti-rabbit IgG HRP linked whole antibody (1:5000, GE Healthcare). Proteins were detected using the ECL Western Blotting Detection reagents, following manufacturer's instructions (GE Healthcare).

For phosphatase treatment experiments, 50 μg of protein from wild-type or transgenic embryos were incubated at 37°C in the presence of 40 units of alkaline phosphatase (20 U/μl, Roche) for 2 hours or overnight. Proteins were then prepared for Western blotting as described above, except proteins were separated on NUPAGE Novex 7% Tris-Acetate pre-cast gels (Invitrogen).

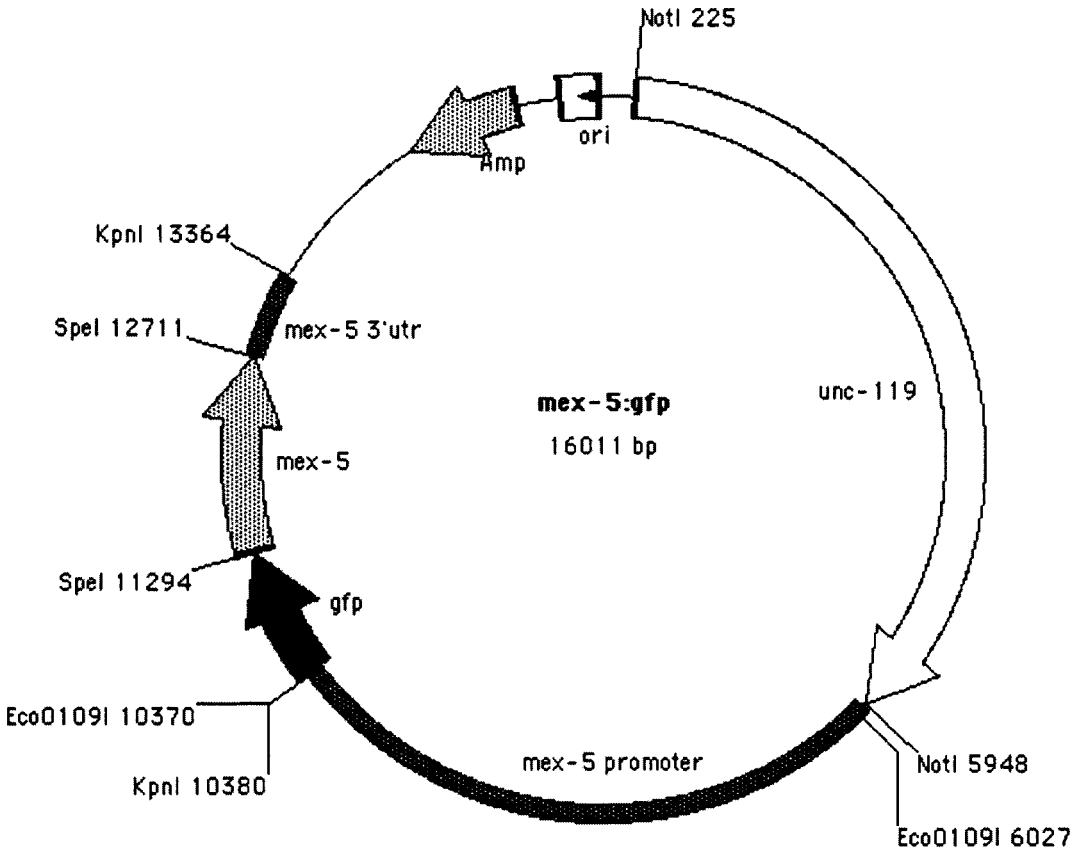

Figure 3. *mex-5:GFP:MEX-5:mex-5(3'UTR)* expression vector. The *mex-5* promoter and 3'UTR and *gfp* coding sequence were cloned into the pBluescript II (KS+) vector. *mex-5* ORF were inserted at a unique *SpeI* site immediately downstream of *gfp*. The *unc-119(+)* genomic fragment that rescues the *unc-119(-)* mutant phenotype was inserted at a unique *NotI* site.

TABLE 1: Transgenic Strains created for this study

Strain	Transforming Plasmid	Genotype[a]
JJ1512	pJT02	*zuIs62 [pie-1:GFP:MEX-5:pie-1(3'UTR)]*
JJ1586	pJT16	*zuIs80 [pie-1:GFP:MEX-5$^{\Delta aa119\text{-}468}$:pie-1(3'UTR)]*
JJ1925	pJT22	*zuIs193 [pie-1::GFP::MEX-5$^{\Delta ZF2}$::pie-1(3'UTR)]*
JJ1591	pJT29	*zuIs83 [pie-1:GFP:MEX-5$^{\Delta aa323\text{-}468}$:pie-1(3'UTR)]*
JJ1592	pJT30	*zuIs84 [pie-1:GFP:MEX-5$^{\Delta aa372\text{-}468}$:pie-1(3'UTR)]*
JJ1588	pJT31	*zuIs81 [pie-1:GFP:pie-1(3'UTR)]*
JJ1605	pJT32	*zuIs86 [pie-1:GFP:MEX-5$^{\Delta aa1\text{-}117}$:pie-1(3'UTR)]*
JJ1607	pJT33	*zuIs88 [pie-1:GFP:MEX-5$^{\Delta aa1\text{-}355}$:pie-1(3'UTR)]*
JJ1648	pJT34	*zuIs106 [pie-1:GFP:MEX-5$^{\Delta ZF1}$:pie-1(3'UTR)]*
JJ1929	pJT35	*zuIs195 [pie-1::GFP::MEX-5$^{ZF1\text{-}SSSH\ ZF2\text{-}SSSH}$::pie-1(3'UTR)]*
JJ1628	pJT37	*zuIs98 [pie-1:GFP:MEX-5$^{\Delta aa1\text{-}297}$:pie-1(3'UTR)]*
JJ1627	pJT38	*zuIs101 [pie-1:GFP:MEX-5$^{\Delta aa1\text{-}255}$:pie-1(3'UTR)]*
JJ1632	pJT39	*zuIs102 [pie-1:GFP:MEX-5$^{\Delta aa1\text{-}198}$:pie-1(3'UTR)]*
JJ1649	pJT42	*zuIs107 [pie-1:GFP:MEX-5$^{ZF1\text{-}SSSH}$:pie-1(3'UTR)]*
JJ1688	pJT44	*zuEx105 [pie-1:GFP:MEX-5$^{ZF2\text{-}SSSH}$:pie-1(3'UTR)]*
JJ1657	pJT45	*zuIs113 [pie-1:GFP:MEX-5$^{\Delta aa447\text{-}468}$:pie-1(3'UTR)]*
JJ1696	pJT60	*zuIs119 [pie-1:GFP:MEX-5^{AAAATS}:pie-1(3'UTR)]*
JJ1699	pJT61	*zuEx113 [pie-1:GFP:MEX-5^{AAAATA}:pie-1(3'UTR)]*
JJ1703	pJT62	*zuIs121 [pie-1:GFP:MEX-5^{ASSTTS}:pie-1(3'UTR)]*
JJ1711	pJT63	*zuIs124 [pie-1:GFP:MEX-5^{TASTTS}:pie-1(3'UTR)]*
JJ1714	pJT64	*zuIs126 [pie-1:GFP:MEX-5^{TSATTS}:pie-1(3'UTR)]*
JJ1705	pJT65	*zuEx117 [pie-1:GFP:MEX-5^{TSSATS}:pie-1(3'UTR)]*
JJ1717	pJT66	*zuIs129 [pie-1:GFP:MEX-5^{S458A}:pie-1(3'UTR)]*
JJ1748	pJT76	*zuIs149 [pie-1:GFP:MEX-5^{S458D}:pie-1(3'UTR)]*
JJ1773	pJT77	*zuEx135 [pie-1:GFP:MEX-5^{S458E}:pie-1(3'UTR)]*

TABLE 1 continued

Strain	Transforming Plasmid	Genotype[a]
JJ1815	pJT82	*zuIs168 [mex-5:GFP:MEX-5:mex-5(3'UTR)]*
JJ1823	pJT85	*zuIs170 [mex-5:GFP:MEX-5^{S458A}:mex-5(3'UTR)]*
JJ1843	pJT86	*zuIs176 [mex-5:GFP:MEX-5^{TSSTAA}:mex-5(3'UTR)]*
JJ1895	pJT90	*zuIs189 [mex-5:GFP:PAR-1:mex-5(3'UTR)]*
JJ1905	pJT93	*zuIs192 [pie-1:GFP:PAR-4:pie-1(3'UTR)]*

[a] All transgenes include the rescuing *unc-119(+)* genomic fragment

TABLE 2: Primers for deletion constructs

Plasmid	Primers[a]
pJT16	5′-GAACTAGTATGAAAGCGGCATCA-3′ 5′-CACTAGTTCCTGACTGCATGACT-3′
pJT22	PCR #1 5′-ATGGCATGGATGAACTATAC-3′ 5′-GCAGAATCCAGTTCCTCCACG-3′ PCR #2 5′-GAACTAGTATGAAAGCGGCATCA-3′ 5′-GAATTCCTTGTCCGTTGGCAGCTTTGTCTTGTACTTGTTG-3′ Fusion PCR 5′-GAACTAGTATGAAAGCGGCATCA-3′ 5′-GGATCCACTAGTCTAATAGTGTCCTCT-3′
pJT29	5′-GAACTAGTATGAAAGCGGCATCA -3′ 5′-CGATACTAGTTCTTGCACAGCTT-3′
pJT30	5′-GAACTAGTATGAAAGCGGCATCA -3′ 5′-CGATACTAGTCTTCTGGAATGAC-3′
pJT32	5′-AGTCACTAGTCAAGTCATGCAGTCAGGACAACCA-3′ 5′-GGATCCACTAGTCTAATAGTGTCCTCT-3′
pJT33	5′-GATCACTAGTATGTCTCACGATGACCAG-3′ 5′-GGATCCACTAGTCTAATAGTGTCCTCT-3′
pJT34	PCR #1 5′-GAACTAGTATGAAAGCGGCATCA -3′ 5′-GATCAAGCTTAGTCTTGTAGTTGGGTGG-3′ PCR #2 5′-GGATCCACTAGTCTAATAGTGTCCTCT-3′ 5′-GATCAAGCTTCTCAAAGAGCTCAGAGCT-3′
pJT37	5′-GATCACTAGTCTCAAAGAGCTCAGA-3′ 5′-GGATCCACTAGTCTAATAGTGTCCTCT-3′
pJT38	5′-GATCACTAGTCGTGGATTCCCAATT-3′ 5′-GGATCCACTAGTCTAATAGTGTCCTCT-3′

TABLE 2 continued

Plasmid	Primers[a]
pJT39	5′-GATCACTAGTCGTGATAATCGCAAC-3′ 5′-GGATCCACTAGTCTAATAGTGTCCTCT-3′
pJT45	5′-GAACTAGTATGAAAGCGGCATCA-3′ 5′-GACTAGTTTAGTTCATCGGTGGATT-3′

[a] *SpeI* sites incorporated into primers are underlined. *HindIII* sites are double-underlined.

TABLE 3: Primers for site-directed mutagenesis

Plasmid	Mutation	Primers[a]
pJT42.1	C276S	5′-CTACAAGACTCGTCTTAGCATGATGCACGCATCTG-3′ 5′-CAGATGCGTGCATCATGCTAAGACGAGTCTTGTAG-3′
pJT42.2	C286S	5′-CATCTGGAATCAAACCAAGTGATATGGGTGCTCGA-3′ 5′-TCGAGCACCCATATCACTTGGTTTGATTCCAGATG-3′
pJT42.3	C292S	5′-GATATGGGTGCTCGAAGCAAGTTTGCTCATGGG-3′ 5′-CCCATGAGCAAACTTGCTTCGAGCACCCATATC-3′
pJT44.1	C320S	5′-GTACAAGACAAAGCTGAGCAAGAACTTTGCGCGTG-3′ 5′-CACGCGCAAAGTTCTTGCTCAGCTTTGTCTTGTAC-3′
pJT44.2	C331S	5′-GAGGAACTGGATTCAGCCCGTATGGACTTCG-3′ 5′-CGAAGTCCATACGGGCTGAATCCAGTTCCTC-3′
pJT44.3	C337S	5′-CCGTATGGACTTCGTAGCGAGTTTGTTCATCCAAC-3′ 5′-GTTGGATGAACAAACTCGCTACGAAGTCCATACGG-3′
pJT60	T450A S451A S453A T454A	5′-TGAACAAGCGTCGCGCAGCTCTCGCCGCGAAGTGGACATCTG-3′ 5′-CAGATGTCCACTTCGCGGCGAGAGCTGCGCGACGCTTGTTCA-3′
pJT61	T450A S451A S453A T454A S458A	5′-TGAACAAGCGTCGCGCAGCTCTCGCCGCGAAGTGGACAGCTG-3′ 5′-CAGCTGTCCACTTCGCGGCGAGAGCTGCGCGACGCTTGTTCA-3′
pJT62	T450A	5′-GAACAAGCGTCGCGCATCTCTCAGCACGA-3′ 5′-TCGTGCTGAGAGATGCGCGACGCTTGTTC-3′
pJT63	S451A	5′-CAAGCGTCGCACAGCTCTCAGCACGAAGT-3′ 5′-ACTTCGTGCTGAGAGCTGTGCGACGCTTG-3′
pJT64	S453A	5′-CGTCGCACATCTCTCGCCACGAAGTGGACATCT-3′ 5′-AGATGTCCACTTCGTGGCGAGAGATGTGCGACG-3′
pJT65	T454A	5′-GCACATCTCTCAGCGCGAAGTGGACATCTGA-3′ 5′-TCAGATGTCCACTTCGCGCTGAGAGATGTGC-3′
pJT66	S458A	5′-GCACGAAGTGGACAGCTGAGGAAAATCTCGG-3′ 5′-CCGAGATTTTCCTCAGCTGTCCACTTCGTGC-3′
pJT86[b]	T457A S458A	5′-CTCAGCACGAAGTGGGCGGCTGAGGAAAATCTC-3′ 5′-GAGATTTTCCTCAGCCGCCCACTTCGTGCTGAG-3′

[a] Nucleotide substitutions are underlined.

[b] The template for pJT86 was pJT66. In all other mutagenesis reactions, the template was pJN148.

Results

Identification of MEX-5 domains that regulate its asymmetry in 1-cell embryos

To examine MEX-5 localization in early embryos, I created *gfp:mex-5* fusion proteins, in which Green Fluorescence Protein (GFP) was fused to the MEX-5 protein. Transgene expression was under the control of either the *mex*-5 promoter or a second germline-specific promoter, *pie-1* (Strome et al., 2001) (see Materials and Methods). Integrated strains expressing green fluorescent protein fused to full-length MEX-5 (GFP:MEX-5) had expression patterns apparently identical to those described previously for MEX-5 by immunostaining (Schubert et al., 2000). GFP:MEX-5 was distributed uniformly in oocytes and newly-fertilized embryos. After fertilization, the levels of GFP:MEX-5 increased and GFP:MEX-5 became enriched progressively in the anterior half of the 1-cell embryo as the male and female pronuclei migrated to the center of the embryo and fused to form the zygotic nucleus (Figure 4A).

MEX-5 is a 468 amino acid protein with two CCCH zinc finger (ZF) domains between amino acids 276 and 342. Substituting all three Cys residues of a CCCH finger with Ser residues (SSSH) is predicted to disrupt its structure, and these changes in the PIE-1 ZF1 domain were effective in preventing PIE-1 degradation after the 2-cell stage (Reese et al., 2000). The MEX-5 ZF2 domain is most similar to the ZF1 domain of PIE-1, and previous work demonstrated that this ZF2 domain was necessary and sufficient for MEX-5 degradation at and after the 2-cell stage (DeRenzo et al., 2003). To further examine roles for the ZF2 domain, I generated a transgene expressing MEX-5 with Cys to Ser changes in ZF2 (GFP:MEX-$5^{ZF2\text{-}SSSH}$). As predicted, this fusion

protein was not degraded in somatic blastomeres after the 2-cell stage. However, the protein showed normal asymmetry at the 1-cell stage, suggesting that ZF2-mediated degradation at and after the 2-cell stage is not essential for 1-cell asymmetry (Figure 4C, F).

To identify domains of MEX-5 that are required for asymmetry at the 1-cell stage, worm strains were generated with integrated transgenes expressing C- and N-terminal fragments of MEX-5 fused to GFP (Figure 5). All of the C-terminal deletion proteins examined showed a loss of asymmetry at the 1-cell stage. The smallest of these deletions (GFP:MEX-$5^{\Delta 446\text{-}468}$) removed only the terminal 22 amino acids. Deletion of the N-terminal 198 amino acids (GFP:MEX-$5^{\Delta 1\text{-}198}$) did not appear to affect asymmetry in 1-cell embryos or at later stages. However, a larger deletion (GFP:MEX-$5^{\Delta 1\text{-}297}$) abolished asymmetry in 1-cell embryos. Because this larger deletion removes ZF1 and an additional 71 amino acids, I generated worm strains with integrated transgenes for either GFP:MEX-$5^{ZF1\text{-}SSSH}$ or a ZF1 deletion (GFP:MEX-$5^{\Delta ZF1}$). Both fusion proteins showed normal anterior localization, indicating that the ZF1 domain is not essential for asymmetry (Figure 4B). Likewise, when both ZF1 and ZF2 were mutated together (GFP:MEX-$5^{ZF1\text{-}SSSH\ ZF2\text{-}SSSH}$), transgenic embryos showed no loss of asymmetry in 1-cell embryos, indicating that neither ZF1 nor ZF2 are necessary for MEX-5 asymmetry at the 1-cell stage (data not shown).

MEX-5 asymmetry requires phosphorylation at Ser458

The above results suggest that at least two regions of MEX-5 are necessary for its asymmetry: the region between amino acids 199 and 270 N-terminal to the ZF1

domain, and the C-terminal 22 amino acids. The N-terminal domain has no obvious motifs, and none of the Ser or Thr sites are predicted to be phosphorylated (NetPhos 2.0) (Blom et al., 1999) (Figure 6A). This C-terminal domain contains six Ser or Thr residues, five of which are predicted to have a high probability of phosphorylation (NetPhos 2.0) (Blom et al., 1999). Four of these residues are conserved in the *C. elegans* MEX-6 protein and in the *C. remanei* and *C. briggsae* orthologs of MEX-5 (Figure 6B). To determine if MEX-5 is a phosphoprotein, protein extracts were prepared from embryos collected from wild-type hermaphrodites (see Materials and Methods). Extracts were treated with alkaline phosphatase (AP) and proteins separated by Western blot. After treatment with AP, the MEX-5 band was more compact, and had a faster mobility, suggesting that MEX-5 is phosphorylated in vivo (Figure 7A).

Each Ser or Thr residue within the C-terminal domain was substituted with Ala, either individually or in combination (Figure 8). 1-cell asymmetry was not observed when all residues were substituted with Ala (Figure 8C). Single substitutions of each of the first four Ser or Thr residues had no apparent effect on asymmetry (Figure 8D and data not shown). However, Ala substitutions of the sixth residue, Ser458, markedly reduced or abolished asymmetry (Figure 8E), and no asymmetry was visible in any embryos when both Thr457 and Ser458 were substituted with Ala. Conversely, asymmetry was retained when all of the Ser and Thr residues except Thr457 and Ser458 were substituted with Ala simultaneously (Figure 8F). These results suggest that Ser458 is critical for MEX-5 asymmetry, with a potential minor contribution for Thr457. Ser or Thr residues can often be replaced by Asp or Glu residues, which can

act as phosphomimetics. However, in integrated lines expressing GFP:MEX-5^{S458D} or GFP:MEX-5^{S458E}, no asymmetry was detected at the 1-cell stage (Figure 8G).

An antiserum was raised against a synthetic peptide with phospho-Ser458 in place of Ser458 (see Materials and Methods). In Western blots, the anti-MEX-5(pS458) antiserum stained a band at the same molecular weight as MEX-5, and bands at the predicted weights for GFP:MEX-5 fusion proteins; relatively little staining was detected of GFP:MEX-5^{S458A} (Figure 7B). Therefore, these results strongly suggest that MEX-5 is phosphorylated on Ser458 in vivo.

Although Ser458 is critical for MEX-5 asymmetry at the 1-cell stage, I did not detect any differences between anti-MEX-5 and anti-MEX-5(pS458) immunostaining in embryos or gonads (Figure 9). Thus, our results suggest that MEX-5 asymmetry is not associated with a major change in Ser458 phosphorylation. The anti-MEX-5(pS458) immunostaining patterns appeared specific for MEX-5, except for small cytoplasmic punctae that were not stained by anti-MEX-5 and that persisted in *mex-5* mutant embryos (Figure 9A).

The Ser/Thr kinases PAR-1 and PAR-4 are necessary for MEX-5 phosphorylation

To identify kinases that might phosphorylate Ser458, I investigated predicted serine/threonine kinases that met two criteria. First, I identified kinases that were enriched in the *C. elegans* germline, based on analysis of microarray experiments and the presence of mRNA in gonads detected by in situ hybridization (Reinke et al., 2000; Reinke et al., 2004) (Nematode Expression Pattern Database, http://nematode.lab.nig.ac.jp/). This list was further refined by identifying kinases that

caused embryonic phenotypes when mutated or depleted by dsRNA interference (WormBase, http://www.wormbase.org; Table 4). For 39 of 41 mutant or dsRNA-treated embryos, there were no differences in staining between anti-MEX-5(pS458) and anti-MEX-5 antisera, although both antisera could have similar abnormal staining patterns. However, depletion of either the PAR-1 or PAR-4 kinases resulted in aberrant staining patterns. These abnormalities (see below) did not appear to result from general defects in polarity, because mutants defective in the *par* polarity genes *par-2*, *par-3*, *par-5*, and *par-6* did not have similar defects in MEX-5(pS458) expression (data not shown). Mutants defective in the *par-1* or *par-4* genes lack MEX-5 asymmetry at the 1-cell stage (Figure 10B) (Schubert et al., 2000). I found that wild-type animals exposed to *par-1* dsRNA showed low or no anti-MEX-5(pS458) staining in the gonad or in 1-cell embryos, although these animals had wild-type levels of MEX-5 staining (data not shown). Similarly, there was no apparent staining of anti-MEX-5(pS458) in *par-1(it51)* animals that have a predicted kinase-dead PAR-1 protein (Figure 10) (Guo and Kemphues, 1995). Temperature-sensitive *par-4(it47ts)* animals that were grown at the permissive temperature of 15°C had normal, equivalent staining patterns of anti-MEX-5 and anti-MEX-5(pS458) in gonads and in 1-cell embryos (data not shown). The pattern of anti-MEX-5 staining remained similar at the restrictive temperature of 25°C. In contrast, there was a progressive decrease in anti-MEX-5(pS458) staining in maturing oocytes, such that staining was not detectable in the most mature oocyte. In 1-cell embryos, anti-MEX-5(pS458) staining was present only on cytoplasmic punctae; these punctae were not stained by the anti-MEX-5 antibody (Figure 10). A similar, aberrant anti-MEX-5(pS458) staining pattern was observed in the non-conditional *par-4* mutants

par-4(it33) and *par-4(it75)*; these mutants and *par-4(it47ts)* mutants have mutations that are predicted to abolish PAR-4 kinase activity (Watts et al., 2000).

The above results indicate that PAR-1 and PAR-4 are necessary for MEX-5(S458) phosphorylation in the gonad; PAR-1 is required for phosphorylation throughout the gonad, and PAR-4 is required to maintain phosphorylation in the most mature oocytes. Because PAR-1 and PAR-4 activities and Ser458 are required for MEX-5 asymmetry at the 1-cell stage, a simple model is that the lack of MEX-5 asymmetry in *par-1* or *par-4* mutant embryos results solely from the failure to phosphorylate Ser458. All sequenced *par-4* mutants have mutations within the PAR-4 kinase domain (Watts et al., 2000). However, several alleles of *par-1*, including *par-1(b274), par-1(e2012)* and *par-1(it60),* have mutations outside of the PAR-1 kinase domain (Guo and Kemphues, 1995). Thus, I examined anti-MEX-5 and anti-MEX-5(pS458) staining in this class of *par-1* mutants. Each of these mutants failed to generate MEX-5 asymmetry at the 1-cell stage; however, all showed anti-MEX-5(pS458) staining in gonads and in 1-cell stage embryos (Figure 10B and data not shown). Thus, these alleles of *par-1* are similar to mutations in *par* genes like *par-3* that have anti-MEX-5(pS458) staining but lack MEX-5 asymmetry. I conclude that PAR-1 is required directly or indirectly to phosphorylate Ser458, but that PAR-1 has an additional function(s) that is required for MEX-5 asymmetry at the 1-cell stage.

Creation of GFP:PAR-1 and GFP:PAR-4 transgenic strains

PAR-1 and PAR-4 may affect MEX-5 phosphorylation by directly interacting with MEX-5, or through an indirect mechanism. To distinguish between these

possibilities, I generated transgenic strains expressing GFP:PAR-1 and GFP:PAR-4 for use with in vitro kinase assays. Integrated strains were generated that expressed either GFP:PAR-1 or GFP:PAR-4. GFP:PAR-1 was expressed throughout the gonad at actin-rich regions between germ cells and at the cortex of oocytes (Figure 11A,C). This expression pattern resembled the pattern of PAR-1 immunostaining (Guo and Kemphues, 1995). GFP:PAR-4 was also expressed throughout the gonad at actin-rich regions between germ cells. In oocytes, GFP:PAR-4 expression was primarily cytoplasmic, with weak localization at the cortex (Figure 11B, D). This pattern was similar to the expression of PAR-4 as detected by immunostaining (Watts et al., 2000).

GFP:MEX-5 localization dynamics in 1-cell embryos

Three general mechanisms may regulate MEX-5 asymmetry in 1-cell embryos: restricted translation, directed transport to the anterior, or degradation in the posterior. In examination of GFP-expressing embryos in utero, I observed a significant increase in GFP expression levels, in comparison to oocytes and newly-fertilized embryos (Figure 12). This observation was repeated in embryos stained with anti-MEX-5. At the time when the pronuclei fused to form the zygotic nucleus, the levels of MEX-5 at the anterior pole was approximately 2-fold greater than in newly-fertilized embryos (Table 5). Similarly, there was an approximately 2.5-fold decrease in MEX-5 levels at the posterior pole, compared to newly-fertilized embryos (Table 5). The increase in protein levels required the MEX-5 open reading frame, as similar increases in GFP expression were not observed in embryos expressing GFP alone (data not shown). However, *mex-5* non-coding sequences were not required, as similar results were obtained using both

the *mex-5:GFP* and *pie-1:GFP* expression vectors. Therefore, while levels of MEX-5 protein increase in early embryos, MEX-5 asymmetry is not explained by translational regulation.

Several proteins, including PAR-3 and PAR-6, were shown to be anteriorly localized as part of a wave of cortical contracts that transport actin-rich cytoskeletal proteins from the posterior to the anterior following fertilization (Munro et al., 2004). This cortical contraction requires the non-muscle myosin protein, NMY-2 (Guo and Kemphues, 1996; Cheeks et al., 2004; Munro et al., 2004). To determine if MEX-5 is also anteriorly localized by cortical flow, NMY-2:GFP and GFP:MEX-5 localization were compared. While I was unable to compare both fusion proteins within the same embryo, I was able to make comparisons at well-characterized stages in the 1-cell embryo. At the time of fertilization, both NMY-2:GFP and GFP:MEX-5 are distributed symmetrically in the embryo. Shortly after fertilization, a smooth zone appears at the posterior cortex, proximal to the male pronucleus (Hird and White, 1993; Munro et al., 2004). The appearance of this smooth zone is coincident with loss of NMY-2:GFP from this region (Munro et al., 2004). However, GFP:MEX-5 expression remained symmetric. Shortly thereafter, a pseudocleavage furrow appears approximately 50% the length of the embryo, which separates the posterior, smooth cortex from the anterior, ruffled cortex. At this time, NMY-2:GFP has formed a cap around the anterior pole, and very little NMY-2:GFP is detected in the posterior (Munro et al., 2004). At this stage, clearing of GFP:MEX-5 from the posterior pole was initiated. GFP:MEX-5 did not reach its maximal asymmetry until the fusion of the male and female pronuclei to

form the zgotic nucleus. I conclude that GFP:MEX-5 localization is not coincident with anterior cortical contraction, and instead occurs slightly after.

To better understand the dynamics of MEX-5 localization, I investigated the use of photoactivatable GFP (PA-GFP) proteins to activate MEX-5 fluorescence in specific regions of the embryo. These PA-GFP fusion proteins do not fluoresce under standard epifluorescence conditions, but when targeted with a 413 nm laser, GFP fluorescence is visible (Patterson and Lippincott-Schwartz, 2002). Transgenic embryos expressing *nmy-2:PA-GFP* fused to a germline protein have been successfully generated in *C. elegans* (J. Nance and E. Munro, personal communication). I obtained four independent lines that expressed the PA-GFP:MEX-5 fusion protein as detected by immunostaining with an anti-GFP antiserum. However, I was unsuccessful in activating PA-GFP fluorescence following exposure to laser.

To investigate the possibility that MEX-5 asymmetry is generated by posterior degradation, I asked whether depletion of proteins involved in the proteasome-mediated degradation pathway would stabilize posterior MEX-5 levels. I tested 32 proteasome-specific genes by feeding dsRNA to L4 larvae expressing GFP:MEX-5 . Since many proteasome subunits result in sterility or embryonic arrest in meiosis, I analyzed genes that were not reported to cause a sterility defect. Of the 32 genes tested, 14 resulted in no detectable phenotypes, and 3 resulted in embryos that arrested in meiosis. Since anterior-posterior polarization requires progression from meiosis into mitosis (Bowerman and Kurz, 2006), these embryos were not analyzed further. The remaining 14 genes resulted in defects at either the 1-cell stage or later. For example, embryos depleted of members of the *rpn* gene family (*rpn-1, -2, -3, -6,* or *-7)* arrested as

multinucleated, 1-cell embryos, suggesting a failure in cytokinesis. In these embryos, GFP:MEX-5 expression appeared to be symmetric. However, it was not clear whether this lack of asymmetry was due to the apparent cytokinesis defect, or due to failure to degrade GFP:MEX-5. Embryos depleted of *rpn-9, rpn-10 or rpn-12* expressed GFP:MEX-5 asymmetrically in 1-cell embryos, but GFP:MEX-5 failed to degrade in somatic blastomeres at and after the 4-cell stage. Embryos depleted of *rbx-1* showed a range of phenotypes, but in all cases in which embryos progressed through the first cell cycle, GFP:MEX-5 expression appeared asymmetric. The remaining genes (B0393.6, T10F2.4, *uba-2*, and *ubc-9*) resulted in postembryonic defects, with no apparent effect on GFP:MEX-5 expression. These results indicate that for the genes tested, the proteasome pathway does not appear to affect MEX-5 stability in 1-cell embryos. However, due to the importance of the proteasome pathway in oogenesis and progression through the first cell cycle, I cannot rule out a role for protein degradation in MEX-5 asymmetry.

GFP:MEX-5 restores PIE-1 localization in early *mex-5;mex-6* embryos

Previous work demonstrated that in 1-cell embryos with loss of function of both *mex-5* and *mex-6*, the germline protein PIE-1 is no longer restricted to the posterior pole, and instead is distributed uniformly throughout the embryo (Schubert et al., 2000). Conversely, when MEX-5 levels were high, levels of germline proteins, including MEX-1, were low (Schubert et al., 2000). These observations suggest that MEX-5 exclusion from the posterior is necessary to ensure proper expression of germline proteins. To test this model, I asked whether the perdurance of MEX-5 in the posterior

of 1-cell embryos deleteriously affected embryo development by examining GFP:MEX-5 and GFP:MEX-5S458A expression in the absence of *mex-5* and *mex-6* function. Embryos with the genotype GFP:MEX-5;*unc-30(e191) mex-5(zu199);mex-6(pk440)* (hereafter referred to as GFP:MEX-5;*mex-5;mex-6* embryos) were viable; 98.9% (n=267) hatched. This result suggests that the level of protein expression from the transgene was sufficient to compensate for the loss of both *mex-5* and *mex-6*.

Conversely, GFP:MEX-5^{S458A};*mex-5;mex-6* embryos failed to hatch (0% viability, n=200). However, several observations indicated that GFP:MEX-5 ^{S458A} activity rescued some of the mutant phenotypes seen in *mex-5(zu199);mex-6(pk440)* double mutant embryos. First, *mex-5(zu199);mex-6(pk440)* embryos have a Skn-like phenotype in that they fail to make intestine or pharynx (Schubert et al., 2000). GFP:MEX-5 ^{S458A};*mex-5;mex-6* embryos were stained with the monoclonal antibody 3NB12 to visualize pharyngeal tissue (Priess and Thomson, 1987), and were examined by polarization optics to visualize birefringent granules produced by intestine (Laufer et al., 1980). 9.1% (n=88) of embryos made pharyngeal tissue, and 45.5% (n=99) produced intestine, indicating that GFP:MEX-5 ^{S458A} was able to restore some tissue types to *mex-5;mex-6* embryos. However, GFP:MEX-5 ^{S458A} was insufficient to rescue two other phenotypes of *mex-5;mex-6* double mutant embryos. First, in 93.3% (n=15) of GFP:MEX-5 ^{S458A};*mex-5;mex-6* 1-cell embryos, PIE-1 was uniformly distributed. However, the levels of PIE-1 staining in these embryos was not noticeably reduced compared to PIE-1 levels in *mex-5;mex-6* double-mutant embryos. Second, in *mex-5;mex-6* double mutant embryos, germline proteins fail to degrade in somatic blastomeres due to a requirement for MEX-5 and MEX-6 in ZIF-1-mediated

proteolysis. Interestingly, GFP:MEX-5 ^{S458A} expression in GFP:MEX-5 ^{S458A};*mex-5;mex-6* embryos perdured in all blastomeres after the 4-cell stage, in contrast to the pattern of somatic degradation observed with GFP:MEX-5 in GFP:MEX-5;*mex-5;mex-6* embryos. Because the ectopic expression of MEX-5 at these later stages could influence cell fate specification, I was unable to directly assess the effects of posteriorly-expressed GFP:MEX-5^{S458A} on embryonic development.

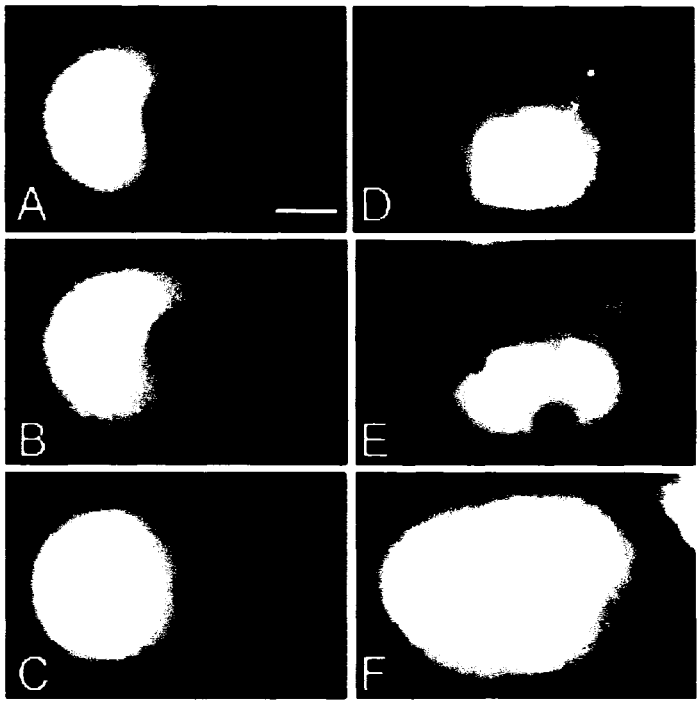

Figure 4. Localization of GFP:MEX-5 fusion proteins in early embryos. (A,D) GFP:MEX-5; (B,E) GFP:MEX-5$^{ZF1\text{-}SSSH}$; (C,F) GFP:MEX-5$^{ZF2\text{-}SSSH}$. GFP:MEX-5 is anteriorly localized at the 1-cell stage in each construct (A-C), but fails to degrade in the anterior somatic blastomeres of GFP:MEX-5$^{ZF2\text{-}SSSH}$ 4-cell embryos (F). Embryos shown in this and subsequent figures are approximately 45 μm in length. Scale bar equals 10 μm.

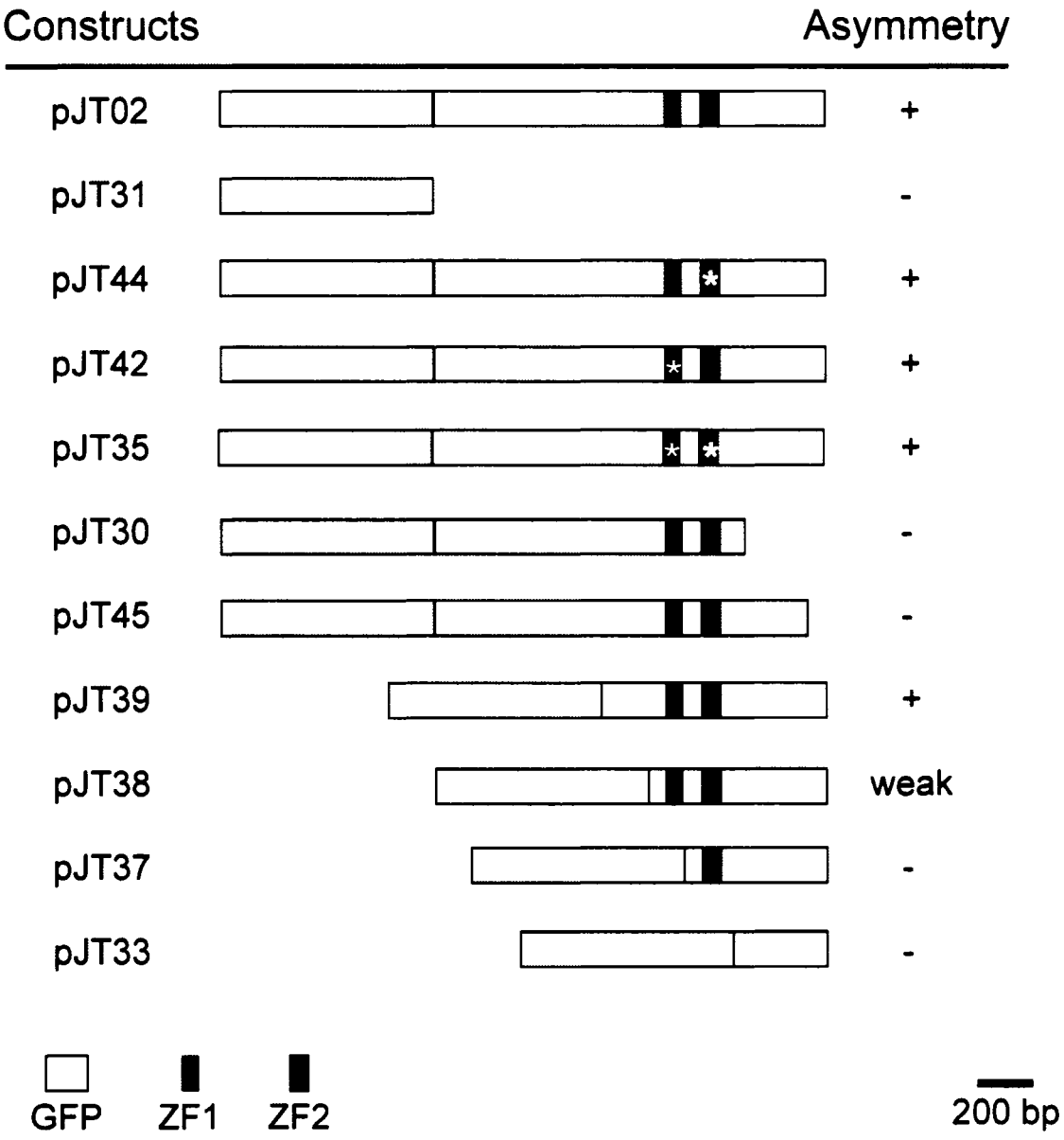

Figure 5. Identification of domains necessary for MEX-5 asymmetry. Diagram showing GFP:MEX-5 fusion proteins drawn to scale, highlighting the positions of GFP, ZF1 and ZF2 sequences. For all constructs, at least 25 1-cell embryos were scored for GFP:MEX-5 localization at the time when the male and female pronuclei have fused in the center of the embryo to form the zygotic nucleus. Detailed genotypes for each construct are listed in Table 1.

A. N-terminal domain (amino acids 199-271)

```
C.e. MEX-5  RD--NRNRNIQFRYHRVMEHDELPID
C.e. MEX-6  RD---RNRNSQSRYQCPIEHDDLPID
C.b. MEX-5  RDNQARNRNIQLRYHRVMEHDDLPIE
C.r. MEX-5  RDTHARNRNIQLRYHRVMEHDELPID
            **    **** * **:  :***:***:

C.e. MEX-5  EISKITLDNHNDDTMSAEKENHFHEH
C.e. MEX-6  EISKITIDNHNDDTMSAEKENRFNKN
C.b. MEX-5  ELSEIKLDHHNDDTMSAEKEN-----
C.r. MEX-5  EISDIG----HDDTMSAEKENHMLAQ
            *:*.*      :**********

C.e. MEX-5  RGEKFGRRGFPIPETDSQQPPN
C.e. MEX-6  RVEKLGRRGFAKPEVDSQLPHN
C.b. MEX-5  NGEKVARRGFTNSDIETQQPAN
C.r. MEX-5  HGEKTARRGFKNAEE---QPPN
            . **  .****   .: :.   * *
```

B. C-terminal domain (amino acids 446-468)

```
C.e. MEX-5  KRRTSLSTKWTSEENLGLRGHY
C.e. MEX-6  RSRPSFSTKWTSVENLGLRGHY
C.b. MEX-5  KRRTSLNTKWTSEENLGLHGHY
C.r. MEX-5  KRRTSLSTKWTSEENLGLHGHY
            : *.*:.***** ******:***
```

Figure 6. Ser and Thr residues in MEX-5 domains. (A) Region of MEX-5 between amino acids 199 and 270, N-terminal to ZF1 domain. (B) C-terminal 22 amino acids (amino acids 446-468). The *C. elegans* (C.e.) MEX-5 sequence is shown aligned to *C. elegans* MEX-6, and to MEX-5 orthologs in the related species *C. briggsae* (C.b.) and *C. remanei* (C.r.) Ser and Thr residues are boxed. Ser and Thr residues with predicted to have a high probability of phosphorylation are shaded (Blom et al., 1999).

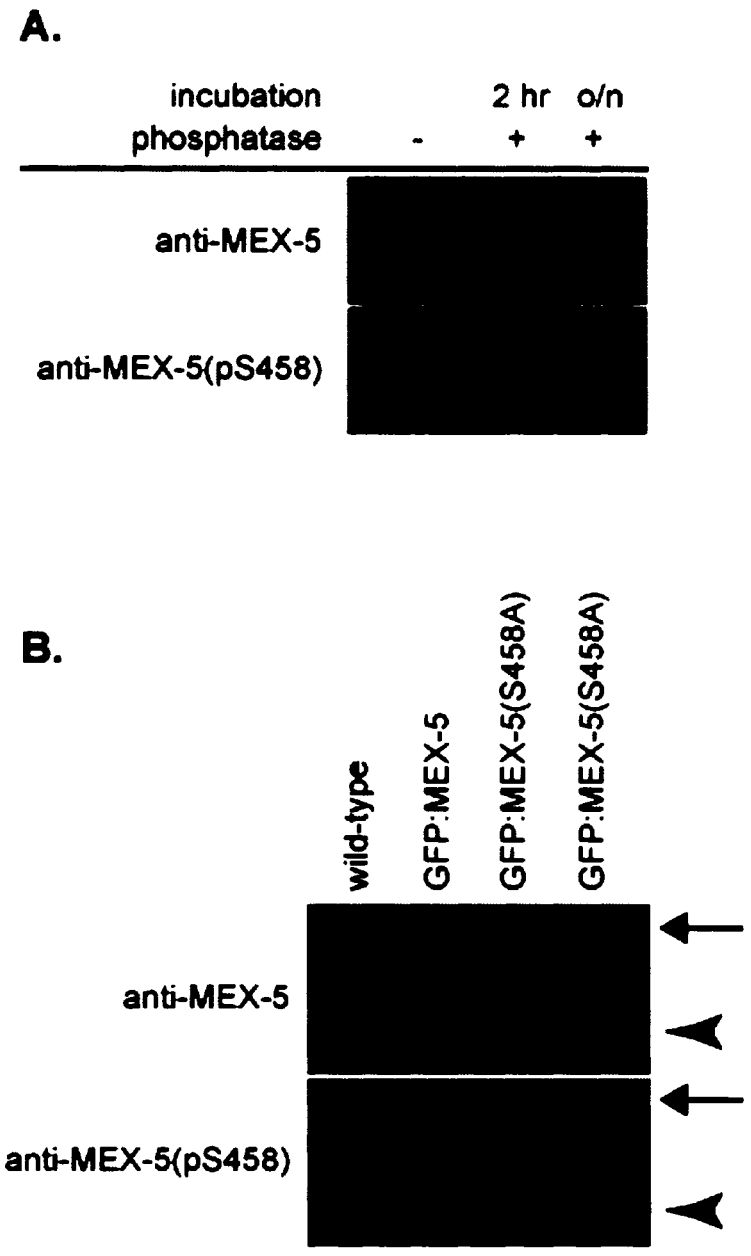

Figure 7. MEX-5 is a phosphoprotein. (A) Protein extracts from wild-type embryos were treated with alkaline phosphatase for 2 hrs or overnight and analyzed by Western blot with the anti-MEX-5 antibody. Blots were exposed to film for 19 min. (B) Protein extracts from embryos from wild-type, GFP:MEX-5 or GFP:MEX-5^{S458A} (two independent lines) strains were analyzed by Western blot with the anti-MEX-5 antibody and anti-MEX-5(pS458) antiserum. Arrowheads indicate endogenous MEX-5, and arrows indicate GFP fusion proteins. Blots were exposed to film for 6 min.

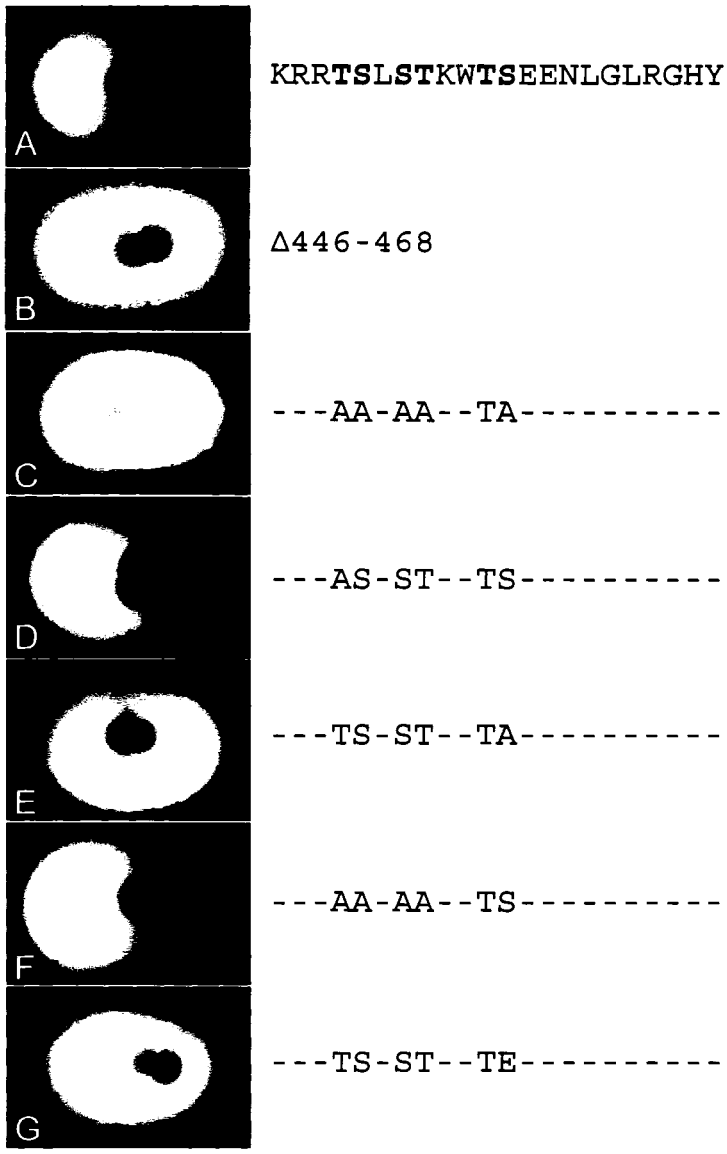

Figure 8. Ser458 is necessary for MEX-5 asymmetry. (A) 1-cell embryo expressing a full-length GFP:MEX-5 fusion protein. For simplicity, only the C-terminal 22 amino acids are shown. (B) GFP:MEX-5$^{\Delta 446\text{-}468}$; (C) GFP:MEX-5^{AAAATA}, showing loss of asymmetry; (D) GFP:MEX-5^{AAAATS}, showing anterior localization of GFP; (E) GFP:MEX-5^{ASSTTS}, showing asymmetric GFP. Similar results were obtained when S451, S453 or T454 were substituted with Ala. (F) GFP:MEX-5^{S458A} results in loss of asymmetry; (G) Phosphomimetic substitutions of S458 with either Asp or Glu did not result in GFP:MEX-5 asymmetry.

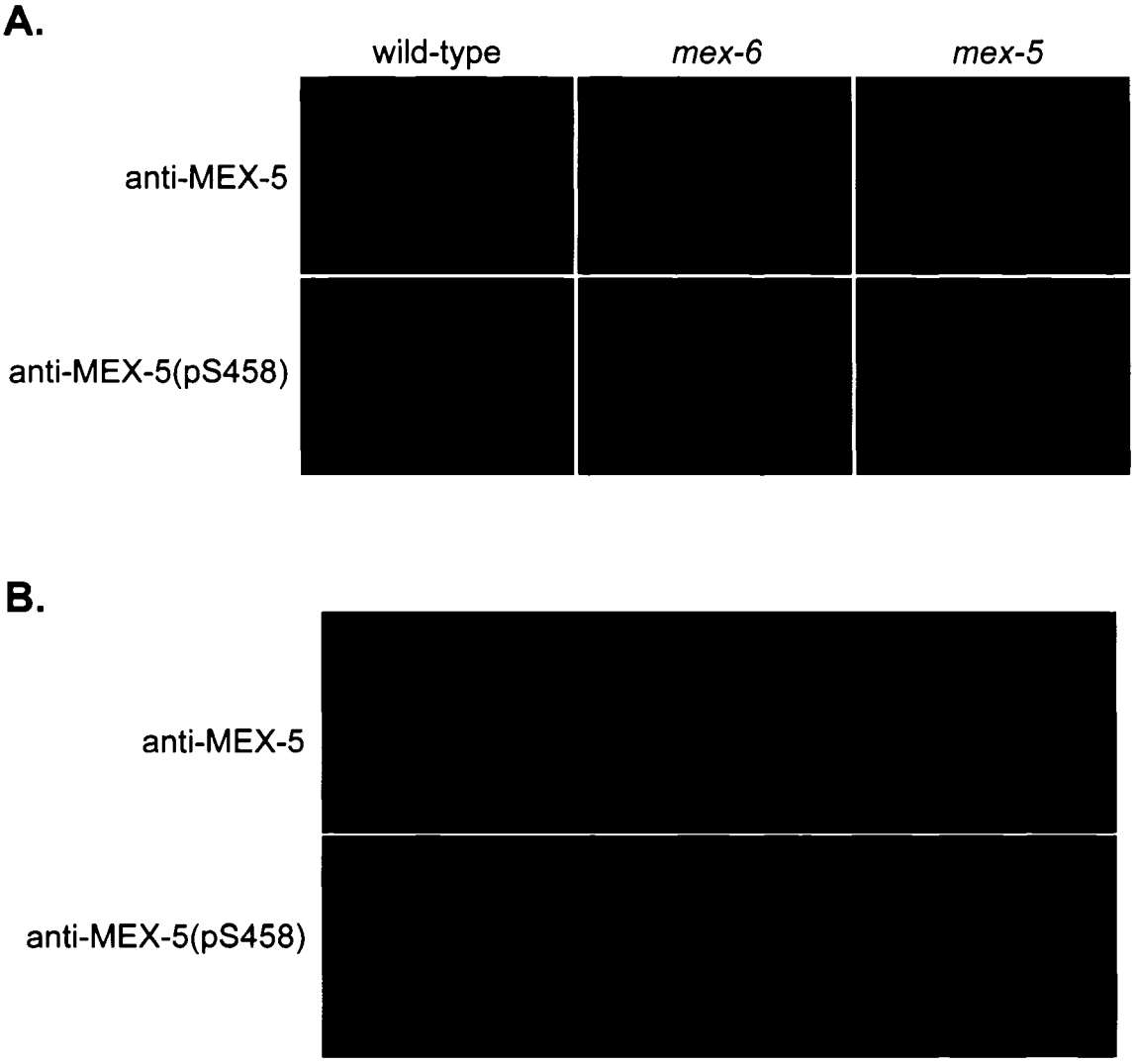

Figure 9. MEX-5 is phosphorylated in the germline. (A) 1-cell embryos from wild-type, *mex-6(pk440)* and *mex-5(zu199)* mothers were immunostained for anti-MEX-5 and anti-MEX-5(pS458). In both wild-type and *mex-6(pk440)* embryos, anti-MEX-5(pS458) staining was co-incident with anti-MEX-5. The anti-MEX-5(pS458 antiserum is specific for MEX-5 as it does not stain *mex-5(zu199)* embryos. The antiserum also recognizes non-specific cytoplasmic foci, since staining of these foci is apparent in *mex-5(zu199)* embryos. (B) Both anti-MEX-5 and anti-MEX-5(pS458) staining are present starting at the bend of the gonad, where germ cells enter oogenesis, suggesting that phosphorylation of MEX-5 at Ser458 occurs at the onset of MEX-5 expression.

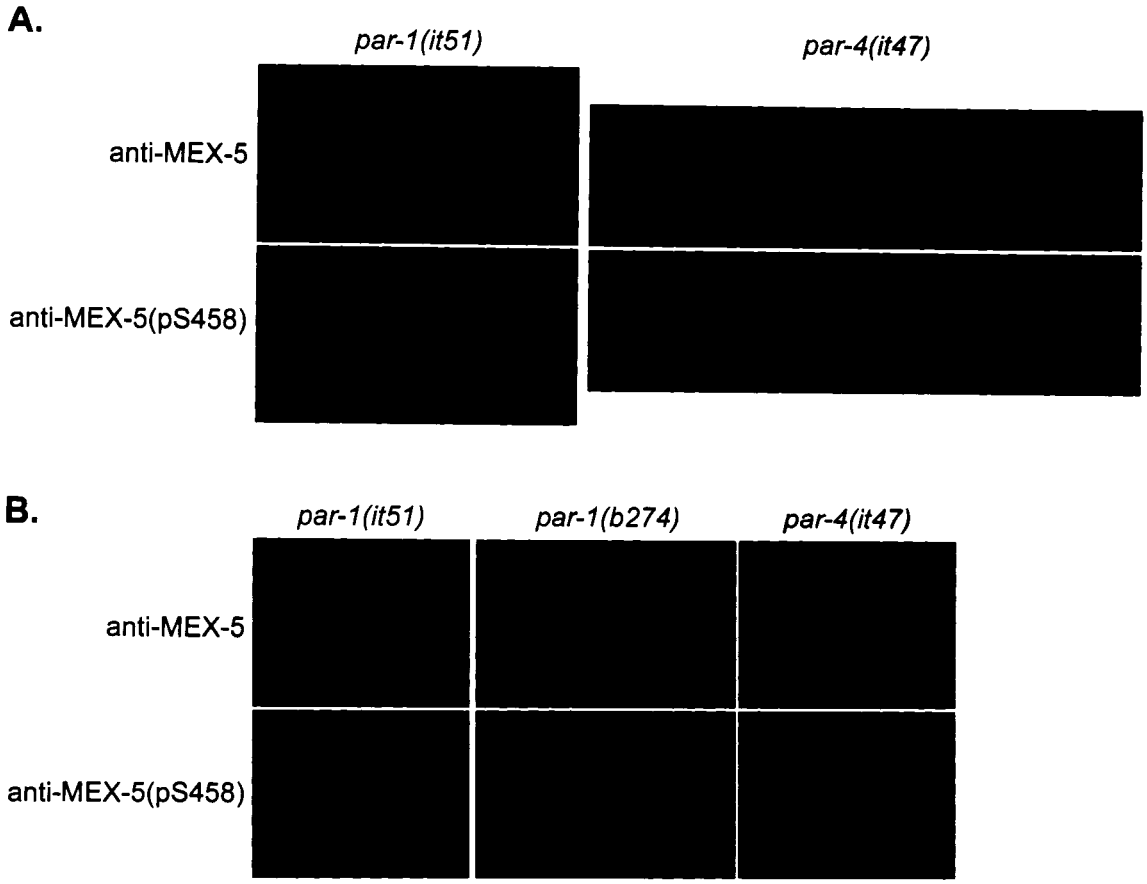

Figure 10. MEX-5 phosphorylation requires PAR-1 and PAR-4. (A) Gonads from *par-1(it51)* and *par-4(it47)* hermaphrodites were stained for anti-MEX-5 and anti-MEX-5(pS458). Both *par-1(it51)* and *par-4(it47)* had high levels of anti-MEX-5 staining (compare to Figure 8B), confirming previously published observations. However, *par-1(it51)* had little or no staining with anti-MEX-5(pS458), except for non-specific staining of sperm. In *par-4(it47)* gonads, levels of anti-MEX-5(pS458) staining were initially high, then progressively decreased in mature oocytes. (B) Both *par-1(it51)* and *par-4(it47)* 1-cell embryos had undetectable levels of anti-MEX-5(pS458) staining in cytoplasm, while *par-1(b274)* had high levels of cytoplasmic staining. In all embryos, anti-MEX-5(pS458) also stained bright punctae; the identity of these punctae is unknown.

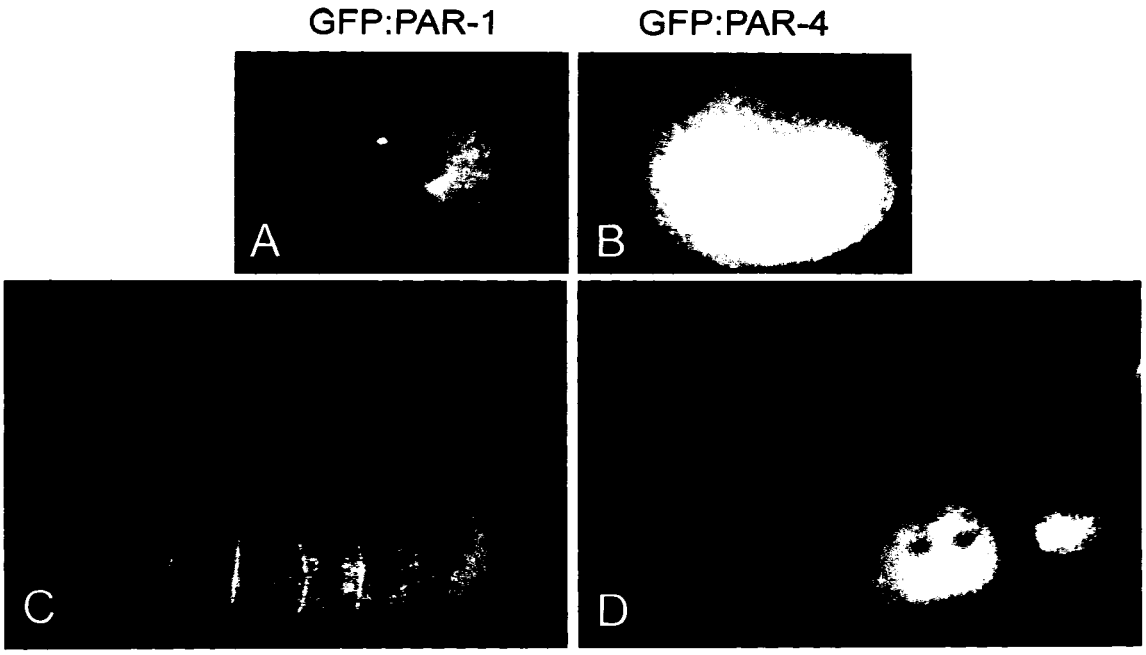

Figure 11. GFP:PAR-1 and GFP:PAR-4 recapitulate endogenous protein expression patterns. Embryos and gonads from GFP:PAR-1 (A, C) and GFP:PAR-4 (B, D) hermaphrodites were stained with anti-GFP antiserum.

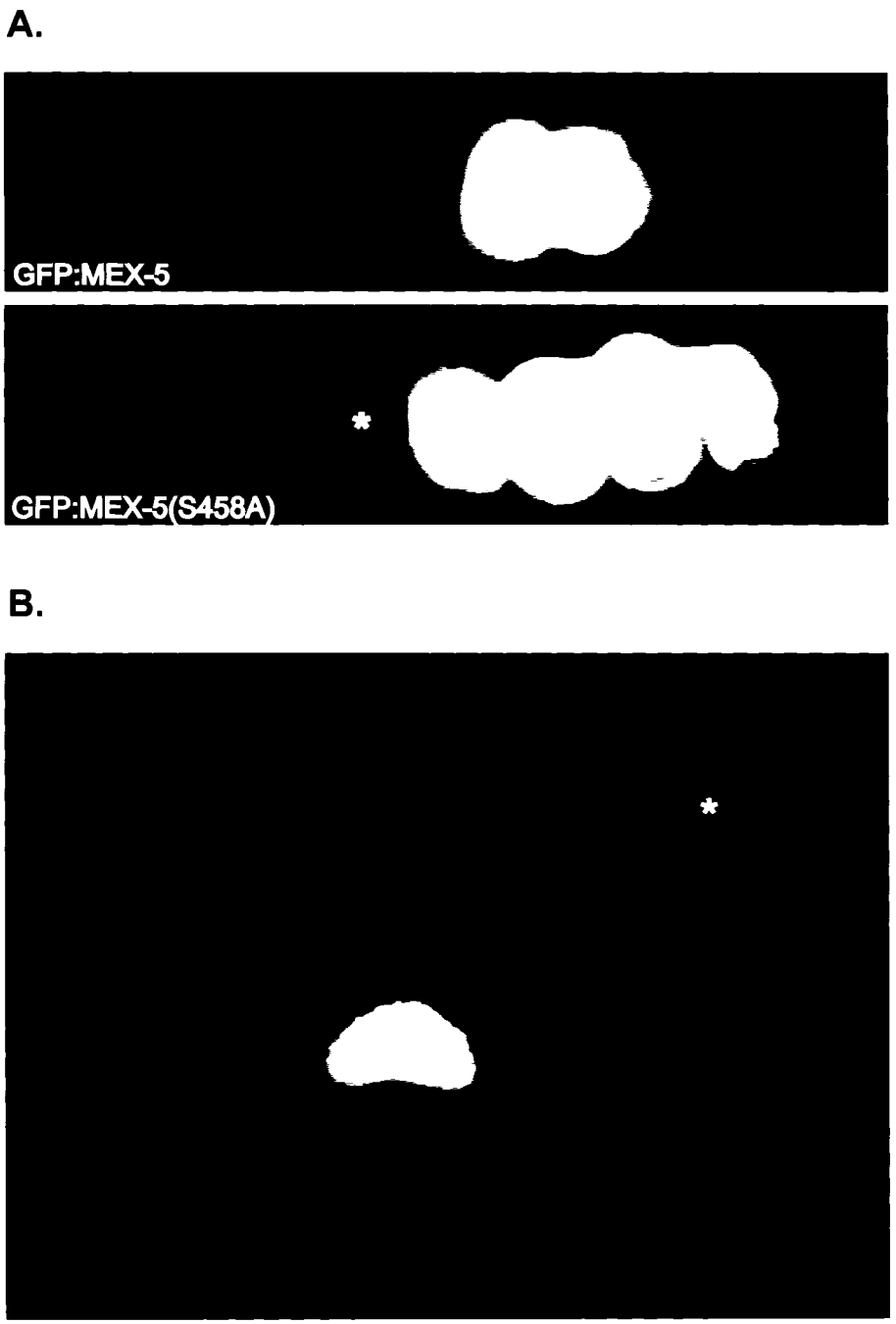

Figure 12. MEX-5 levels increase in 1-cell embryos. (A) Images of oocytes and embryos from live animals expressing GFP:MEX-5 (top) and GFP:MEX-5^{S458A} (bottom) fusion proteins. Red arrowheads mark the spermatheca. Oocytes are positioned to the left of the spermatheca. (B) Immunostaining with anti-MEX-5 in newly-fertilized, 1-cell and 2-cell embryos (counterclockwise, from right). In all panels, newly-fertilized embryos are marked with asterisks.

TABLE 4: Predicted Ser/Thr Kinases Analyzed in this Study

WormBase ID	Gene Name	Kinase Family[a]	Method of Analysis
B0205.7	*kin-3*	CK2	RNAi (feeding)
B0207.4	*air-2*	Aurora	RNAi (feeding)
B0414.7	*mtk-1*	MEKK	RNAi (feeding) [b]
B0495.2		CDK	RNAi (feeding) [b]
C03C10.1	*kin-19*	CK1	RNAi (feeding) [b]
C05D10.2		MAPK	RNAi (feeding) [b]
C09G4.3	*dom-6*		RNAi (feeding)
C10H11.9	*let-502*	Rho-kinase	RNAi (feeding)
C14B9.4	*plk-1*	Polo-like	RNAi (feeding)
C29F9.7	*pat-4*	ILK	RNAi (feeding)
F09E5.1	*pkc-3*	PKC	RNAi (feeding)
F22D6.5	*prp-4*	DYRK	RNAi (feeding) [b]
F23C8.8		MARK	RNAi (feeding)
F28B12.3	*vrk-1*	VRK	RNAi (feeding)
F35G12.3	*sel-5*	Nak	RNAi (feeding) [b]
F43C1.2	*mpk-1*	MAPK	RNAi (feeding) [b]
F49E11.1	*mbk-2*	DYRK	RNAi (feeding) *mbk-2(ne992)*
F55G1.8	*plk-3*	Polo-like	RNAi (feeding) [b]
F59E12.2	*zyg-1*	unique	RNAi (feeding) [b]
F59E12.3		uncharacterized	RNAi (feeding)
H25P06.2	*cdk-9*	CDK	RNAi (feeding)
H39E23.1	*par-1*	MARK	RNAi (feeding) *par-1(b274)* *par-1(e2012)* *par-1(it51)* *par-1(it60)* *par-1(zu310)*
K03E5.3	*cdk-2*	CDK	RNAi (feeding)
K04C1.5		uncharacterized	RNAi (feeding) [b]
K07C11.2	*air-1*	Aurora	RNAi (feeding)
R06C7.8	*bub-1*	Bub	RNAi (feeding)
R10D12.10		TTBKL	RNAi (feeding)
T01G9.6	*kin-10*	CK2	RNAi (feeding)
T05G5.3	*cdk-1*	CDK	RNAi (feeding)
T17E9.1	*kin-18*	MAP4K	RNAi (feeding)
T20F10.1		NDR	RNAi (feeding)
W06F12.1	*lit-1*	MAPK	RNAi (feeding)
W10G6.2	*sgk-1*	SGK	RNAi (feeding)
Y106G6E.6	*csnk-1*	CK1	RNAi (feeding)

TABLE 4 continued

WormBase ID	Gene Name	Kinase Family[a]	Method of Analysis
Y18D10A.5	*gsk-3*	GSK	RNAi (feeding)
Y39H10A.7	*chk-1*	CAMK	RNAi (feeding)
Y52D3.1		MAP4K	RNAi (feeding) [b]
Y53C12A.1	*wee-1.3*	WEE	RNAi (feeding)
Y54E10BL.6	*mek-2*	MAPKK	RNAi (feeding)
Y59A8B.14	*par-4*	LKB1	*par-4(it33)* *par-4(it47ts)* *par-4(it75)*
Y71F9B.7	*plk-2*	Polo-like	RNAi (feeding)

[a] Kinase family classification taken from Manning (Manning, 2005)
[b] No phenotype observed by RNAi(feeding)

TABLE 5: Changes in MEX-5 expression levels in 1-cell embryos

	Pixel intensity[a]	
Stage	**Anterior**	**Posterior**
Newly-fertilized[b]	97.3±18.1 (n=6)	100.5±17.7 (n=6)
1-cell[c]	210.4±12.8 (n=4)	39.7±6.8 (n=4)

[a] Values represent the average pixel intensities ±standard deviation and sample size *(n)*.

[b] Newly-fertilized embryos were measured at the time when the male and female pronuclei were just visible by DAPI staining.

[c] 1-cell embryos were measured when the male and female pronuclei fused to form a single zygotic nucleus.

Discussion

In this study, I have demonstrated that phosphorylation of the CCCH zinc finger protein MEX-5 at Ser458 is critical for its asymmetry in 1-cell embryos. This phosphorylation occurs prior to fertilization and requires the activity of two Ser/Thr kinases, PAR-1 and PAR-4. These results provide the first evidence that MEX-5 is a target of at least two PAR proteins, and also provide the first known report of a role for PAR-1 and PAR-4 in development of the germline. While MEX-5 asymmetry is critical in embryos for exclusion of germline proteins from the anterior, this asymmetry is actually set up prior to fertilization with the phosphorylation of MEX-5 by PAR-1 and PAR-4 (Figure 13). I propose that the coordinate activities of PAR-1 and PAR-4 are necessary to prime MEX-5 to quickly respond to events that polarize the embryo following fertilization.

MEX-5 asymmetry is controlled by multiple processes

MEX-5 and MEX-6 are members of a *C. elegans* CCCH zinc finger family that includes the germline proteins PIE-1, POS-1 and MEX-1 (Guedes and Priess, 1997; Tabara et al., 1999; Reese et al., 2000; Schubert et al., 2000). Previous experiments suggested that the asymmetric expression of these proteins is regulated by two distinct pathways: one pathway that localizes these proteins to their respective poles in 1-cell embryos, and a second pathway that degrades these proteins in somatic blastomeres (Reese et al., 2000; Schubert et al., 2000; Cuenca et al., 2003; DeRenzo et al., 2003). The zinc finger domains of each of these proteins are necessary for their degradation in

somatic blastomeres after the 1-cell stage (DeRenzo et al., 2003), but the mechanisms that result in asymmetry in 1-cell embryos are unclear.

This study expands on these previous observations by identifying a MEX-5 domain that is uniquely required for MEX-5 asymmetry in 1-cell embryos. Mutation of the MEX-5 Ser458 to Ala significantly reduced MEX-5 asymmetry at the 1-cell stage, but did not prevent degradation of MEX-5 in somatic blastomeres. Conversely, mutation of the Cys residues in the ZF2 domain did not prevent anterior localization of MEX-5 in 1-cell embryos, but did prevent later MEX-5 degradation. These results demonstrate that at least two distinct processes control MEX-5 asymmetry in early embryos, one of which requires ubiquitin-mediated proteolysis. Three general processes may result in MEX-5 asymmetry in 1-cell embryos: restricted translation, targeted transport, and localized degradation. As I discuss below, none of these processes are mutually exclusive, and it is likely that the embryo utilizes several processes concurrently to ensure that MEX-5 expression is restricted to the anterior.

In examination of transgenic strains expressing GFP:MEX-5 fusion proteins, I observed significant increases in the expression of GFP:MEX-5 throughout 1-cell embryos, compared to oocytes and newly-fertilized embryos. These increases were observed prior to the appearance of MEX-5 asymmetry, suggesting that MEX-5 levels are regulated in part by *de novo* translation. Because maternal *mex-5* mRNA is distributed uniformly in 1-cell embryos, translation must occur either through interactions with asymmetrically-localized translational regulators, or through global translation followed by localized recruitment of translated proteins. During *Drosophila* oogenesis, the expression of several maternal proteins, including Bicoid, Nanos and

Oskar, is regulated by restricted translation (Johnstone and Lasko, 2001). In *C. elegans,* no examples of restricted translation have been described for 1-cell embryos. However, translational regulation has been observed for several proteins after the 1-cell stage, including the Notch-like receptor GLP-1. Asymmetric expression of GLP-1 is initiated at the 2-cell stage; this expression is regulated through the 3'UTR of *glp-1* (Evans et al., 1994; Ogura et al., 2003). SPN-4, a RNP-like RNA binding protein, promotes GLP-1 translation in anterior blastomeres, while the CCCH protein POS-1 represses GLP-1 translation in posterior blastomeres (Ogura et al., 2003). Neither POS-1 nor SPN-4 are likely to regulate MEX-5 translation since *pos-1(-)* and *spn-4(-)* embryos show apparently normal MEX-5 localization (Gomes et al., 2001; Tenlen et al., 2006). Furthermore, the *mex-5* 3'UTR is unlikely to affect MEX-5 expression or localization after fertilization since these events were observed for GFP:MEX-5 fusion proteins under the control of either the *mex-5* or *pie-1* 3'UTR.

Directed transport of proteins is a common process in generating asymmetries. In *Drosophila* oocytes, cell fate determinants such as Oskar and Nanos are localized to the posterior pole by a microtubule-dependent mechanism (van Eeden and St Johnston, 1999) After fertilization of *C. elegans* oocytes, directed movement of cortical and cytoplasmic proteins results in the polarization of early embryos. Sperm entry initiates a flow of actomyosin cytoskeletal proteins away from the posterior pole and toward the anterior pole, resulting in the anterior accumulation of several proteins, including non-muscle myosin, catenins, cadherins, and at least two PAR proteins, PAR-3 and PAR-6 (Munro et al., 2004). This anterior cortical flow displaces cytoplasmic proteins toward the posterior, including germline-specific P granules (Gönczy and Rose, 2005). Since

MEX-5 asymmetry is established shortly after PAR asymmetry, it is possible that MEX-5 is also transported to the anterior by cortical flow. However, comparisons of the timing of GFP:MEX-5 anterior localization with that of non-muscle myosin (NMY-2:GFP) suggest that GFP:MEX-5 anterior localization is not concurrent with cortical flow and instead occurs shortly after. Alternatively, MEX-5 asymmetry may be the result of directed transport to the anterior, against the posteriorly-directed cytoplasmic flow. This transport would involve either binding to a carrier protein that translocates MEX-5 to the anterior, or "capture" of MEX-5 by an anteriorly-localized protein(s). While a candidate cytoplasmic carrier protein has yet to be identified, the anterior PAR proteins PAR-3, PAR-6 and PKC-3 are goods candidates for capturing MEX-5 in the anterior. Both PAR-3 and PAR-6 are PDZ domain proteins and have been shown to be involved in protein-protein interactions in multiple systems, while PKC-3 is an atypical protein kinase (Suzuki and Ohno, 2006). The PAR-3/PAR-6/PKC-3 complex may act directly to bind and stabilize MEX-5 in the anterior, or may recruit another protein to the anterior that interacts with MEX-5.

MEX-5 asymmetry may be alternatively explained by a combination of the mechanisms described above with localized protein degradation. Protein degradation has emerged as an important mechanism to prevent inappropriate protein expression and to ensure the timely progression of developmental events (DeRenzo and Seydoux, 2004; Bowerman and Kurz, 2006). For example, in *C. elegans*, P granules are transported to the posterior pole by cytoplasmic flow, and any remaining P granules in the anterior are rapidly degraded, ensuring the restriction of these complexes to the germline (Hird et al., 1996; Cheeks et al., 2004). In *Drosophila*, *oskar* mRNA is

transported to the posterior by microtubule-dependent processes, where it is translated and stabilized. Any mRNA or protein present in the anterior is degraded (Riechmann et al., 2002).

Multiple E3 ubiquitin ligase complexes have been identified in *C. elegans*, each with different substrate specificities (DeRenzo and Seydoux, 2004). The Hect E3 ubiquitin ligase EEL-1 targets SKN-1 for degradation after the 8-cell stage, but does not affect degradation of other proteins, including MEX-5 and the germline proteins (Page et al., 2007). A complex that includes the cullin CUL-2, elongin C homolog ELC-1 and SOCS box protein ZIF-1 targets MEX-5 and other CCCH proteins for degradation in somatic blastomeres. However, this complex is not likely to cause MEX-5 degradation at the 1-cell stage because neither mutating the MEX-5 ZF2 domain nor *zif-1*(RNAi) affected MEX-5 asymmetry in 1-cell embryos. A different complex that includes CUL-3 and the BTB domain protein MEL-26 targets the katanins MEI-1 and MEI-2 for degradation shortly after fertilization. However, I showed that loss of *cul-3* function does not affect MEX-5 asymmetry in 1-cell embryos. Depletion of other proteins involved in proteolysis likewise did not identify any components with a function in MEX-5 asymmetry. However, for many of these components, no phenotypes were observed following depletion by RNAi. It is possible that many of these proteins are refractive to RNAi, or have redundant function (Takahashi et al., 2002). To this end, recent work has shown that the cullins CUL-2 and CUL-5 have overlapping activities in oocyte maturation and progression through meiosis. Neither *cul-2(-)* or *cul-5(-)* animals showed defects in oocyte maturation or fertilization, but many *cul-2(-);cul-5(-)* double-mutant animals were sterile. However, *cul-5(-)* animals with weak loss of function of

cul-2 did produce embryos that progressed beyond the first cell cycle but failed to hatch (Sasagawa et al., 2007). Since these embryos progressed beyond the first mitosis, it would be interesting to examine MEX-5 expression for possible mislocalization.

Intriguing potential regulators of MEX-5 proteolysis are the posteriorly-localized PAR proteins, PAR-1 (discussed below) and PAR-2. As with the other PAR proteins, PAR-2 restricts MEX-5 to the anterior, as MEX-5 expression extends more posteriorly in *par-2(-)* 1-cell embryos (Cuenca et al., 2003). PAR-2 is a RING finger protein, as are several components of E3 ubiquitin ligase complexes, including RBX-1 (Kipreos, 2005). Based on this homology, it has been proposed that PAR-2 is a putative E3 ubiquitin ligase (Suzuki and Ohno, 2006). It is possible that PAR-2 could act to recruit other proteasome components to the posterior cortex through interactions with its RING finger domain. Interestingly, the RING finger domain may be necessary for PAR-2 protein stability, as expression of GFP:PAR-2 fusion proteins was significantly higher when the RING finger domain was deleted compared to the full-length GFP:PAR-2 protein (Hao et al., 2006). Loss of function of *cul-2* results in ectopic cortical localization of PAR-2 in some 1-cell embryos, suggesting that CUL-2 is necessary to maintain anterior-posterior domains in the early embryos, perhaps through direct interactions with PAR-2 (Liu et al., 2004; Sonneville and Gonczy, 2004). However, no direct association between PAR-2 and proteasome components has yet been described.

While the details remain to be elucidated, embryonic MEX-5 expression appears to be translationally upregulated, and translation may be coupled with directed transport, posterior degradation or both to generate MEX-5 asymmetry. The analysis of

photoactivated or photoconvertible GFP:MEX-5 fusion proteins would provide a helpful tool in understanding the dynamics of MEX-5 localization, particularly in the role of directed transport or degradation.

PAR-1 has multiple roles in MEX-5 asymmetry

Epistasis analysis demonstrated that *mex-5* functions downstream of each of the *par* genes, as well as *nmy-2* and *pkc-3* (Schubert et al., 2000; Cuenca et al., 2003). *par-1* appears to act most immediately upstream of *mex-5* since *par-1* mutant embryos show no defects in localization of any other *par* gene (Schubert et al., 2000). Since *par-1*, *par-4* and *pkc-3* encode predicted Ser/Thr kinases (Guo and Kemphues, 1995; Tabuse et al., 1998; Watts et al., 2000), these kinases were considered likely candidates to regulate phosphorylation of MEX-5 at Ser458. Indeed, I identified PAR-1 and PAR-4 as uniquely required for MEX-5 phosphorylation.

From this work and others, at least two roles for PAR-1 in regulating MEX-5 asymmetry have been identified. First, PAR-1 is required to phosphorylate MEX-5 in the maternal germline. This activity occurs at the onset of MEX-5 translation in the distal arm of the gonad, as germ cells exit arrest at the pachytene stage of meiotic prophase, and enter oogenesis. Although previous studies demonstrated that PAR-1 was expressed in the maternal germline, no activity for PAR-1 prior to fertilization has been described (Guo and Kemphues, 1995). It is not known whether MEX-5 phosphorylation is required in the germline, or if phosphorylation after fertilization would result in the same MEX-5 asymmetry. To address this question, it would be useful to identify temperature-sensitive alleles of *par-1* that affect its kinase activity. In

addition to defects in MEX-5 phosphorylation, *par-1(RNAi)*-treated animals also show defects in development of the maternal germline, as germ cells appear to prematurely cellularize and the production of fertilized embryos eventually ceases (data not shown). Similar defects are also seen in *par-1(it60)*, a putative null allele that produces fewer embryos than other *par-1* mutant alleles. Since *mex-5(-);mex-6(-)* double-mutant hermaphrodites have apparently normal germlines, these observations raise the possibility that PAR-1 may have additional targets in the germline.

A second function for PAR-1 was revealed from *par-1* mutant alleles in which MEX-5 phosphorylation occurred at wild-type levels, but no asymmetry was observed in 1-cell embryos. These results confirmed earlier observations that PAR-1 kinase activity was not sufficient for MEX-5 asymmetry, since both PAR-1 and MEX-5 are expressed uniformly in *par-3* mutant embryos (Etemad-Moghadam et al., 1995; Schubert et al., 2000). After the 1-cell stage, PAR-1 activity is required to stabilize multiple proteins in the posterior, including the germline proteins PIE-1, POS-1 and MEX-1 (DeRenzo and Seydoux, 2004), and P granules (Cheeks et al., 2004). In the absence of *par-1*, MEX-5 and MEX-6 are expressed uniformly in early embryos. MEX-5 and MEX-6 expression activates the ZIF-1-E3 ubiqutin ligase complex, leading to the degradation of the CCCH proteins. An analogous role for PAR-1 occurs in *Drosophila* oocytes, where PAR-1 stabilizes Oskar proteins in the posterior through phosphorylation (Riechmann et al., 2002). Oskar protein in the anterior is then targeted for degradation by an unknown mechanism. Therefore, PAR-1 may act in the posterior 1-cell embryos to antagonize MEX-5 and MEX-6 activity (Schubert et al., 2000; Cuenca et al., 2003).

Two models may explain the function of PAR-1 in restricting MEX-5 to the anterior. First, localization of PAR-1 to the posterior cortex, which requires the activity of the RING finger protein PAR-2, may destabilize MEX-5 in the posterior and result in its degradation (Cuenca et al., 2003). Support for this model comes from observations that MEX-5 activity is reduced in *par-3* mutant embryos (Cuenca et al., 2003). Since PAR-1 is mislocalized throughout *par-3(-)* embryos, this result implies negative regulation of MEX-5 by PAR-1 (Cuenca et al., 2003). While PAR-1 contains an ubiquitin-associated (UBA) domain, which is also found in other proteins involved in proteolysis (Hofmann and Bucher, 1996), none of the *par-1* alleles examined in this study have mutations within the UBA domain. Additionally, this model requires that the mechanisms that degrade MEX-5 in the posterior act specifically on MEX-5 and not on the germline proteins. In an alternative model, PAR-1 may activate another protein that is required to exclude MEX-5 from the posterior. In *Drosophila* and mammalian cells, PAR-1 acts with 14-3-3 proteins to phosphorylate PAR-3 homologs and exclude PAR-3 from the posterior of *Drosophila* oocytes and from the basal membranes of epithelial cells (Benton et al., 2002; Benton and St Johnston, 2003). Since the *C. elegans* 14-3-3 protein PAR-5 is also necessary for MEX-5 asymmetry (Morton et al., 2002; Cuenca et al., 2003), PAR-5 is a potential candidate to interact with PAR-1.

Based on interactions between PAR-1 and MEX-5 as described above, I suggest that MEX-5 is a direct substrate for PAR-1 kinase activity. First, in a screen of over 40 Ser/Thr kinases, only PAR-1 and PAR-4 had any effect on levels of MEX-5 phosphorylation in the maternal germline and embryos. Second, MEX-5 phosphorylation at Ser458 was completely abolished in mutants expressing a putative

kinase-dead PAR-1 protein; PAR-4 was not sufficient to initiate MEX-5 phosphorylation. Finally, *par-1* functions immediately upstream of *mex-5* in the establishment of anterior-posterior polarity; to date, no genes have been identified that act downstream of *par-1* in regulating MEX-5 asymmetry. However, a search of the MEX-5 protein sequence did not reveal any motifs known to be PAR-1 kinase target sites (Benton and St Johnston, 2003; Nishimura et al., 2004; Riechmann and Ephrussi, 2004; Ossipova et al., 2005). It is possible that PAR-1 does not phosphorylate MEX-5 directly, but instead activates another kinase that then phosphorylates MEX-5. Therefore, assessing the ability of PAR-1 to directly phosphorylate MEX-5 by in vitro kinase assays would be an important first step in understanding molecular pathway leading to MEX-5 phosphorylation.

PAR-4 kinase activity maintains, but does not initiate, MEX-5 phosphorylation

This study demonstrated that PAR-4 kinase activity is required in the *C. elegans* germline to maintain MEX-5 phosphorylation at Ser458. In *par-4* mutant gonads, levels of MEX-5(pS458) are initially high in young, more distal oocytes, but progressively decrease in more mature oocytes, and are undetectable in the most mature oocyte. This lack of phosphorylation is also observed in 1-cell embryos. This observation suggests that this decrease in staining with anti-MEX-5(pS458) is due to an increase in phosphatase activity in maturing oocytes. PAR-4 may protect MEX-5 from the activity of phosphatases either by directly phosphorylating MEX-5, or by inhibiting phosphatase activity. The decrease in levels of MEX-5 phosphorylation in *par-4* oocytes has striking similarities to an increase in levels of activated mitogen-activated

protein kinase (MAPK) in mature oocytes in response to sperm cues (Miller et al., 2001). The activation of MAPK in these oocytes is associated with changes in activities of other proteins (Leacock and Reinke, 2006). For example, up-regulation of protein phosphatases may result in dephosphorylation of MEX-5 in the absence of PAR-4 activity. Depletion of phosphatases with known activities in the gonad, including LIP-1 and PAA-1 (Hajnal and Berset, 2002; Kamath et al., 2003) did not restore MEX-5(pS458) levels in proximal oocytes of *par-4* mutants (data not shown). However, in several experiments, the combined depletion of PAR-4 and a phosphatase resulted in severely defective gonads, precluding analysis of MEX-5 phosphorylation. Analysis of MAPK pathway components in *par-4* mutants would address the role of activated MAPK on MEX-5 phosphorylation.

PAR-4 expression in the gonad shows an abrupt transition from localization at actin-rich boundaries between germ cells in the distal arm of the gonad, to primarily cytoplasmic localization in maturing oocytes (Watts et al., 2000) (this study). This change in PAR-4 localization suggests that cytoplasmic expression of PAR-4 is necessary for its role in maintaining MEX-5 phosphorylation, and may explain why PAR-4 is insufficient to initiate MEX-5 phosphorylation at the transition from germ cells to oocytes. Alternatively, PAR-1 kinase activity may be necessary for PAR-4 activation and/or relocalization (see below).

PAR-4 homologs, including XEEK1 (*Xenopus*) and LKB1 (*Drosophila* and mammals), have conserved roles in cell polarity and signal transduction (Su et al., 1996; Hemminiki et al., 1998; Jenne et al., 1998; Martin and St Johnston, 2003). Mutations in the human *lkb1* locus cause Peutz-Jeghers syndrome, leading to a predisposition to

tumorigenesis, possibly as the result of a loss of cell polarity (Hemminiki et al., 1998; Jenne et al., 1998; Baas et al., 2004; Forcet et al., 2005). In mammalian cells, the pseudokinase STRAD and mouse protein 25 (MO25) are obligate co-factors of LKB1 activity (Baas et al., 2003). STRAD is required to induce LKB1 activation, resulting in actin cytoskeleton reorganization and the formation of brush borders and cell-cell junctions (Baas et al., 2004). *C. elegans* has one homolog of STRAD, Y52D3.1 (WormBase), but no obvious homologs of MO25. The protein encoded by the Y52D3.1 locus has yet to be characterized, and depletion of Y52D3.1 by RNAi in wild-type animals had no obvious effect on embryo development (WormBase). However, Y52D3.1(RNAi) in *par-4* mutant animals may uncover potential interactions between PAR-4 and this STRAD homolog. LKB1 is also required to activate multiple components of the Wnt/β-catenin signaling pathway, including GSK-3β kinase. Loss of function mutations in *lkb1* result in a decrease in phosphorylation of β-catenin in both *Xenopus laevis* and human cell culture (Ossipova et al., 2003; Lin-Marq et al., 2005). Loss of function of GSK-3 in early *C. elegans* embryos does not affect MEX-5 asymmetry or phosphorylation (this study), but is required for degradation of OMA-1 and OMA-2 in the transition from oogenesis to embryogenesis (Nishi and Lin, 2005; Shirayama et al., 2006; Stitzel et al., 2006). LKB1 has been shown to phosphorylate target proteins at two unique motifs, matching the consensus sequence LxT and CGSPxY (Spicer et al., 2003). The MEX-5 C-terminal domain has a single LxT motif (LST, amino acids 452-454). However, substitution of Thr454 with Ala had no effect on GFP:MEX-5 asymmetry in early embryos.

One question from these studies is whether the mechanisms that maintain MEX-5 phosphorylation in the germline are also used in the early embryo. Is PAR-4 necessary for this maintenance in 1-cell embryos? Or is MEX-5 protected from phosphatase activity through interactions with proteins in the anterior of each germ cell precursor? Analysis of the temperature-sensitive allele *par-4(it47)* may address this question by identifying when PAR-4 activity is critical for MEX-5 asymmetry. Additionally, identification of mutations in *par-4* that occur outside kinase domain may shed light on such a function.

Do PAR-1 and PAR-4 regulate each other's activities in *C. elegans*?

The relationship between PAR-1 and PAR-4 in other organisms is somewhat controversial. In *Drosophila*, genetic data and kinase assays demonstrated that PAR-1 phosphorylates and activates the *Drosophila* PAR-4 homolog, LKB1, but LKB1 does not directly phosphorylate or activate PAR-1 (Martin and St Johnston, 2003). Conversely, experiments in mouse models and human cell culture lines demonstrated that LKB1 directly phosphorylates Par1/MARK at conserved motifs (Spicer et al., 2003; Woods et al., 2003; Lizcano et al., 2004). In *C. elegans*, PAR-1 and PAR-4 have similar phenotypes, but do not appear to be fully redundant, since PAR-4 is unable to initially phosphorylate MEX-5 in the absence of PAR-1 kinase activity, nor is PAR-1 able to maintain MEX-5 phosphorylation in the absence of PAR-4. Although *par-1* and *par-4* mutant embryos have similar phenotypes after the 1-cell stage, *par-4* mutant embryos have apparently normal spindle positioning at the 1-cell stage (Morton et al., 1992), suggesting that PAR-1 activity occurs prior to PAR-4 activity. In mammalian

cells, LKB1 was shown to phosphorylate the PAR-1 homolog PAR1A/MARK3 at the LxT and CGSPxY motifs (Spicer et al., 2003). The *C. elegans* PAR-1 protein (H39E23.1; WormBase) includes five LKB1 consensus phosphorylation sites: four sites that match the consensus LxT motif, and one CGSPPY motif. However, it is unknown whether PAR-4 is able to phosphorylate PAR-1 at these or other residues.

In some *par-4(it47ts)* mutant 2- and 4-cell embryos, there was a detectable increase in staining with anti-MEX-5(pS458) in the germline blastomere (data not shown). Since there are no apparent differences in PAR-1 protein localization in *par-4* mutant embryos as compared to wild-type (data not shown), it is possible that enrichment of PAR-1 in the germline blastomere results in *de novo* phosphorylation of MEX-5 protein. These observations suggest that PAR-1 retains some function in the absence of *par-4*. However, similar increases in anti-MEX-5(pS458) staining were not observed in any of the *par-1* alleles, suggesting that either PAR-4 is inactive in these alleles, or that PAR-4 kinase activity is not sufficient to initiate phosphorylation of MEX-5. PAR-4 expression appears to be unaffected in *par-1(b274)* mutant gonads and embryos (Watts et al., 2000), but it is unknown whether PAR-4 retains kinase activity in the absence of PAR-1 function. Results from this study support previous suggestions that *par-1* and *par-4* function in independent pathways, rather than as part of a linear pathway (Bowerman et al., 1997). However, it is possible that PAR-4 expression requires PAR-1 kinase activity, so *par-1(it51)* mutant embryos should also be stained for PAR-4.

Further evidence that PAR-1 and PAR-4 share some overlapping functions came from my observations of maternal germline defects in *par-1(RNAi)* and *par-4(it47ts)*

single mutant hermaphrodites. While oogenesis proceeded normally for the first 18 – 24 hours following entry into adulthood, after 24 hours, rounded cells, enclosed in a complete membrane, began to appear in both the distal and proximal gonad arms. Eventually, both *par-1(RNAi)* and *par-4(it47ts)* mutant animals ceased to make fertilized embryos, even though sperm was still detected in the spermatheca. In *par-1(RNAi);par-4(it47ts)* double-mutant embryos, this germline defect was observed much sooner following entry into adulthood – often within 8 hours, and brood sizes were much smaller. It is not know whether the rounded cells observed in the gonad are prematurely-cellularized oocytes, or if they express somatic cell fate markers, as was recently described in gonads depleted of both *gld-1* and *mex-3* (Ciosk et al., 2006). Analysis of *par-1(RNAi);par-4(it47ts)* double mutant gonads with the oocyte-specific markers MEX-3 and OMA-1 would resolve this question. No role for germline development has been previously described for PAR-1. Recently, PAR-4 was shown to be necessary for germline quiescence in metabolically-arrested (dauer) larvae. Loss of function of PAR-4 results in excess proliferation of germ cells; this function requires the activity of the AMPK homolog AAK-2 (Narbonne and Roy, 2006). It would be interesting to explore whether PAR-4 also regulates germ cell proliferation in adult gonads.

Kinase signaling pathways and cell fate specification

In recent years, kinase signaling has emerged as a major signal transduction pathway in establishment of anterior-posterior polarity and cell fate specification in multiple organisms (Brajenovic et al., 2004; Gotta, 2005). In *C. elegans*, kinases play

an integral role in the progression through each stage of early embryo development. Oocyte maturation and competence for fertilization requires the mitogen-activated protein kinase (MAPK) pathway, which is activated in response to signals from sperm (Miller et al., 2001). Following fertilization, exit from meiosis and entry into mitosis requires both minibrain kinase (MBK-2) and glycogen synthase kinase 3 (GSK-3) (Pellettieri et al., 2003; Nishi and Lin, 2005; Shirayama et al., 2006; Stitzel et al., 2006). The maintenance of anterior-posterior polarity requires in part the exclusion of PAR-2 from the anterior cortex by phosphorylation by PKC-3 (Hao et al., 2006). My research suggests that MEX-5 is the first known downstream target of any of the PAR kinases in *C. elegans* 1-cell embryos, and provides insight into how polarity information from the PAR proteins is transduced into somatic and germline fate decisions. Since both MEX-5 and MBK-2 are necessary to restrict germline proteins such as PIE-1 to the posterior (Schubert et al., 2000; Pellettieri et al., 2003), these results suggest that at least two independent kinase signaling cascades are necessary for the asymmetry of germline proteins. Finally, the phosphorylation of MEX-5 during oogenesis raises the possibility that MEX-5 plays another, undescribed role in development of the maternal germline. It will be important to determine whether MEX-5 is an *in vivo* substrate of PAR-1 and/or PAR-4 kinase activity, and to understand how MEX-5 phosphorylation leads to its asymmetry.

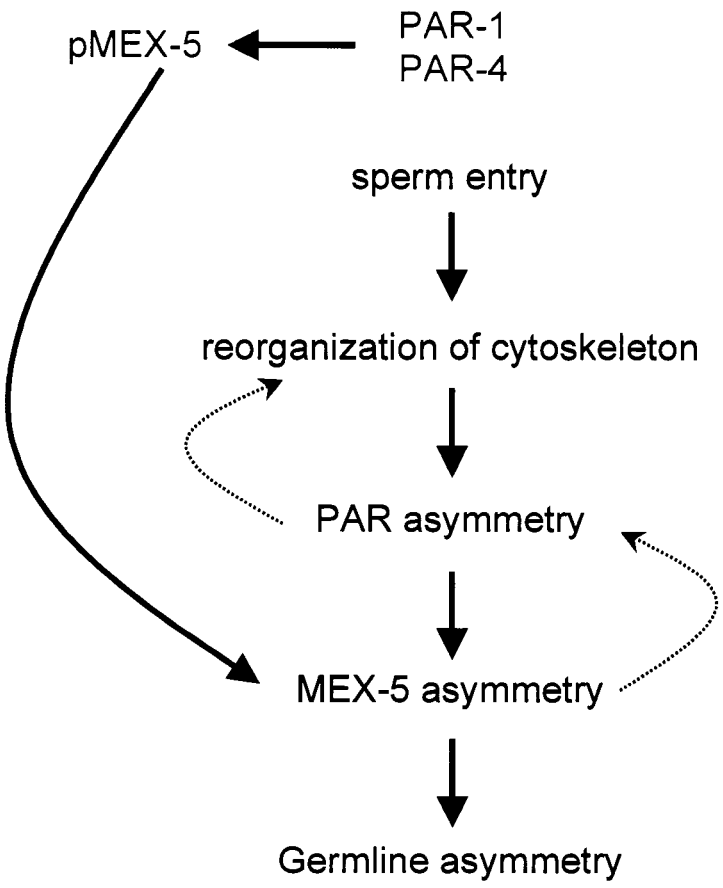

Figure 13. Revised model for establishment of germline asymmetry in 1-cell embryos. Phosphorylation of MEX-5 at Ser458 by PAR-1 and/or PAR-4 occurs in the gonad prior to fertilization, and is required for MEX-5 asymmetry in 1-cell embryos.

Conclusions and Future Direction

The CCCH zinc finger proteins MEX-5 and MEX-6 are necessary for the proper localization of cell fate regulators, including germline proteins, in early *C. elegans* development. However, while MEX-5 was shown to act downstream of the PAR polarity proteins in 1-cell embryos, the mechanisms resulting in MEX-5 asymmetry are unknown. In this study, I describe several findings that indicate that MEX-5 asymmetry requires phosphorylation by two Ser/Thr kinases, PAR-1 and PAR-4. First, I identified two regions within MEX-5 that are necessary for its asymmetry: a region between amino acids 199 and 270 N-terminal to the ZF1 domain, and the C-terminal 22 amino acids. This C-terminal domain includes six Ser and Thr sites that are conserved in MEX-6 and two MEX-5 orthologs. I demonstrated that MEX-5 is a phosphoprotein, and that phosphorylation at Ser458 is necessary for MEX-5 asymmetry in 1-cell embryos. Using an antiserum against MEX-5 phosphorylated at Ser458 [MEX-5(pS458)] I demonstrated that MEX-5 is phosphorylated in the gonad when MEX-5 expression is first detected in young oocytes, and is maintained in all oocytes. A screen of predicted Ser/Thr kinases identified two kinases, PAR-1 and PAR-4, that affected levels of MEX-5 phosphorylation in the gonad. MEX-5 phosphorylation was undetectable in *par-1(it51)* embryos expressing a kinase-dead PAR-1 protein, although MEX-5 protein levels were similar to wild-type. In *par-4* mutant embryos expressing a kinase-dead PAR-4 protein, MEX-5 was phosphorylated at wild-type levels in the young oocytes, but levels progressively decreased in oocytes until it was undetectable in the most

mature oocytes. These results demonstrate that the Ser/Thr kinases PAR-1 and PAR-4 have multiple roles in MEX-5 asymmetry.

Phosphorylation of MEX-5 C-terminal domain

The identification of MEX-5 as a phosphoprotein raises several questions about phosphorylation in the C-terminal domain. My results show that the serine residue Ser458 is critical for MEX-5 asymmetry and is phosphorylated in vivo. For some phosphoproteins in other systems, negatively-charged amino acids such as Asp or Glu can mimic a consitutively phosphorylated Ser or Thr residue. However, substitution of Ser458 with either Asp or Glue did not result in MEX-5 asymmetry. Thus, proteins that interact with phospho-MEX-5 may require high-affinity binding to the Ser458 site, or MEX-5 asymmetry may require dynamic phosphorylation of Ser458 that is not apparent in my fixed and stained preparations of *C. elegans* gonads and embryos. For example, my finding that PAR-4 is required to maintain MEX-5 phosphorylation specifically in late oocytes suggests that dynamic events may occur in normal development.

Although GFP:MEX-5^{S458A} fusion protein lacked detectable asymmetry at the 1-cell stage in most embryos, weak asymmetry was detectable in a few embryos. It is possible that phosphorylation at Ser458 creates a recognition site for another protein that is necessary for MEX-5 asymmetry, and that substituting this Ser with Ala does not completely prevent recognition of this site. For example, surrounding residues may compensate for the loss of phosphorylation at Ser458, such as by serving as an alternate phosphate acceptor site. This possibility is supported by the observation that no asymmetry is detected in embryos expressing the GFP:MEX-5^{TSSTAA} fusion protein. To

determine the contribution of Ser and Thr sites to MEX-5 asymmetry, it will be of interest to map phosphorylated residues in the C-terminal domain by mass spectrometry (Garcia et al., 2005).

While my research shows that MEX-5 phosphorylation is dependent on PAR-1 and PAR-4 kinase activity, I have not yet been able to determine whether MEX-5 is phosphorylated directly by either kinase. Analysis of MEX-5 proteins purified from wild-type, *par-1(it51)* and *par-4(it47ts)* strains, as well as GFP:MEX-5^{S458A} fusion proteins purified from transgenic strains, would identify both primary and secondary phosphorylation sites. In particular, analysis of MEX-5 phosphorylation in *par-1* and *par-4* mutant backgrounds may identify potential motifs phosphorylated by PAR-1- and PAR-4-dependent kinase activities. Confirmation of the specificities of these motifs as PAR-1 or PAR-4 substrates would add novel motifs to the list of known recognition sites for these kinases in other organisms.

In addition to the MEX-5 C-terminal domain, I identified an N-terminal region from amino acids 199 to 270 that is important for MEX-5 asymmetry. It is not known which sequences within this region are necessary for this asymmetry. No obvious protein-interaction motifs are present in this region (ScanSite, http://scansite.mit.edu), and none of the Ser and Thr sites are predicted to be phosphorylated (NetPhos Server 2.0; (Blom et al., 1999)). Further deletion analysis of this region could be useful in identifying specific residues that are critical for asymmetry, and the domain itself could be used to screen for interacting proteins by the yeast two-hybrid system.

Generation of MEX-5 asymmetry in 1-cell embryos

Observations of protein localization by live GFP imaging has resulted in important insight into the process by which MEX-5 and other proteins are localized in early embryos (Reese et al., 2000; Cuenca et al., 2003; Cheeks et al., 2004; Munro et al., 2004). These previous experiments, in combination with this study, lead us to propose that MEX-5 asymmetry is achieved through a combination of any of three processes: directed transport, translation, and localized degradation. An important goal will be to understand the contribution of each process to the generation of MEX-5 asymmetry.

By examining MEX-5 asymmetry with respect to cellular behaviors at the 1-cell stage, I showed that most MEX-5 asymmetry occurs after anterior cortical flow. This result could mean that MEX-5 asymmetry is only indirectly dependent on cortical flow. It remains possible that a small fraction of MEX-5 localization is affected directly by flow. To better analyze possible relationship between cortical flow and MEX-5 localization, it would be useful to create transgenic strains expressing both MEX-5 and NMY-2, fused to different GFP variants (such as GFP:MEX-5 and RFP:NMY-2). Such strains could also be useful in genetic screens to identify other genes necessary for MEX-5 asymmetry. Performing either forward screens (by mutagenizing worm strains) or reverse screens (by feeding worms bacteria expressing dsRNA), 1-cell embryos can be analyzed directly for effects on GFP:MEX-5 localization. Since NMY-2 localization is necessary for MEX-5 asymmetry, the presence of RFP:NMY-2 in the strain would allow for discarding of mutants in which RFP:NMY-2 failed to localize to the anterior.

Visualization of MEX-5 localization using photoactivatable GFP reporter proteins would be very useful in understanding MEX-5 dynamics. In such experiments, a small region of the posterior pole of 1-cell embryos is irradiated with the appropriate excitation wavelength. These studies could provide important insight into the dynamics of MEX-5 asymmetry; translocation of the GFP signal from one region of the embryo to another would suggest a role for directed transport. Conversely, the disappearance of signal from an irradiated posterior region of the embryo could suggest a role for protein degradation. I attempted to perform these types of experiments with a photoactivated GFP reporter protein (PA-GFP) (Patterson and Lippincott-Schwartz, 2002), under the control of the *nmy-2* promoter and 3'UTR. However, I was unable to activate GFP fluorescence in 1-cell embryos, even though PA-GFP:MEX-5 fusion protein was detectable by immunostaining for GFP. I found that the level of protein expression in embryos was much lower than in gonads, where other groups have been able to activate PA-GFP fusion proteins successfully (J. Nance and E. Munro, unpublished). Because the *nmy-2* 3'UTR used to construct the fusion protein might influence translation levels, future experiments should explore replacing the 3'UTR with others that are known to promote embryonic expression. Alternatively, a photoconvertible form of GFP ("Kaede") was developed which converts from green to red fluorescence upon exposure to UV light (Ando et al., 2002). Compared to PA-GFP fusion proteins, which require activation with a laser at 413 nm, the Kaede GFP is visible under standard epifluorescence conditions. If the Kaede GFP reporter construct is capable of expression in the *C. elegans* germline, then it may facilitate selection of transgenic embryos expressing detectable levels of GFP fusion proteins in embryos.

mex-5 mRNA is made maternally, and is translated in oocytes prior to embryogenesis. If embryonic mRNA translation contributes to MEX-5 asymmetry, it may be possible to address this by inhibiting translation in the early embryo with the drug cycloheximide (Zdinak et al., 1997), or by depleting the function of translational regulators, such as IFG-1 and EFT-3 (Rhoads et al., 2006). Injection of cycloheximide into the oocytes of adults expressing GFP:MEX-5 should distinguish the dynamics of pre-existing MEX-5 protein from the behavior of MEX-5 translated in embryos.

PAR-1-mediated localization of MEX-5

I have shown that PAR-1 kinase activity is required for phosphorylation of Ser458 and for MEX-5 asymmetry, but that phosphorylation at Ser458 is not sufficient for the PAR-1-dependent localization of MEX-5 to the anterior. These results suggest that PAR-1 has additional, direct or indirect, effects on MEX-5 localization that do not involve Ser458. Identifying these additional roles will be crucial for a full understanding of the role of PAR-1 in MEX-5 asymmetry. MEX-5 is phosphorylated but not expressed asymmetrically in *par-1(b274), par-1(e2012)* and *par-1(it60)* mutant embryos. Identifying mutations in *par-1(b274), par-1(e2012)* and *par-1(it60)* genomic sequences may shed light on the role of PAR-1 in MEX-5 asymmetry; the residues altered by the mutations have not been determined, but are known not to occur in the kinase domain or C-terminal domain (Guo and Kemphues, 1995). PAR-1 includes a UBA domain, which is also found in E2 and E3 ubiquitin ligases, and may be important for interactions among proteins in the ubiquitin-mediated degradation pathway (Hofmann and Bucher, 1996). However, I did not identify any mutations within the

UBA domain of any of these *par-1* alleles. Other mutations may lead to the identification of domains necessary for cortical localization of PAR-1. The proteins encoded by *par-1(b274)* and *par-1(e2012)* alleles are expressed in 1-cell embryos, but fail to localize to the posterior cortex after fertilization.

A putative allele of *par-1* previously identified in our lab (Schubert, 2000) resembles the *par-1(b274)*, *par-1(e2012)* and *par-1(it60)* alleles in that MEX-5 is phosphorylated but symmetrically expressed in 1-cell embryos. This *par-1(zu310)* allele is temperature-sensitive, producing 100% inviable embryos at the restrictive temperature of 25°C. Further characterization of this allele, in particular determining the genetic lesion resulting in the Par phenotype, and examining the localization of the protein produced by this allele, may yield useful information on the role of PAR-1 in MEX-5 asymmetry. Determining the temperature-sensitive period of *zu310* could indicate when PAR-1 function is critical. These experiments may be most informative by combining the *zu310* allele with various GFP:MEX-5 fusion proteins to assess when PAR function is necessary for MEX-5 localization.

If a role for PAR-1 in MEX-5 destabilization is supported by analysis of the experiments described above, then it is possible that other members of the ubiquitin-mediated degradation pathway may also be necessary. I examined GFP:MEX-5 asymmetry in embryos depleted of proteasome subunits by RNAi, but in many of these experiments either no phenotype was observed, or embryos arrested prior to the transition from meiosis to the first mitotic division; MEX-5 asymmetry requires exit from meiosis, which is marked by the extrusion of a polar body near the anterior pole of the embryo, and the appearance of the male and female pronuclei. A possible approach

to resolve the role of degradation in MEX-5 asymmetry is the use of proteasome inhibitors, such as *clasto*-lactacystin β-lactone. These inhibitors are irreversible and were shown to act quickly in 1-cell embryos following delivery of inhibitors by laser-induced holes in the eggshell (Labbe et al., 2004). Maximal MEX-5 asymmetry occurs approximately 10 minutes after the appearance of the pronuclei, and before formation of the single zygotic nucleus (Cuenca et al., 2003) (my observations). Therefore, exposing embryos to proteasome inhibitors when the pronuclei first become visible might provide sufficient time for inhibition.

A more general approach to identifying potential regulators of MEX-5 asymmetry is through yeast two-hybrid screens, and mass spectrometry analysis of protein complexes purified by immunoprecipitation. For example, antiserum against GFP can be used to purify GFP:PAR-1-bound protein complexes, which may reveal candidate proteins involved in protein degradation or kinase signal transduction. Similar experiments can be performed to purify GFP:MEX-5-bound protein complexes from both wild-type and *par-1(-)* embryos. Differences in protein composition of complexes purified from these backgrounds may provide important clues to mechanisms that result in MEX-5 asymmetry. Similar comparisons should be made for proteins purified from complexes bound to GFP:MEX-5 and GFP:MEX-5^{S458A}.

PAR-4 and the maintenance of MEX-5 asymmetry

The observation of a progressive decrease in phosphorylation at Ser458 of MEX-5 in *par-4(it47ts)* mutants suggests a model in which PAR-4 may be required in oocytes to counter the effects of increased phosphatase activity on phosphorylated

MEX-5, either by directly phosphorylating MEX-5, or by indirectly inhibiting phosphatase activity. Activation of the MAPK signaling cascade in the proximal oocytes may trigger removal of phosphates from MEX-5, which is counteracted by PAR-4. To test this model, it will be important to analyze MEX-5 phosphorylation in *par-4* mutant gonads with non-activated MAPK. Depletion of sperm in old hermaphrodites results in the downregulation of activated MAPK (Miller et al., 2001). However, gonads from old *par-4* mutants that are depleted of sperm have defects in oogenesis, complicating analysis of MEX-5 phosphorylation. A mutation in the *fem-1* gene results in hermaphrodites that fail to make sperm, and instead produce only oocytes (Nelson et al., 1978; Doniach and Hodgkin, 1984). Prior to mating, these oocytes lack detectable levels of activated MAPK (Miller et al., 2001; Page et al., 2001). Therefore, if activated MAPK in mature oocytes is responsible for the decrease in MEX-5 phosphorylation in the *par-4* background, then MEX-5 phosphorylation should be restored in all oocytes in *fem-1;par-4* double mutant gonads. As a corollary experiment, examination of the effect of precocious activation of MAPK on phosphorylated MEX-5 would also be useful. A mutation in the *efl-1* gene results in activation of MAPK in young, more distal oocytes (Page et al., 2001). If MAPK activation is correlated with MEX-5 dephosphorylation, then *efl-1;par-4* double mutant gonads would be expected to have decreased levels of phosphorylated MEX-5 in more distal oocytes.

An unresolved question is whether PAR-4 has a role in maintaining MEX-5 phosphorylation in embryos. At no time during early embryo development do the levels of MEX-5(pS458) appear to be significantly different from MEX-5 levels. It is possible

that PAR-4 continues to protect MEX-5 phosphorylation after fertilization. Alternatively, MEX-5 may interact with a protein(s) in the anterior that protects Ser458 from the activity of phosphatases. To ask whether PAR-4 is required for this maintenance, MEX-5(pS458) levels should be examined in *par-1(b274);par-4(it47ts)* double mutant embryos. MEX-5(pS458) levels are symmetric in 1-cell *par-1(b274)* embryos, so any role for PAR-4 in the maintenance of phosphorylation should be apparent in a decrease in levels of MEX-5(pS458) compared to levels of MEX-5. Due to the roles of both PAR-1 and PAR-4 in germline development, it is a concern that few or no embryos would be produced by the double mutants, as was observed in *par-1(RNAi);par-4(it47ts)* double mutant hermaphrodites. However, since *par-1(b274)* single mutant animals do not have the same germline defects seen in *par-1(RNAi)*-treated animals, it is possible that *par-1(b274);par-4(it47ts)* double mutant animals would produce sufficient numbers of embryos for analysis.

The identification of other proteins that interact with PAR-4 in the germline, as activators or substrates, may yield more information on the role of PAR-4 in MEX-5 phosphorylation, and reveal other roles for PAR-4 in germline development. To this end, strains expressing GFP:PAR-4 can be used in experiments to purify PAR-4-interacting proteins by immunoprecipation with antibodies against GFP, and analyze complexed proteins by mass spectrometry. Alternatively, possible substrates of PAR-4 may be identified in yeast two-hybrid screens.

MEX-5, MEX-6 and localization of germline proteins

An unresolved question is the role of MEX-6 in cell fate specification. MEX-5 can substitute fully for MEX-6 activity, as null mutants for *mex-6* are viable. Conversely, MEX-6 cannot substitute for MEX-5 activity, as *mex-5* mutants are inviable and the phenotype of *mex-5;mex-6* double mutant embryos is more severe than *mex-5* single mutants. It is possible that MEX-6 and MEX-*5* identical functions, but that MEX-5 levels are insufficient for normal development. In support of this hypothesis, we recently demonstrated that the germline CCCH protein POS-1 suppressed the *mex-5* mutant phenotype, and that this suppression required *mex-6* function. We proposed a model in which POS-1 functions in part to restrict MEX-6 accumulation, possibly through translational regulation of the *mex-6* 3'UTR (Tenlen et al., 2006).

To test whether the *mex-5;mex-6* phenotype is due to protein levels or to a unique function for MEX-6, it would be useful to raise antibodies against MEX-6. While existing GFP:MEX-6 transgenic strains show similar localization patterns as MEX-5, our genetic experiments suggest that there may be subtle differences in the expression of endogenous MEX-6 not apparent with the GFP:MEX-6 fusion proteins (Tenlen et al., 2006). Furthermore, an antibody against MEX-6 would allow for comparisons of the levels of endogenous protein between MEX-5 and MEX-6 in wild-type, *mex-5* and *mex-6* mutant embryos.

To ask whether protein levels explain the differences in *mex-5* and *mex-5;mex-6* mutant embryos, transgenic strains should be created that express the MEX-6 coding sequence under the control of the *mex-5* promoter and 3'UTR. If MEX-5 and MEX-6

are truly redundant proteins, then the *mex-5*-driven GFP:MEX-6 fusion protein should be able to rescue the *mex-5* single mutant phenotype. Protein levels can be monitored by Western blot hybridization to ensure that expression from the transgene is at similar levels to rescuing GFP:MEX-5 transgenes.

In conclusion, the work of our lab and others has demonstrated the importance of the PAR polarity proteins in cell fate specification in early *C. elegans* embryos, and identified the CCCH zinc finger proteins MEX-5 and MEX-6 as key intermediates between the PAR proteins and downstream cell fate regulators. However, it was unclear whether MEX-5 and MEX-6 were direct or indirect targets of PAR activity, nor had the mechanisms leading to MEX-5 asymmetry in 1-cell embryos been described. In this study, I have identified MEX-5 as the first known target of the PAR proteins in the early *C. elegans* embryo. The discovery that MEX-5 phosphorylation is regulated by PAR-1 and PAR-4 in the gonad is the first published report of a role for any of the *C. elegans* PAR proteins in setting up anterior-posterior polarity prior to fertilization. Given the importance of the PAR proteins in polarization of many cell types across metazoans, this study uncovers new roles for the Ser/Thr kinases PAR-1 and PAR-4 in cell polarity, and enhances our understanding of the signaling pathways regulated by the PARs.

Bibliography

Ando, R., Hama, H., Yamamoto-Hino, M., Mizuno, H. and Miyawaki, A. (2002). An optical marker based on the UV-induced green-to-red photoconversion of a fluorescent protein. *Proc Natl Acad Sci U S A* **99**, 12651-6.

Baas, A. F., Boudeau, J., Sapkota, G. P., Smit, L., Medema, R., Morrice, N. A., Alessi, D. R. and Clevers, H. C. (2003). Activation of the tumour suppressor kinase LKB1 by the STE20-like pseudokinase STRAD. *Embo J* **22**, 3062-72.

Baas, A. F., Kuipers, J., van der Wel, N. N., Batlle, E., Koerten, H. K., Peters, P. J. and Clevers, H. C. (2004). Complete polarization of single intestinal epithelial cells upon activation of LKB1 by STRAD. *Cell* **116**, 457-66.

Benton, R., Palacios, I. M. and St Johnston, D. (2002). Drosophila 14-3-3/PAR-5 is an essential mediator of PAR-1 function in axis formation. *Dev Cell* **3**, 659-71.

Benton, R. and St Johnston, D. (2003). Drosophila PAR-1 and 14-3-3 inhibit Bazooka/PAR-3 to establish complementary cortical domains in polarized cells. *Cell* **115**, 691-704.

Betschinger, J., Mechtier, K. and Knoblich, J. A. (2003). The Par complex directs asymmetric cell division by phosphorylating the cytoskeletal protein Lgl. *Nature* **422**, 326-330.

Blom, N., Gammeltoft, S. and Brunak, S. (1999). Sequence and structure-based prediction of eukaryotic protein phosphorylation sites. *J Mol Biol* **294**, 1351-1362.

Bowerman, B., Draper, B. W., Mello, C. C. and Priess, J. R. (1993). The maternal gene *skn-1* encodes a protein that is distributed unequally in early *C. elegans* embryos. *Cell* **74**, 443-52.

Bowerman, B., Eaton, B. A. and Priess, J. R. (1992). *skn-1*, a maternally expressed gene required to specify the fate of ventral blastomeres in the early *C. elegans* embryo. *Cell* **68**, 1061-75.

Bowerman, B., Ingram, M. K. and Hunter, C. P. (1997). The maternal *par* genes and the segregation of cell fate specification activities in early *Caenorhabditis elegans* embryos. *Development* **124**, 3815-26.

Bowerman, B. and Kurz, T. (2006). Degrade to create: developmental requirements for ubiquitin-mediated proteolysis during early *C. elegans* embryogenesis. *Development* **133**, 773-84.

Boyd, L., Guo, S., Levitan, D., Stinchcomb, D. T. and Kemphues, K. J. (1996). PAR-2 is asymmetrically distributed and promotes association of P granules and PAR-1 with the cortex in *C. elegans* embryos. *Development* **122**, 3075-84.

Brajenovic, M., Joberty, G., Kuster, B., Bouwmeester, T. and Drewes, G. (2004). Comprehensive proteomic analysis of human Par protein complexes reveals an interconnected protein network. *J Biol Chem* **279**, 12804-11.

Brenner, S. (1974). The genetics of *Caenorhabditis elegans*. *Genetics* **77**, 71-94.

Carballo, E., Lai, W. S. and Blackshear, P. J. (1998). Feedback inhibition of macrophage tumor necrosis factor-alpha production by tristetraprolin. *Science* **281**, 1001-5.

Cheeks, R. J., Canman, J. C., Gabriel, W. N., Meyer, N., Strome, S. and Goldstein, B. (2004). *C. elegans* PAR proteins function by mobilizing and stabilizing asymmetrically localized protein complexes. *Curr Biol* **14**, 851-62.

Ciosk, R., DePalma, M. and Priess, J. R. (2006). Translational regulators maintain totipotency in the *Caenorhabditis elegans* germline. *Science* **311**, 851-3.

Cowan, C. R. and Hyman, A. A. (2004). ASYMMETRIC CELL DIVISION IN C. ELEGANS: Cortical Polarity and Spindle Positioning. *Annu Rev Cell Dev Biol* **20**, 427-53.

Cox, D. N., Chao, A., Baker, J., Chang, L., Qiao, D. and Lin, H. (1998). A novel class of evolutionarily conserved genes defined by piwi are essential for stem cell self-renewal. *Genes Dev* **12**, 3715-27.

Cuenca, A. A., Schetter, A., Aceto, D., Kemphues, K. and Seydoux, G. (2003). Polarization of the *C. elegans* zygote proceeds via distinct establishment and maintenance phases. *Development* **130**, 1255-65.

DeRenzo, C., Reese, K. J. and Seydoux, G. (2003). Exclusion of germ plasm proteins from somatic lineages by cullin-dependent degradation. *Nature* **424**, 685-9.

DeRenzo, C. and Seydoux, G. (2004). A clean start: degradation of maternal proteins at the ooctye-to-embryo transition. *Trends Cell Biol* **14**, 420-426.

Doniach, T. and Hodgkin, J. (1984). A sex-determining gene, *fem-1*, required for both male and hermaphrodite development in *Caenorhabditis elegans*. *Dev Biol* **106**, 223-35.

Draper, B. W., Mello, C. C., Bowerman, B., Hardin, J. and Priess, J. R. (1996). MEX-3 is a KH domain protein that regulates blastomere identity in early *C. elegans* embryos. *Cell* **87**, 205-16.

Duncan, F. E., Moss, S. B., Schultz, R. M. and Williams, C. J. (2005). PAR-3 defines a central subdomain of the cortical actin cap in mouse eggs. *Dev Biol* **280**, 38-47.

Ephrussi, A. and Lehmann, R. (1992). Induction of germ cell formation by *oskar*. *Nature* **358**, 387-392.

Etemad-Moghadam, B., Guo, S. and Kemphues, K. J. (1995). Asymmetrically distributed PAR-3 protein contributes to cell polarity and spindle alignment in early *C. elegans* embryos. *Cell* **83**, 743-52.

Evans, T. C., Crittenden, S. L., Kodoyianni, V. and Kimble, J. (1994). Translational control of maternal *glp-1* mRNA establishes an asymmetry in the *C. elegans* embryo. *Cell* **77**, 183-94.

Forcet, C., Etienne-Manneville, S., Gaude, H., Fournier, L., Debilly, S., Salmi, M., Baas, A., Olschwang, S., Clevers, H. and Billaud, M. (2005). Functional analysis of Peutz-Jeghers mutations reveals that the LKB1 C-terminal region exerts a crucial role in regulating both the AMPK pathway and the cell polarity. *Human Molecular Genetics* **14**, 1283-1292.

Garcia, B. A., Shabanowitz, J. and Hunt, D. F. (2005). Analysis of protein phosphorylation by mass spectrometry. *Methods* **35**, 256-64.

Goldstein, B. and Hird, S. N. (1996). Specification of the anteroposterior axis in Caenorhabditis elegans. *Development* **122**, 1467-74.

Gomes, J. E., Encalada, S. E., Swan, K. A., Shelton, C. A., Carter, J. C. and Bowerman, B. (2001). The maternal gene *spn-4* encodes a predicted RRM protein required for mitotic spindle orientation and cell fate patterning in early *C. elegans* embryos. *Development* **128**, 4301-14.

Gotta, M. (2005). At the heart of cell polarity and the cytoskeleton. *Dev Cell* **8**, 629-33.

Gruidl, M. E., Smith, P. A., Kuznicki, K. A., McCrone, J. S., Kirchner, J., Roussell, D. L., Strome, S. and Bennett, K. L. (1996). Multiple potential germ-line helicases are components of the germ-line-specific P granules of Caenorhabditis elegans. *Proc Natl Acad Sci U S A* **93**, 13837-42.

Guedes, S. and Priess, J. R. (1997). The *C. elegans* MEX-1 protein is present in germline blastomeres and is a P granule component. *Development* **124**, 731-9.

Guo, S. and Kemphues, K. J. (1995). *par-1*, a gene required for establishing polarity in *C. elegans* embryos, encodes a putative Ser/Thr kinase that is asymmetrically distributed. *Cell* **81**, 611-20.

Guo, S. and Kemphues, K. J. (1996). A non-muscle myosin required for embryonic polarity in *Caenorhabditis elegans*. *Nature* **382**, 455-8.

Gönczy, P. and Rose, L. S. (2005). Asymmetric cell division and axis formation in the embryo. In *WormBook* (ed. The *C. elegans* Research Community). doi/10.1895/wormbook.1.30.1, http://www.wormbook.org.

Hajnal, A. and Berset, T. (2002). The *C.elegans* MAPK phosphatase LIP-1 is required for the G(2)/M meiotic arrest of developing oocytes. *Embo J* **21**, 4317-26.

Hamill, D. R., Severson, A. F., Carter, J. C. and Bowerman, B. (2002). Centrosome maturation and mitotic spindle assembly in *C. elegans* require SPD-5, a protein with multiple coiled-coil domains. *Dev Cell* **3**, 673-84.

Hao, Y., Boyd, L. and Seydoux, G. (2006). Stabilization of cell polarity by the *C. elegans* RING protein PAR-2. *Dev Cell* **10**, 199-208.

Hemminiki, A., Markie, D., Tomlinson, I., Avizienyte, E., Roth, S., Loukola, A., Bignell, G., Warren, W., Aminoff, M., Höglund, P. et al. (1998). A serine/threonine kinase gene defective in Peutz-Jeghers syndrome. *Nature* **391**, 184-187.

Hird, S. N., Paulsen, J. E. and Strome, S. (1996). Segregation of germ granules in living *Caenorhabditis elegans* embryos: cell-type-specific mechanisms for cytoplasmic localisation. *Development* **122**, 1303-12.

Hird, S. N. and White, J. G. (1993). Cortical and cytoplasmic flow polarity in early embryonic cells of Caenorhabditis elegans. *J Cell Biol* **121**, 1343-55.

Hobert, O. (2002). PCR fusion-based approach to create reporter gene constructs for expression analysis in transgenic *C. elegans*. *Biotechniques* **32**, 728-30.

Hodgkin, J. (1997). Genetics. In *C. elegans II*, (ed. D. L. Riddle T. Blumenthal B. J. Meyer and J. R. Priess). Plainview, NY: Cold Spring Harbor Laboratory Press.

Hofmann, K. and Bucher, P. (1996). The UBA domain: a sequence motif present in multiple enzyme classes of the ubiquitination pathway. *Trends Biochem Sci* **21**, 172-173.

Hung, T. J. and Kemphues, K. J. (1999). PAR-6 is a conserved PDZ domain-containing protein that colocalizes with PAR-3 in *Caenorhabditis elegans* embryos. *Development* **126**, 127-35.

Hunter, C. P. and Kenyon, C. (1996). Spatial and temporal controls target *pal-1* blastomere-specification activity to a single blastomere lineage in *C. elegans* embryos. *Cell* **87**, 217-226.

Jenkins, N., Saam, J. R. and Mango, S. E. (2006). CYK-4/GAP provides a localized cue to initiate anteroposterior polarity upon fertilization. *Science* **313**, 1298-301.

Jenne, D. E., Reimann, H., Nezu, J., Friedel, W., Loff, S., Jeschke, R., Muller, O., Back, W. and Zimmer, M. (1998). Peutz-Jeghers syndrome is caused by mutations in a novel serine threonine kinase. *Nat Genet* **18**, 38-43.

Johnstone, O. and Lasko, P. (2001). Translational regulation and RNA localization in *Drosophila* oocytes and embryos. *Annual Review of Genetics* **35**, 365-406.

Kamath, R. S., Fraser, A. G., Dong, Y., Poulin, G., Durbin, R., Gotta, M., Kanapin, A., Le Bot, N., Moreno, S., Sohrmann, M. et al. (2003). Systematic functional analysis of the *Caenorhabditis elegans* genome using RNAi. *Nature* **421**, 231-237.

Kamath, R. S., Martinez-Campos, M., Zipperlen, P., Fraser, A. G. and Ahringer, J. (2001). Effectiveness of specific RNA-mediated interference through ingested double-stranded RNA in *Caenorhabditis elegans*. *Genome Biol* **2**, RESEARCH0002.

Kawasaki, I., Shim, Y. H., Kirchner, J., Kaminker, J., Wood, W. B. and Strome, S. (1998). PGL-1, a predicted RNA-binding component of germ granules, is essential for fertility in C. elegans. *Cell* **94**, 635-45.

Kemphues, K. and Strome, S. (1997). Fertilization and establishment of polarity in the embryo. In *C. elegans II*, (ed. D. L. Riddle T. Blumenthal B. J. Meyer and J. R. Priess), pp. 335-360. Cold Spring Harbor, NY: Cold Spring Harbor Laboratory Press.

Kemphues, K. J., Priess, J. R., Morton, D. G. and Cheng, N. S. (1988). Identification of genes required for cytoplasmic localization in early C. elegans embryos. *Cell* **52**, 311-20.

King, M. L., Messitt, T. J. and Mowry, K. L. (2005). Putting RNAs in the right place at the right time: RNA localization in the frog oocyte. *Biol Cell* **97**, 19-33.

Kipreos, E. T. (2005). Ubiquitin-mediated pathways in *C. elegans*. In *WormBook* (ed. The *C. elegans* Research Community). doi/10.1895/wormbook.1.36.1, http://www.wormbook.org.

Kuznicki, K. A., Smith, P. A., Leung-Chiu, W. M., Estevez, A. O., Scott, H. C. and Bennett, K. L. (2000). Combinatorial RNA interference indicates GLH-4 can compensate for GLH-1; these two P granule components are critical for fertility in *C. elegans*. *Development* **127**, 2907-16.

Labbe, J. C., McCarthy, E. K. and Goldstein, B. (2004). The forces that position a mitotic spindle asymmetrically are tethered until after the time of spindle assembly. *J Cell Biol* **167**, 245-56.

Lai, W. S., Carballo, E., Strum, J. R., Kennington, E. A., Phillips, R. S. and Blackshear, P. J. (1999). Evidence that tristetraprolin binds to AU-rich elements and promotes the deadenylation and destabilization of tumor necrosis factor alpha mRNA. *Mol Cell Biol* **19**, 4311-23.

Laufer, J. S., Bazzicalupo, P. and Wood, W. B. (1980). Segregation of developmental potential in early embryos of *Caenorhabditis elegans*. *Cell* **19**, 569-577.

Leacock, S. W. and Reinke, V. (2006). Expression profiling of MAP kinase-mediated meiotic progression in *Caenorhabditis elegans*. *PLoS Genet* **2**, e174.

Lin-Marq, N., Borel, C. and Antonarakis, S. E. (2005). Peutz-Jeghers LKB1 mutants fail to activate GSK-3-beta, preventing it from inhibiting Wnt signaling. *Mol Gen Genomics* **273**, 184-196.

Liu, J., Vasudevan, S. and Kipreos, E. T. (2004). CUL-2 and ZYG-11 promote meiotic anaphase II and the proper placement of the anterior-posterior axis in *C. elegans*. *Development* **131**, 3513-25.

Lizcano, J. M., Goransson, O., Toth, R., Deak, M., Morrice, N. A., Boudeau, J., Hawley, S. A., Udd, L., Makela, T. P., Hardie, D. G. et al. (2004). LKB1 is a master kinase that activates 13 kinases of the AMPK subfamily, including MARK/PAR-1. *Embo J* **23**, 833-43.

Maduro, M. and Pilgrim, D. (1995). Identification and cloning of *unc-119*, a gene expressed in the *Caenorhabditis elegans* nervous system. *Genetics* **141**, 977-88.

Manning, G. (2005). Genomic overview of protein kinases. In *WormBook* (ed. The *C. elegans* Research Community). doi/10.1895/wormbook.1.60.1, http://www.wormbook.org.

Martin, S. G. and St Johnston, D. (2003). A role for Drosophila LKB1 in anterior-posterior axis formation and epithelial polarity. *Nature* **421**, 379-84.

Mello, C. C., Draper, B. W., Krause, M., Weintraub, H. and Priess, J. R. (1992). The pie-1 and mex-1 genes and maternal control of blastomere identity in early *C. elegans* embryos. *Cell* **70**, 163-76.

Mello, C. C., Schubert, C., Draper, B., Zhang, W., Lobel, R. and Priess, J. R. (1996). The PIE-1 protein and germline specification in C. elegans embryos. *Nature* **382**, 710-2.

Miller, M. A., Nguyen, V. Q., Lee, M. H., Kosinski, M., Schedl, T., Caprioli, R. M. and Greenstein, D. (2001). A sperm cytoskeletal protein that signals oocyte meiotic maturation and ovulation. *Science* **291**, 2144-7.

Morton, D. G., Roos, J. M. and Kemphues, K. J. (1992). *par-4*, a gene required for cytoplasmic localization and determination of specific cell types in *Caenorhabditis elegans* embryogenesis. *Genetics* **130**, 771-90.

Morton, D. G., Shakes, D. C., Nugent, S., Dichoso, D., Wang, W., Golden, A. and Kemphues, K. J. (2002). The *Caenorhabditis elegans par-5* gene encodes a 14-3-3 protein required for cellular asymmetry in the early embryo. *Dev Biol* **241**, 47-58.

Motegi, F. and Sugimoto, A. (2006). Sequential functioning of the ECT-2 RhoGEF, RHO-1 and CDC-42 establishes cell polarity in Caenorhabditis elegans embryos. *Nat Cell Biol* **8**, 978-85.

Munro, E., Nance, J. and Priess, J. R. (2004). Cortical flows powered by asymmetrical contraction transport PAR proteins to establish and maintain anterior-posterior polarity in the early *C. elegans* embryo. *Dev Cell* **7**, 413-24.

Munro, E. M. (2006). PAR proteins and the cytoskeleton: a marriage of equals. *Curr Opin Cell Biol* **18**, 86-94.

Nance, J. (2005). PAR proteins and the establishment of cell polarity during *C. elegans* development. *Bioessays* **27**, 126-35.

Narbonne, P. and Roy, R. (2006). Inhibition of germline proliferation during *C. elegans* dauer development requires PTEN, LKB1 and AMPK signalling. *Development* **133**, 611-619.

Nelson, G. A., Lew, K. K. and Ward, S. (1978). Intersex, a temperature-sensitive mutant of the nematode *Caenorhabditis elegans. Dev Biol* **66**, 386-409.

Nishi, Y. and Lin, R. (2005). DYRK2 and GSK-3 phosphorylate and promote the timely degradation of OMA-1, a key regulator of the oocyte-to-embryo transition in *C. elegans. Dev Biol* **288**, 139-49.

Nishimura, I., Yang, Y. and Lu, B. (2004). PAR-1 kinase plays an initiator role in a temporally ordered phosphorylation process that confers tau toxicity in *Drosophila. Cell* **116**, 671-82.

O'Connell, K. F., Maxwell, K. N. and White, J. G. (2000). The *spd-2* gene is required for polarization of the anteroposterior axis and formation of the sperm asters in the *Caenorhabditis elegans* zygote. *Dev Biol* **222**, 55-70.

Ogura, K.-i., Kishimoto, N., Mitani, S., Gengyo-Ando, K. and Kohara, Y. (2003). Translational control of maternal *glp-1* mRNA by POS-1 and its interacting protein SPN-4 in *Caenorhabditis elegans*. *Development* **130**, 2495-2503.

Ossipova, O., Bardeesy, N., DePinho, R. A. and Green, J. B. A. (2003). LKB1 (XEEK1) regulates Wnt singalling in vertebrate development. *Nat Cell Biol* **5**, 889-894.

Ossipova, O., Dhawan, S., Sokol, S. and Green, J. B. (2005). Distinct PAR-1 proteins function in different branches of Wnt signaling during vertebrate development. *Dev Cell* **8**, 829-41.

Pagano, J. M., Farley, B. M., McCoig, L. M. and Ryder, S. P. (2007). Molecular basis of RNA recognition by the embryonic polarity determinant MEX-5. *J Biol Chem* **282**, 8883-94.

Page, B. D., Diede, S. J., Tenlen, J. R. and Ferguson, E. L. (2007). EEL-1, a Hect E3 ubiquitin ligase, controls asymmetry and perisstence of the SKN-1 transcription factor in the early *C. elegans* embryo. *Development, in press.*

Page, B. D., Guedes, S., Waring, D. and Priess, J. R. (2001). The *C. elegans* E2F- and DP-related proteins are required for embryonic asymmetry and negatively regulate Ras/MAPK signaling. *Mol Cell* **7**, 451-60.

Patterson, G. H. and Lippincott-Schwartz, J. (2002). A photoactivatable GFP for selective photolabeling of proteins and cells. *Science* **297**, 1873-7.

Pellettieri, J., Reinke, V., Kim, S. K. and Seydoux, G. (2003). Coordinate activation of maternal protein degradation during the egg-to-embryo transition in *C. elegans*. *Dev Cell* **5**, 451-62.

Pitt, J. N., Schisa, J. A. and Priess, J. R. (2000). P granules in the germ cells of *Caenorhabditis elegans* adults are associated with clusters of nuclear pores and contain RNA. *Dev Biol* **219**, 315-33.

Portman, D. S. (2006). Profiling *C. elegans* gene expression with DNA microarrays. In *WormBook* (ed. The *C. elegans* Research Community). doi/10.1895/wormbook.1.104.1, http://www.wormbook.org.

Praitis, V., Casey, E., Collar, D. and Austin, J. (2001). Creation of low-copy integrated transgenic lines in *Caenorhabditis elegans*. *Genetics* **157**, 1217-1226.

Priess, J. R., Schnabel, H. and Schnabel, R. (1987). The *glp-1* locus and cellular interactions in early C. elegans embryos. *Cell* **51**, 601-11.

Priess, J. R. and Thomson, J. N. (1987). Cellular interactions in early *C. elegans* embryos. *Cell* **48**, 241-50.

Reese, K. J., Dunn, M. A., Waddle, J. A. and Seydoux, G. (2000). Asymmetric segregation of PIE-1 in *C. elegans* is mediated by two complementary mechanisms that act through separate PIE-1 protein domains. *Mol Cell* **6**, 445-55.

Reinke, V., Gil, I. S., Ward, S. and Kazmer, K. (2004). Genome-wide germline-enriched and sex-biased expression profiles in *Caenorhabditis elegans. Development* **131**, 311-23.

Reinke, V., Smith, H. E., Nance, J., Wang, J., Doren, C. V., Begley, R., Jones, S. J. M., Davis, E. B., Scherer, S., Ward, S. et al. (2000). A global profile of germline gene expression in *C. elegans. Molecular Cell* **6**, 605-616.

Rhoads, R. E., Dinkova, T. D. and Korneeva, N. L. (2006). Mechanism and regulation of translation in *C. elegans.* In *WormBook* (ed. The *C. elegans* Research Community). doi/10.1895/wormbook.1.63.1, http://www.wormbook.org.

Riechmann, V. and Ephrussi, A. (2004). Par-1 regulates *bicoid* mRNA localisation by phosphorylating Exuperantia. *Development* **131**, 5897-907.

Riechmann, V., Gutierrez, G. J., Filardo, P., Nebreda, A. R. and Ephrussi, A. (2002). Par-1 regulates stability of the posterior determinant Oskar by phosphorylation. *Nat Cell Biol* **4**, 337-42.

Sadler, P. L. and Shakes, D. C. (2000). Anucleate *Caenorhabditis elegans* sperm can crawl, fertilize oocytes and direct anterior-posterior polarization of the 1-cell embryo. *Development* **127**, 355-66.

Saffman, E. E. and Lasko, P. (1999). Germline development in vertebrates and invertebrates. *Cell Mol Life Sci* **55**, 1141-63.

Sasagawa, Y., Sato, S., Ogura, T. and Higashitani, A. (2007). *C. elegans* RBX-2-CUL-5- and RBX-1-CUL-2-based complexes are redundant for oogenesis and activation of the MAP kinase MPK-1. *FEBS Lett* **581**, 145-150.

Schisa, J. A., Pitt, J. N. and Priess, J. R. (2001). Analysis of RNA associated with P granules in germ cells of C. elegans adults. *Development* **128**, 1287-98.

Schonegg, S. and Hyman, A. A. (2006). CDC-42 and RHO-1 coordinate acto-myosin contractility and PAR protein localization during polarity establishment in C. elegans embryos. *Development* **133**, 3507-16.

Schubert, C. M. PIE-1, MEX-5, MEX-6 and Soma/Germline Asymmetry in *C. elegans* embryos [Dissertation]. Seattle (WA): University of Washington; 2000. 123 p.

Schubert, C. M., Lin, R., de Vries, C. J., Plasterk, R. H. and Priess, J. R. (2000). MEX-5 and MEX-6 function to establish soma/germline asymmetry in early *C. elegans* embryos. *Mol Cell* **5**, 671-82.

Seydoux, G. (1996). Mechanisms of translational control in early development. *Curr Opin Genet Dev* **6**, 555-61.

Seydoux, G. and Braun, R. E. (2006). Pathway to totipotency: lessons from germ cells. *Cell* **127**, 891-904.

Seydoux, G. and Fire, A. (1994). Soma-germline asymmetry in the distributions of embryonic RNAs in *Caenorhabditis elegans. Development* **120**, 2823-34.

Shirayama, M., Soto, M. C., Ishidate, T., Kim, S., Nakamura, K., Bei, Y., van den Heuvel, S. and Mello, C. C. (2006). The Conserved Kinases CDK-1, GSK-3, KIN-19, and MBK-2 Promote OMA-1 Destruction to Regulate the Oocyte-to-Embryo Transition in *C. elegans. Curr Biol* **16**, 47-55.

Sonneville, R. and Gonczy, P. (2004). *zyg-11* and *cul-2* regulate progression through meiosis II and polarity establishment in *C. elegans. Development* **131**, 3527-43.

Spicer, J., Rayter, S., Young, N., Elliott, R., Ashworth, A. and Smith, D. (2003). Regulation of the Wnt signalling component PAR1A by the Peutz-Jeghers syndrome kinase LKB1. *Oncogene* **22**, 4752-6.

Stitzel, M. L., Pellettieri, J. and Seydoux, G. (2006). The *C. elegans* DYRK Kinase MBK-2 Marks Oocyte Proteins for Degradation in Response to Meiotic Maturation. *Curr Biol* **16**, 56-62.

Strome, S., Powers, J., Dunn, M., Reese, K., Malone, C. J., White, J., Seydoux, G. and Saxton, W. (2001). Spindle dynamics and the role of gamma-tubulin in early *Caenorhabditis elegans* embryos. *Mol Biol Cell* **12**, 1751-64.

Strome, S. and Wood, W. B. (1982). Immunofluorescence visualization of germ-line-specific cytoplasmic granules in embryos, larvae, and adults of *Caenorhabditis elegans. Proc Natl Acad Sci U S A* **79**, 1558-62.

Strome, S. and Wood, W. B. (1983). Generation of asymmetry and segregation of germ-line granules in early *C. elegans* embryos. *Cell* **35**, 15-25.

Su, J.-Y., Erikson, E. and Maller, J. L. (1996). Cloning and characterization of a novel serine/threonine protein kinase expressed in early *Xenopus* embryos. *J Biol Chem* **271**, 14430-14437.

Sulston, J. E., Schierenberg, E., White, J. G. and Thomson, J. N. (1983). The embryonic cell lineage of the nematode *Caenorhabditis elegans*. *Dev Biol* **100**, 64-119.

Suzuki, A., Ishiyama, C., Hashiba, K., Shimizu, M., Ebnet, K. and Ohno, S. (2002). aPKC kinase activity is required for the asymmetric differentiation of the premature junctional complex during epithelial cell polarization. *J Cell Sci* **115**, 3565-73.

Suzuki, A. and Ohno, S. (2006). The PAR-aPKC system: lessons in polarity. *J Cell Sci* **119**, 979-87.

Szczepanska, K. and Maleszewski, M. (2005). LKB1/PAR4 protein is asymmetrically localized in mouse oocytes and associates with meiotic spindle. *Gene Expr Patterns* **6**, 86-93.

Tabara, H., Hill, R. J., Mello, C. C., Priess, J. R. and Kohara, Y. (1999). *pos-1* encodes a cytoplasmic zinc-finger protein essential for germline specification in *C. elegans*. *Development* **126**, 1-11.

Tabuse, Y., Izumi, Y., Piano, F., Kemphues, K. J., Miwa, J. and Ohno, S. (1998). Atypical protein kinase C cooperates with PAR-3 to establish embryonic polarity in *Caenorhabditis elegans*. *Development* **125**, 3607-14.

Takahashi, M., Iwasaki, H., Inoue, H. and Takahashi, K. (2002). Reverse genetic analysis of the *Caenorhabditis elegans* 26S proteasome subunits by RNA interference. *Biol Chem* **383**, 1263-1266.

Tenenhaus, C., Schubert, C. and Seydoux, G. (1998). Genetic requirements for PIE-1 localization and inhibition of gene expression in the embryonic germ lineage of *Caenorhabditis elegans*. *Dev Biol* **200**, 212-24.

Tenlen, J. R., Schisa, J. A., Diede, S. J. and Page, B. D. (2006). Reduced dosage of *pos-1* suppresses Mex mutants and reveals complex interactions among CCCH zinc-finger proteins during *Caenorhabditis elegans* embryogenesis. *Genetics* **174**, 1933-1945.

Timmons, L. and Fire, A. (1998). Specific interference by ingested dsRNA. *Nature* **395**, 854.

Vaccari, T. and Ephrussi, A. (2002). The fusome and microtubules enrich Par-1 in the oocyte, where it effects polarization in conjunction with Par-3, BicD, Egl, and dynein. *Curr Biol* **12**, 1524-8.

van Eeden, F. and St Johnston, D. (1999). The polarisation of the anterior-posterior and dorsal-ventral axes during *Drosophila* oogenesis. *Current Opinion in Genetics and Development* **9**, 396-404.

Vinot, S., Le, T., Maro, B. and Louvet-Vallee, S. (2004). Two PAR6 proteins become asymmetrically localized during establishment of polarity in mouse oocytes. *Curr Biol* **14**, 520-5.

Wallenfang, M. R. and Seydoux, G. (2000). Polarization of the anterior-posterior axis of *C. elegans* is a microtubule-directed process. *Nature* **408**, 89-92.

Watts, J. L., Etemad-Moghadam, B., Guo, S., Boyd, L., Draper, B. W., Mello, C. C., Priess, J. R. and Kemphues, K. J. (1996). *par-6*, a gene involved in the establishment of asymmetry in early *C. elegans* embryos, mediates the asymmetric localization of PAR-3. *Development* **122**, 3133-40.

Watts, J. L., Morton, D. G., Bestman, J. and Kemphues, K. J. (2000). The *C. elegans par-4* gene encodes a putative serine-threonine kinase required for establishing embryonic asymmetry. *Development* **127**, 1467-75.

Williamson, A. and Lehmann, R. (1996). Germ cell development in *Drosophila*. *Annual Review of Cell and Developmental Biology* **12**, 365-391.

Woods, A., Johnstone, S. R., Dickerson, K., Leiper, F. C., Fryer, L. G. D., Neumann, D., Schlattner, U., Wallimann, T., Carlson, M. and Carling, D. (2003). LKB1 is the upstream kinase in the AMP-activated protein kinase cascade. *Curr Biol* **13**, 2004-2008.

Zachariae, W., Shevchenko, A., Andrews, P. D., Ciosk, R., Galova, M., Stark, M. J., Mann, M. and Nasmyth, K. (1998). Mass spectrometric analysis of the anaphase-promoting complex from yeast: identification of a subunit related to cullins. *Science* **279**, 1216-9.

Zdinak, L. A., Greenberg, I. B., Szewczyk, N. J., Barmada, S. J., Cardamone-Rayner, M., Hartman, J. J. and Jacobson, L. A. (1997). Transgene-coded chimeric proteins as reporters of intracellular proteolysis: starvation-induced catabolism of a lacZ fusion protein in muscle cells of *Caenorhabditis elegans*. *J Cell Biochem* **67**, 143-53.

Appendix A: Reduced dosage of *pos-1* suppresses Mex mutant phenotype

DOI: 10.1534/genetics.105.052621

Reduced Dosage of *pos-1* Suppresses Mex Mutants and Reveals Complex Interactions Among CCCH Zinc-Finger Proteins During *Caenorhabditis elegans* Embryogenesis

Jennifer R. Tenlen,*,†,1 Jennifer A. Schisa,‡,1 Scott J. Diede§ and Barbara D. Page*,,2**

**Division of Basic Sciences, Fred Hutchinson Cancer Research Center, Seattle, Washington 98109, **Howard Hughes Medical Institute, Seattle, Washington 98109, †Molecular and Cellular Biology Program, University of Washington, Seattle, Washington 98195, §Children's Hospital and Regional Medical Center, Department of Hematology and Oncology, Seattle, Washington 98105 and ‡Department of Biology, Central Michigan University, Mount Pleasant, Michigan 48859*

Manuscript received January 18, 2006
Accepted for publication September 11, 2006

ABSTRACT

Cell fate specification in the early *C. elegans* embryo requires the activity of a family of proteins with CCCH zinc-finger motifs. Two members of the family, MEX-5 and MEX-6, are enriched in the anterior of the early embryo where they inhibit the accumulation of posterior proteins. Embryos from *mex-5* single-mutant mothers are inviable due to the misexpression of SKN-1, a transcription factor that can specify mesoderm and endoderm. The aberrant expression of SKN-1 causes a loss of hypodermal and neuronal tissue and an excess of pharyngeal muscle, a Mex phenotype (*m*uscle *ex*cess). POS-1, a third protein with CCCH motifs, is concentrated in the posterior of the embryo where it restricts the expression of at least one protein to the anterior. We discovered that reducing the dosage of *pos-1(+)* can suppress the Mex phenotype of *mex-5(−)* embryos and that POS-1 binds the 3′-UTR of *mex-6*. We propose that the suppression of the Mex phenotype by reducing *pos-1(+)* is due to decreased repression of *mex-6* translation. Our detailed analyses of these protein functions reveal complex interactions among the CCCH finger proteins and suggest that their complementary expression patterns might be refined by antagonistic interactions among them.

A fundamental question in development is how sister cells become different from one another. These differences can result from an intrinsic asymmetry present in the mother cell or asymmetry can be triggered by an external cue. In the *Caenorhabditis elegans* embryo, anterior–posterior asymmetry is initially established at fertilization (Goldstein and Hird 1996). The sperm aster activates a cascade of events in the one-cell embryo that results in the asymmetric localization of a group of proteins, called PARs (Sadler and Shakes 2000; Wallenfang and Seydoux 2000; Cuenca *et al.* 2003). The PAR proteins are required to polarize the one-cell embryo, and their asymmetric localization has two major downstream effects. First, PAR proteins control the asymmetric placement of the first mitotic spindle. As a result, at the two-cell stage the anterior blastomere is larger than its posterior sister. Second, the PARs affect the fates of the anterior and posterior cells through the asymmetric localization of cell fate determinants (Rose and Kemphues 1998). The larger anterior cell produces the majority of ectoderm, hypodermis, and neurons in the wild-type worm. The smaller, posterior sister cell generates the endoderm, the germline, and the majority of mesoderm. The mechanisms by which PAR proteins act on the downstream proteins that regulate cell fate have only recently begun to be elucidated (Schubert *et al.* 2000; Cuenca *et al.* 2003).

The PAR proteins, in particular the Ser/Thr kinase PAR-1, are thought to act on members of the CCCH zinc-finger protein family to regulate cell fate. PAR-1 restricts two CCCH proteins, MEX-5 and MEX-6, to the anterior pole of the one-cell embryo. The function of both MEX-5 and MEX-6 proteins is required to limit the accumulation of three other CCCH proteins, PIE-1, POS-1 and MEX-1, such that they are enriched in the posterior of the embryo (Schubert *et al.* 2000; Cuenca *et al.* 2003). PIE-1 acts in the nucleus of germline precursors to repress transcription and in the cytoplasm where it prevents degradation of at least one maternal mRNA and promotes expression of that message (Mello *et al.* 1996; Seydoux *et al.* 1996; Batchelder *et al.* 1999; Tenenhaus *et al.* 2001). POS-1 is critical for both somatic and germline fates (Tabara *et al.* 1999; D'Agostino *et al.* 2006) and acts as a translational repressor by directly binding the 3′-UTR of its target gene (Ogura *et al.* 2003), and MEX-1 affects the accumulation

[1]These authors contributed equally to this work.

[2]*Corresponding author:* Fred Hutchinson Cancer Research Center, 1100 Fairview Ave. N, Mailstop c3-168, Seattle, WA 98109. E-mail: bdpage@gmail.com

of several proteins (Mello *et al.* 1992; Guedes and Priess 1997).

Each member of the above *C. elegans* family of CCCH zinc-finger proteins controls cell fate by its ability to regulate the accumulation and/or expression of other proteins. The molecular mechanism(s) by which this regulation is achieved is unknown for MEX-5, MEX-6, MEX-1, and for the cytoplasmic function of PIE-1. Proteins with CCCH motifs in mammals, flies, and yeast have been associated with diverse aspects of RNA regulation, including processing, localization, and destabilization (Begemann *et al.* 1997; Blackshear 2002; Adereth *et al.* 2005; Ladd *et al.* 2005; Puig *et al.* 2005). For example, the mammalian TTP and the yeast Cth2 CCCH proteins have been shown to regulate expression by binding and targeting mRNAs for degradation (Blackshear 2002; Puig *et al.* 2005). Possibly, the *C. elegans* CCCH proteins use similar mechanisms to control cell fate in the early embryo.

Both CCCH proteins MEX-5 and POS-1 affect SKN-1 via its accumulation and/or its activity (Tabara *et al.* 1999; Schubert *et al.* 2000). SKN-1 is a transcription factor that acts in descendants of the posterior blastomere of the two-cell embryo and is important for the specification of endoderm and a subset of mesodermal tissues (Bowerman *et al.* 1992). In wild-type two-cell embryos, SKN-1 is present at a high level in the posterior cell, and is detected at a lower level in its anterior sister (Bowerman *et al.* 1993). In *mex-5* mutant embryos, SKN-1 protein accumulates to a high level in the anterior blastomere, similar to the level seen in its posterior sister. This misexpression of SKN-1 results in a Mex (*m*uscle *ex*cess) phenotype. In these mutant embryos, the anterior blastomere of the two-cell embryo produces ectopic mesodermal tissues, body-wall muscle, and pharyngeal cells (Schubert *et al.* 2000). Loss of *pos-1* function has a very different effect on SKN-1. Although SKN-1 expression appears wild-type in *pos-1(−)* embryos, loss of *pos-1* appears to reduce SKN-1 activity. Terminally developed *pos-1* mutant embryos lack endoderm and a subset of mesoderm, a phenotype similar to that of *skn-1(−)* embryos (Tabara *et al.* 1999). Thus, the effects of *mex-5(−)* and *pos-1(−)* are very different; loss of *mex-5* causes ectopic accumulation and activity of SKN-1, whereas loss of *pos-1* reduces SKN-1 activity.

In addition to *mex-5*, mutations in three other genes, *mex-1*, *efl-1*, or *dpl-1*, disrupt SKN-1 asymmetry and cause a Mex phenotype (Mello *et al.* 1992; Bowerman *et al.* 1993; Page *et al.* 2001). MEX-1 is a CCCH protein (Guedes and Priess 1997). *efl-1* and *dpl-1* encode proteins similar to the mammalian transcription factors E2F and DP1, respectively (Page *et al.* 2001). These two proteins function in the maternal germline where they upregulate the transcription of genes involved in oogenesis and early embryogenesis. Their targets include *mex-6*, *mex-5*, and *mex-1* (Chi and Reinke 2006); thus, the Mex phenotype of *efl-1(−)* or *dpl-1(−)* embryos is most likely caused by reduced transcription of these CCCH-encoding genes.

We are interested in the interactions among the various proteins that control cell fate in the early embryo. To achieve this objective, we screened for dominant mutations that suppress the temperature-sensitive Mex phenotype of *efl-1(se1)*. We isolated a loss-of-function mutation in the *pos-1* gene. Our analysis indicates that SKN-1 activity is very sensitive to the dosage level of *pos-1(+)*, but that *pos-1* is not essential for SKN-1 to specify mesoderm or endoderm. We propose that POS-1 can indirectly affect SKN-1 in the anterior blastomere, possibly by repressing *mex-6* translation. In addition, our analysis reveals that *mex-5* is required for the asymmetric pattern of two class II messages, *pos-1* and *mex-1*. Taken together, these data indicate mutually restrictive interactions among the anterior and posterior CCCH finger proteins that may contribute to their complementary expression patterns.

MATERIALS AND METHODS

Strains: The standard wild-type strain used in these experiments is the Bristol strain N2. The following mutant alleles were used: LG II, *dpl-1(zu355)*, *unc-4(e120)*, *rol-1(e187)*, *let-23(sy97)*, *mex-1(zu122)*; LG III, *glp-1(e2142)*, *unc-119(ed3)*; LG IV, *mex-5(zu199)*, *unc-30(e191)*; LG V, *rol-4(sc8)*, *efl-1(se1)*, *unc-42(e270)*, *pos-1(zu454)*, *pos-1(zu148)*, *dpy-11(e224)*, *let-406(s206)*; LG X, *lin-2(e1309)*; and MED-1:GFP (Maduro *et al.* 2001). The transgene insertion *zuIs159[pie-1::gfp::mex-6* (*mex-6* 3′-UTR)] was created in this study and is described below. *C. elegans* culture, mutagenesis, and genetics were performed as previously described (Brenner 1974).

Screen for suppressors of *efl-1(se1)*: We screened for modifiers of *efl-1(se1)* using the strain *efl-1(se1);lin-2(e1309)*. This strain was mutagenized with EMS, and the F_1 were shifted to 26° at the L4 stage and screened as adults. We recovered those worms that produced viable progeny (a bag of viable worms). We screened 36,000 F_1 hermaphrodites and isolated 12 dominant suppressors of the *efl-1(se1)* temperature-sensitive phenotype. Upon further examination one of these suppressors was discovered to be allele *zu454* of *pos-1*.

Antibodies and fluorescence: We detected SKN-1, POS-1, and MEX-5 proteins using antibodies and procedures that have been previously described (Bowerman *et al.* 1993; Tabara *et al.* 1999; Schubert *et al.* 2000). We used the monoclonal antibody mAb3NB12 to detect pharyngeal muscle cells (Priess and Thomson 1987), and the expression of *med-1* was detected by the fusion construct MED-1:GFP created and integrated by Maduro *et al.* (2001). The presence of endoderm was scored using polarizing optics for the intestinal-cell-specific gut granules (Bowerman *et al.* 1992).

RNA-mediated interference: To direct RNA-mediated interference against *pos-1* and *mex-1*, we used a pair of nested primers to PCR amplify part of the coding region of these genes from genomic DNA. Each set of internal primers contains the T7 sequence at the 5′-end to use T7 RNA polymerase to generate double-strand RNA (dsRNA). To specifically remove *mex-5* or *mex-6*, we targeted the region described by Schubert *et al.* (2000). To direct RNA-mediated interference against *skn-1*, we used the cDNA yk2d12 in which the *skn-1* insert is flanked by T7 and T3 RNA polymerase binding sites. L4 worms were soaked in dsRNA for ~15 hr at the temperature specified. In the case of *efl-1(se1) pos-1(zu148)/efl-1(se1)*

pos-1(+) heterozygous worms treated with *mex-6(dsRNA)*, we were unable to distinguish heterozygotes from the homozygous *efl-1(se1) pos-1(+)* worms at the L4 stage. Since soaking causes only a transient removal of *mex-6*, we scored the phenotypic outcome for the progeny of each treated worm and later determined the corresponding genotype of each worm on the basis of its viable progeny.

***In situ* hybridization:** cDNA probes for *pos-1* and *mex-1* were generated using asymmetric PCR, digoxigenin-labeled nucleotides, and the cDNAs yk117h11 and pJPSG9, respectively. Fixation and hybridization procedures were essentially as described in SCHISA *et al.* (2001). Briefly, adults were dissected in M9 on a glass coverslip to remove embryos. The coverslips were inverted on a 0.1% polylysine-coated slide and frozen on dry ice. After removal of the coverslip, the slide was immersed in 100% methanol at −20° (5 min), 100% methanol at room temperature (5 min), 90% methanol (1 min), 70% methanol (1 min), and 50% methanol (1 min) and washed twice in PTw (5 min; 1× PBS, 0.1% Tween 20). Embryos were treated with proteinase K (20 μg/ml; 15 min) at 37° and washed in 2 mg/ml glycine in PTw (2 min) and PTw (5 min). Embryos were fixed for 20 min at room temperature in 4% formaldehyde in PBS and then washed in PTw (5 min), 2 mg/ml glycine in PTw (5 min), PTw (5 min), and 2× SSC (5 min).

Hybridization buffer consisted of 100 μg/ml salmon sperm DNA, 50 μg/ml heparin, 0.1% Tween 20, 50% formamide, and 5× SSC. Embryos were prehybridized for 10 min at 48°. Probes were boiled in hybridization buffer for 10 min and put on ice prior to applying to the sample tissue on a microscope slide. The tissue was covered with a glass coverslip, sealed with rubber cement, and incubated at 37°or 48° for 12–18 hr. After hybridization, the slide was washed at 48° with hybridization buffer (15 min, 30 min). The slide was then washed twice in 2× SSC (10 min). For alkaline phosphatase detection, the slide was washed in PBT (1× PBS, 0.1% BSA, 0.1% Triton X-110) twice for 5 min at room temperature and 5-bromo-4-chloro-3-indolyl phosphate and 4-nitro blue tetrazolium chloride substrates were added. To stop the detection reaction, embryos were washed twice in 150 mM NaCl, 50 mM Tris–HCl pH 7.8, 0.1% BSA, 0.1% Tween-20. Embryos were placed in PBS containing 0.08 μg/ml DAPI and covered with mounting media.

Yeast trihybrid: We used the yeast trihybrid system designed by PUTZ *et al.* (1996). This assay for RNA–protein interactions was also used by OGURA *et al.* (2003) to demonstrate that POS-1 binds the *glp-1* 3′-UTR. Therefore, we used their *pos-1* fusion construct in our experiments and tested its interaction with the *glp-1* 3′-UTR as a positive control. We also used their mutant *pos-1(ne51)* construct as a negative control. The *pos-1(ne51)* mutant allele has a missense mutation that alters the second zinc finger in the POS-1 protein (OGURA *et al.* 2003). This mutation most likely disrupts *pos-1* function, and OGURA *et al.* (2003) did not detect binding of the *glp-1* 3′-UTR with this mutant *pos-1*. We constructed the fusion RNA between Rev response element (RRE) and the *mex-6* 3′-UTR by using a *mex-6* PCR product. Our PCR primers were 5′-cgcgacgcgtccatttttga tttacccactgagagtcc-3′ and 5′-agaatgcggccgcaggcgcagggtatttttggg aatgg-3′. The 5′-end of each primer contains a restriction enzyme site, *MluI* and *NotI*, respectively, allowing for unidirectional cloning. The PCR product was digested and cloned into the pRevRX vector. The wild-type 226-bp sequence of the *mex-6* 3′-UTR was confirmed by sequencing.

The yeast strain PJ69-4A was cotransformed with plasmids containing the *pos-1* fusion and the *mex-6* 3′-UTR fusion. Transformants were selected on synthetic complete media lacking leucine and tryptophan. The RNA–protein interactions were detected by growth on synthetic complete plates lacking tryptophan, leucine, and histidine and supplemented with 5 mM 3-amino-1,2,4-triazole, a His3p inhibitor.

Construction and integration of *gfp:mex-6* fusion: Standard techniques were used to manipulate and amplify DNA. A *pie-1*promoter::*gfp*::*mex-6* transgene, pJT78, was created by modification of a previously described *pie-1*::*gfp* expression vector (STROME *et al.* 2001). The *mex-6*-coding sequence was PCR amplified from *mex-6* cDNA yk733b2 using primers with *SpeI* adapters at the 5′-ends. (Complete primer sequences are available upon request.) The *mex-6* PCR product was cloned downstream of *gfp* into the *SpeI* site of the *pie-1* promoter::*gfp* plasmid. Sequencing was performed to confirm that the *mex-6* insert was in the correct orientation and in-frame with the *gfp* sequence. A unique *NotI* site was created in the plasmid by mutagenesis of one of two *NotI* sites. The *unc-119*(+) genomic fragment was inserted into this *NotI* site (MADURO and PILGRIM 1995). A *pie-1*promoter::*gfp*::*mex-6* (*mex-6* 3′-UTR) transgene, pJT79, was created by modification of pJT78. A *KpnI* fragment of pJT78, containing *gfp*::*mex-6* and *pie-1* 3′-UTR, was removed and used as a template for PCR amplification of *gfp*::*mex-6*. Genomic DNA was used as a template to amplify 939 bp of *mex-6* 3′-UTR immediately downstream of the TAG codon. A two-step fusion PCR method was used to fuse *gfp*::*mex-6* and *mex-6* 3′-UTR sequences (HOBERT 2002). The final fusion PCR product included *KpnI* sites at both the 5′- and 3′-ends, and was cloned into the *KpnI* site of pJT78.

Strains expressing *pie-1*promoter::*gfp*::*mex-6* (*mex-6* 3′-UTR) were obtained by microparticle bombardment of *unc-119(ed3)* worms with the *pie-1* promoter::*gfp*::*mex-6* (*mex-6* 3′-UTR) plasmid described above (PRAITIS *et al.* 2001).

RESULTS

Reducing the gene dosage of *pos-1(+)* suppresses the Mex phenotype of *efl-1*, *dpl-1*, and *mex-5* mutant embryos: We identified the mutant *zu454* in a genetic screen for suppressors of the maternal-effect lethal *efl-1(se1)* Mex phenotype (MATERIALS AND METHODS). The *zu454* mutation resulted in dominant maternal-effect suppression of *efl-1(se1)*. Over 50% of the embryos from mothers that were *efl-1(se1) pos-1(zu454)/efl-1(se1) pos-1(+)* formed viable pretzel-shaped progeny, compared to only 5% of the embryos from *efl-1(se1)* homozygous control mothers (Table 1).

After outcrossing the *zu454* allele from the *efl-1(se1)* background, a nonconditional, maternal-effect lethal phenotype was observed. The dead embryos resembled those produced by *pos-1(−)* mothers (TABARA *et al.* 1999); when terminally differentiated, the *zu454* embryos lacked endoderm and produced varying amounts of pharyngeal tissue. The *zu454* mutation mapped to the *pos-1* locus, and complementation analysis demonstrated that *zu454* is a mutation in the *pos-1* gene.

We sequenced the newly isolated *pos-1* allele, *zu454*, and discovered a transition of a C to T that conceptually results in a nonsense codon at codon 92. Thus, in this mutant the POS-1 protein would be truncated to a length of 91 amino acids instead of its normal length of 264 amino acids. The wild-type POS-1 protein contains two CCCH zinc-finger motifs, each of which is required for POS-1 function (TABARA *et al.* 1999; OGURA *et al.* 2003). Both domains would be absent in the *zu454* truncated POS-1 protein, suggesting that the

TABLE 1

Mutations in *pos-1* dominantly suppress the morphological defect of *dpl-1*, *efl-1*, and *mex-5* mutant embryos

Strain	% normal morphology (*n*)
Wild type	96 (237)
efl-1(se1)	5 (110)
efl-1(se1) pos-1(zu454)/efl-(se1) pos-1(+)	63 (188)
efl-1(se1) pos-1(zu148)/efl-(se1) pos-1(+)	63 (300)
dpl-1(zu355)	8 (294)
dpl-1(zu355);pos-1(zu454)/pos-1(+)	43 (545)
mex-5(zu199)	1 (180)
mex-5(zu199);pos-1(zu454)/pos-1(+)	50 (490)
mex-5(zu199);pos-1(zu148)/pos-1(+)	68 (250)
mex-5(RNAi)	1 (171)
pos-1(zu454)/pos-1(+);mex-5(RNAi)	67 (209)
mex-1(zu122)	0 (272)
mex-1(zu122);pos-1(zu454)/pos-1(+)	0 (>200)

N2 and *efl-1(se1)* hermaphrodites were incubated at 26°. All other hermaphrodites were incubated at 22°. Suppression of embryonic morphology was assayed by the number of embryos that hatched or formed pretzels.

suppressing mutation of *pos-1* results in a nonfunctional protein.

To confirm that a reduction of *pos-1(+)* function can suppress the *efl-1(se1)* phenotype, we tested whether the null *pos-1* allele *zu148* (TABARA *et al.* 1999) suppressed the *efl-1(se1)* Mex phenotype. This mutant *pos-1* allele strongly suppressed the *efl-1(se1)* temperature-sensitive Mex phenotype (Table 1; Figure 1), equal to the levels observed with the newly isolated *pos-1* allele. Thus, reduction of *pos-1(+)* gene dosage appears to be sufficient for suppression of the *efl-1(se1)* Mex phenotype.

The *efl-1(se1)* Mex phenotype is very similar to the Mex phenotype of *dpl-1* and *mex-5* single-mutant embryos (PAGE *et al.* 2001). Therefore, we tested whether the Mex phenotypes of *dpl-1(−)* and *mex-5(−)* were also suppressed by reducing the gene dosage of *pos-1(+)* and found that both were strongly suppressed by mutations in *pos-1* (Table 1). The *mex-5(−);pos-1(−)/pos-1(+)* double-mutant strain was viable.

We also tested whether reducing *pos-1(+)* dosage could dominantly suppress *mex-1* mutant embryos. *mex-1* mutant embryos resemble *mex-5*, *dpl-1*, and *efl-1* single-mutant embryos with respect to their terminally differentiated phenotype, and all four mutant embryos accumulate high levels of SKN-1 in the anterior blastomere and its daughters, compared to wild-type embryos (MELLO *et al.* 1992; BOWERMAN *et al.* 1993; SCHUBERT *et al.* 2000; PAGE *et al.* 2001). However, unlike *mex-5*, *dpl-1*, and *efl-1* mutants, *mex-1* is not suppressed by reducing Ras/MAPK signaling (PAGE *et al.* 2001). *mex-1(−)* was also not suppressed by reducing *pos-1(+)* dosage as *mex-1; pos-1(−)/pos-1(+)* mothers produced all dead progeny with the Mex phenotype (Table 1), consistent with the previous distinction between *mex-1(−)* embryos and those Mex embryos caused by mutations in *mex-5*, *dpl-1*, or *efl-1*.

Reduction of *pos-1(+)* dosage does not alter the terminal phenotype of *mex-5;mex-6* double-mutant embryos: MEX-5 and MEX-6 encode highly similar proteins that function redundantly in the embryo (SCHUBERT *et al.* 2000; HUANG *et al.* 2002). In a two-cell *mex-5(−)* embryo, SKN-1 is the only protein whose asymmetry is consistently disrupted, and the resulting embryos are inviable. In contrast, no disruption of embryonic asymmetry has been detected in *mex-6* mutant embryos, and these embryos are viable. *mex-5;mex-6* double-mutant embryos show a severe disruption in the asymmetry of multiple proteins. At the two-cell stage, proteins such as MEX-3 and GLP-1, that are expressed anteriorly in both wild-type and *mex-5(−)* embryos, are absent in *mex-5(−);mex-6(−)* embryos. Conversely, the proteins PIE-1, MEX-1, and POS-1, that accumulate posteriorly in wild-type and *mex-5(−)* two-cell embryos, are detected in both blastomeres in the double mutant (SCHUBERT *et al.* 2000).

Since reduced dosage of *pos-1(+)* can make *mex-5(−)* embryos viable, we tested whether reduction or loss of *pos-1(+)* function could affect the terminal phenotype of *mex-5;mex-6* double-mutant embryos. A terminal *mex-5(−);mex-6(−)* embryo possesses ectopic body-wall muscle and hypodermal cells but lacks pharyngeal muscle and endoderm (SCHUBERT *et al.* 2000). An additional characteristic of this double-mutant embryo is that it generates a small number of neurons (~10/embryo), whereas a wild-type embryo possesses 269 neurons. To determine if reduction of *pos-1(+)* dosage could affect the *mex-5(−);mex-6(−)* phenotype, we examined terminally developed embryos from *pos-1(zu454)/pos-1(+); mex-5(RNAi);mex-6(RNAi)* mothers. We detected no difference between these embryos and those from *mex-5(−);mex-6(−)* double-mutant mothers (Table 2). To test whether a complete loss of *pos-1* function could affect the *mex-5(−);mex-6(−)* terminal phenotype, we also examined *pos-1(zu454);mex-5(RNAi);mex-6(RNAi)* embryos. Scoring for both the presence of endoderm and the number of neurons produced, we detected no difference in the terminal phenotype of *pos-1;mex-5;mex-6* triple-mutant embryos compared to *mex-5;mex-6* double-mutant embryos (Table 2). Thus, reduction of *pos-1(+)* did not suppress or modify the *mex-5(−);mex-6(−)* terminal phenotype.

Reduction of *pos-1(+)* dosage suppresses the Mex phenotype by eliminating ectopic SKN-1 activity but not ectopic SKN-1 accumulation: To further analyze the ability of *pos-1(−)* to suppress the Mex phenotype of *efl-1* and *mex-5* mutant embryos, we examined the expression of the *med-1* gene. Expression of *med-1* is dependent on SKN-1 activity and correlates with SKN-1 specification of mesoderm and/or endoderm. Consistent with this correlation, *med-1* is a direct target of SKN-1 (MADURO

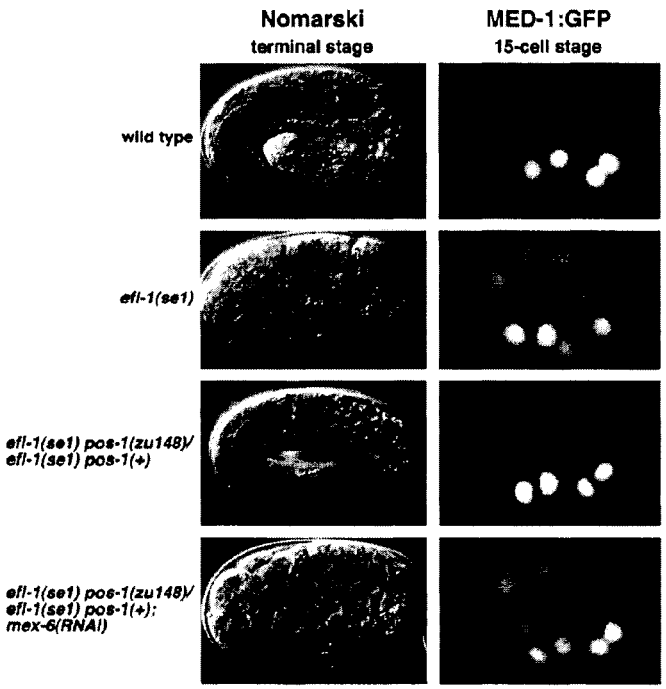

FIGURE 1.—Reducing the gene dosage of *pos-1(+)* suppresses the Mex phenotype of *efl-1(se1)*. (Left) Nomarski images of terminally developed embryos from wild-type, *efl-1(se1)*, *efl-1(se1) pos-1(zu148)/efl-1(se1) pos-1(+)*, and *efl-1(se1) pos-1(zu148)/efl-1(se1) pos-1(+);mex-6(RNAi)* mothers. Note that embryos from both wild-type and *efl-1(se1) pos-1(zu148)/efl-1(se1) pos-1(+)* mothers form pretzel-shaped progeny, whereas embryos from *efl-1(se1)* and *efl-1(se1) pos-1(zu148)/efl-1(se1) pos-1(+);mex-6(RNAi)* mothers do not form pretzels. (Right) MED-1:GFP expression in embryos at the 15-cell stage. The MED-1:GFP expression pattern in wild-type embryos is identical to that seen in embryos from *efl-1(se1) pos-1(zu148)/efl-1(se1) pos-1(+)* mothers. In both types of embryo, MED-1:GFP is expressed in only a subset of descendants from the posterior blastomere of the two-cell stage. Embryos from *efl-1(se1)* and *efl-1(se1) pos-1(zu148)/efl-1(se1) pos-1(+);mex-6(RNAi)* mothers express MED-1:GFP ectopically in the descendants of the anterior blastomere of the two-cell stage. All embryos are oriented with the anterior to the left. The length of the embryo is 50 μm.

et al. 2001). Because *efl-1* and *mex-5* mutant embryos have a SKN-1-dependent Mex phenotype (SCHUBERT *et al.* 2000; PAGE *et al.* 2001), we confirmed that *med-1* is ectopically expressed in these mutant embryos, using a *med-1:gfp* fusion construct from MADURO *et al.* (2001). In wild-type embryos, this construct is expressed in a subset of descendants from the posterior blastomere of the two-cell embryo, and this expression pattern is similar to that of the endogenous MED-1 protein (MADURO *et al.* 2001). In *efl-1* and *mex-5* mutant embryos, MED-1:GFP was ectopically expressed in the descendants of the anterior blastomere ($n = 24$ for *efl-1* and $n = 21$ for *mex-5*), consistent with these embryos generating ectopic mesodermal tissues from this blastomere (Figure 1; data not shown). We next determined whether the MED-1:GFP expression pattern changed in *efl-1* and *mex-5* mutant embryos suppressed by reduction in *pos-1(+)* dosage. All embryos examined from *efl-1(se1) pos-1(zu148)/efl-1(se1) pos-1(+)* mothers, incubated at the *efl-1(se1)* restrictive temperature, or from *pos-1(zu148)/pos-1(+);mex-5(RNAi)* mothers, expressed MED-1:GFP in a wild-type pattern ($n = 25$ for *efl-1* and $n = 24$ for *mex-5*) (Figure 1; data not shown). The restoration of wild-type MED-1 expression indicates that a haploid level of *pos-1(+)* suppresses the Mex phenotype by acting upstream of *med-1* expression and by preventing either ectopic SKN-1 activity or misexpression of SKN-1.

In *mex-5*, *efl-1*, and *dpl-1* single-mutant embryos, SKN-1 is present at high levels in the anterior blastomere and its daughters, compared to the lower levels observed in

TABLE 2

Mutations in *pos-1* do not alter the terminal phenotype of *mex-5;mex-6* double-mutant embryos

Strain	% *mex-5(−);mex-6(−)* phenotype	% *pos-1(−)* phenotype	*n*
mex-5(RNAi);mex-6(RNAi)	100	0	120
pos-1(zu454)/pos-1(+);mex-5(RNAi);mex-6(RNAi)	100	0	83
pos-1(zu454);mex-5(RNAi);mex-6(RNAi)	100	0	67
pos-1(zu454)	0	100	96

Hermaphrodites were incubated at 22°. The *mex-5(−);mex-6(−)* phenotype was distinguished from the *pos-1(−)* phenotype by a neuronal GFP marker. A *mex-5;mex-6* double-mutant embryo produces ~10 GFP expressing cells, while a *pos-1(−)* embryo produces >30 GFP positive cells.

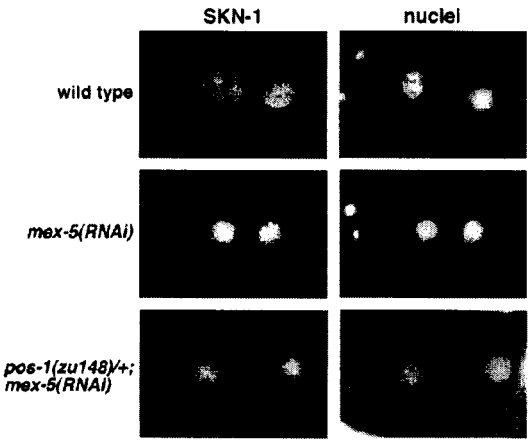

FIGURE 2.—Reducing the gene dosage of *pos-1(+)* does not alter SKN-1 misexpression in *mex-5* mutant embryos. (Left) SKN-1 protein in two-cell embryos from wild-type, *mex-5(RNAi)*, and *pos-1(zu148)/+;mex-5(RNAi)* mothers. Embryos from both *mex-5(RNAi)* and *pos-1(zu148)/+;mex-5(RNAi)* mothers show misexpression of SKN-1 in the anterior blastomere. (Right) The corresponding embryos stained with DAPI to show the nuclei.

these cells in wild-type embryos. In Mex mutant embryos suppressed via reduced Ras/MAPK signaling, SKN-1 accumulation is restored to the wild-type pattern, indicating that the Ras/MAPK pathway functions upstream of SKN-1 (PAGE *et al.* 2001). To determine if reduction of *pos-1(+)* also suppresses the misexpression of SKN-1 in Mex mutants, we stained embryos from *pos-1(zu148)/pos-1(+);mex-5(RNAi)* mothers with anti-SKN-1 serum. In all two-cell and four-cell embryos examined ($n = 42$), we detected a high level of SKN-1 in the anterior blastomere(s); this pattern appeared identical to that seen in *mex-5(RNAi)* control embryos (Figure 2). The majority of embryos from *pos-1(zu148)/pos-1(+); mex-5(RNAi)* mothers that were allowed to terminally differentiate had normal morphology (67%, $n = 209$; Table 1). These results suggest that reducing *pos-1(+)* does not restore the wild-type pattern of SKN-1 accumulation and indicate that reducing *pos-1(+)* affects SKN-1 activity. This result is consistent with analysis of SKN-1 in *pos-1(−)* single-mutant embryos. In these mutant embryos, SKN-1 accumulation appears wild type even though SKN-1 activity is decreased (TABARA *et al.* 1999; MADURO *et al.* 2001).

POS-1 is not required for SKN-1 to specify mesodermal or endodermal tissue: Because our suppression analysis indicates that SKN-1 activity is very sensitive to *pos-1(+)* dosage, we more closely explored the interaction between these two genes. We examined whether *skn-1(+)* could specify mesoderm in the absence of *pos-1(+)*. To accomplish this aim, we looked at two markers indicative of this SKN-1 activity: *med-1:gfp* expression and *glp-1*-independent production of pharyngeal tissue (MELLO *et al.* 1992; BOWERMAN *et al.* 1997; MADURO *et al.* 2001). We scored for the presence of these markers in *pos-1;mex-1* double-mutant embryos. Similar to *efl-1* and *mex-5* mutant embryos, *mex-1* mutant embryos have a terminal Mex phenotype that is dependent on SKN-1 (MELLO *et al.* 1992; SCHUBERT *et al.* 2000; PAGE *et al.* 2001), and as expected, *mex-1(−)* embryos express the SKN-1 target gene *med-1* ectopically (MADURO *et al.* 2001). We examined the expression of the *med-1:gfp* fusion in *pos-1(zu454);mex-1(RNAi)* double-mutant embryos and detected ectopic expression of MED-1:GFP, although the GFP signal was weaker in the double mutant compared to *mex-1* single-mutant embryos (in 12/16 *pos-1(zu454);mex-1(RNAi)* embryos, MED-1:GFP was detected in AB descendants; all 16 embryos were Mex when terminally developed.) This experiment indicates that POS-1 is not required for SKN-1 to specify mesoderm.

To confirm this interpretation of the *pos-1;mex-1* double mutant, we constructed a *pos-1;mex-1* mutant in the background of *glp-1(e2142)* and stained for pharyngeal muscle in those embryos produced at the restrictive temperature for *glp-1(e2142)*. In *glp-1* mutant embryos, the only pharyngeal muscle produced is dependent on the autonomous function of SKN-1 (MELLO *et al.* 1992; BOWERMAN *et al.* 1997). Previous analysis of *pos-1* mutant embryos suggested that the presence of pharyngeal muscle is dependent on *glp-1* (TABARA *et al.* 1999). We confirmed that *glp-1(e2142);pos-1(zu148)* double-mutant embryos did not produce pharyngeal muscle ($n = 13$; Figure 3). In contrast, all *glp-1(e2142);pos-1(zu148);mex-1(RNAi)* triple-mutant embryos produced pharyngeal muscle, demonstrating that SKN-1 specifies mesoderm without POS-1 ($n = 18$) (Figure 3).

Our above analysis concentrated on the effect that loss of *pos-1(+)* has on ectopic SKN-1 function. We examined the amount of pharyngeal muscle, a mesodermal tissue, produced because ectopic anterior SKN-1 activity results in production of this tissue (MELLO *et al.* 1992; BOWERMAN *et al.* 1997). SKN-1 function in its wild-type site of action is associated with production of both mesodermal and endodermal tissues (BOWERMAN *et al.* 1992). When we first examined the *pos-1(zu454)* mutant embryos in the *efl-1(se1)* background, we observed that the majority of *efl-1(se1) pos-1(zu454)* embryos generate endoderm, unlike *pos-1* single-mutant embryos. To confirm that this observation was due to *efl-1(se1)* and not to a secondary mutation in our mutagenized background, we constructed the *efl-1(se1) pos-1(zu148)* double mutant and examined the embryos from *efl-1(se1) pos-1(zu148)* mothers. At 23°, 6% of *pos-1(zu148)* mutant embryos produced endoderm ($n = 144$), whereas 70% of *efl-1 pos-1* double-mutant embryos made endoderm ($n = 90$). To confirm that the endoderm present in *efl-1 pos-1* mutant embryos was due to *skn-1(+)*, we reduced *skn-1* function by RNAi in the *efl-1(se1) pos-1(zu148)*

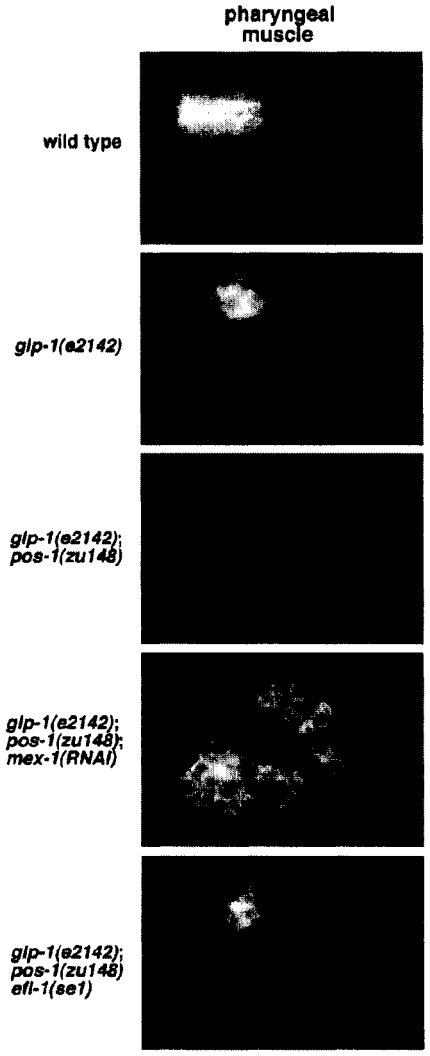

FIGURE 3.—POS-1 is not required for SKN-1 to specify pharyngeal muscle. Terminally developed embryos were stained for pharyngeal muscle with the antibody mAb3NB12. The mothers were incubated for 16 hr at 26°, the restrictive temperature for both *glp-1(e2142)* and *efl-1(se1)*, and then transferred to prewarmed plates for 12 more hours. Terminally developed embryos from the second plate were subsequently stained for pharyngeal muscle. The presence of pharyngeal muscle independent of *glp-1* function is due to autonomous SKN-1 function (MELLO *et al.* 1992).

background. We detected endoderm in only 12% of *efl-1(se1) pos-1(zu148);skn-1(RNAi)* triple-mutant embryos ($n = 103$). Thus, for the majority of *efl-1 pos-1* double-mutant embryos, production of endoderm is dependent on *skn-1(+)*, and in the *efl-1(se1)* mutant background, SKN-1 can specify endoderm in the absence of *pos-1(+)*.

Since *efl-1(se1)* suppressed the loss of endoderm in *pos-1* mutant embryos, we determined whether *efl-1(se1)* also suppressed the loss of mesoderm. To score this suppression, we examined the presence of pharyngeal muscle in *glp-1(e2142);efl-1(se1) pos-1(zu148)* triple-mutant embryos produced at the restrictive temperature for *glp-1(e2142)* and *efl-1(se1)*. As stated above, no *glp-1(e2142);pos-1(zu148)* double-mutant embryos produced pharyngeal muscle ($n = 13$); however, 64% of *glp-1(e2142);efl-1(se1) pos-1(zu148)* embryos produced pharyngeal muscle ($n = 150$) (Figure 3). Thus, in the *efl-1(se1)* mutant background, SKN-1 can specify both endodermal and mesodermal tissues without *pos-1(+)* function. To determine whether SKN-1 was functioning at its normal site of action to specify these tissues, we looked at the expression of MED-1:GFP in *efl-1 pos-1* double-mutant embryos. We detected the wild-type pattern of MED-1:GFP expression in all *efl-1(se1) pos-1(zu148)* embryos examined ($n = 22$).

At this point, the data indicated that the level of *pos-1(+)* is important for SKN-1 to specify mesoderm and endoderm in certain backgrounds, but that *pos-1(+)* was not necessary for this SKN-1 activity. These conclusions lead us to examine two hypotheses that might explain why reduction in *pos-1(+)* dosage suppresses Mex mutants. These hypotheses are not mutually exclusive: (1) POS-1 is misexpressed in the above Mex mutants, and this ectopic POS-1 is important for ectopic SKN-1 activity and (2) POS-1(+) affects SKN-1 activity by acting as a translational repressor; *i.e.*, POS-1 represses translation of a SKN-1 inhibitor.

***efl-1* and *mex-5* mutant embryos have an asymmetric POS-1 expression pattern but a symmetric *pos-1* mRNA distribution:** In wild-type two-cell embryos, POS-1 and SKN-1 are more concentrated in the posterior blastomere than in the anterior; however, both proteins are detected at a low level in the anterior blastomere (BOWERMAN *et al.* 1993; TABARA *et al.* 1999). Our genetic analysis demonstrates that the ectopic activity of SKN-1 is very sensitive to *pos-1(+)* levels. Could the ectopic activity of SKN-1 in the *efl-1, dpl-1* and *mex-5* single mutants be due in part to POS-1 misexpression?

To test this possibility, we examined the localization of the POS-1 protein and *pos-1* mRNA in Mex mutant embryos. In early *efl-1* and *mex-5* mutant embryos, POS-1 accumulation appeared asymmetric, similar to its pattern in wild-type two-cell and four-cell embryos (Figure 4). This observation suggests that ectopic SKN-1 activity in *efl-1* and *mex-5* mutant embryos is not due to ectopic POS-1 accumulation.

In wild-type embryos, *pos-1* mRNA is asymmetrical at the two-cell stage in a pattern similar to that of the protein; a high level of *pos-1* mRNA appears in the posterior blastomere, and a lower level of *pos-1* mRNA is present in the anterior blastomere (TABARA *et al.* 1999).

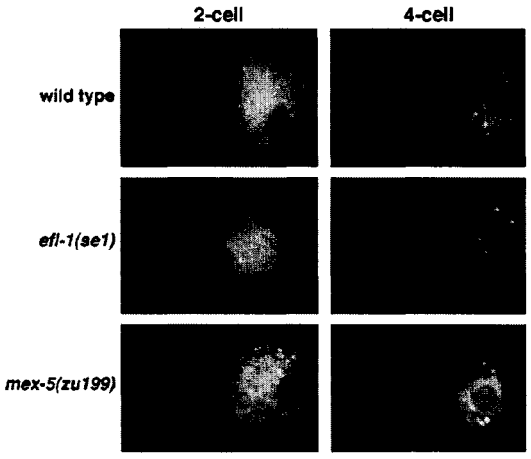

FIGURE 4.—In *efl-1* and *mex-5* mutant embryos, POS-1 accumulation appears wild type. In wild-type embryos, POS-1 accumulation is asymmetric; POS-1 is present at a higher level in the posterior blastomere and in its daughters at the two-cell and four-cell stages (100%, $n = 28$ for the two-cell stage and $n = 31$ for the four-cell stage). A similar pattern of asymmetry is seen in *efl-1* and *mex-5* mutant embryos [for *efl-1(se1)*, 100%, $n = 12$ for the two-cell stage and $n = 13$ for the four-cell stage; for *mex-5(zu199)*, 100%, $n = 16$ for the two-cell stage and $n = 20$ for the four-cell stage].

TABLE 3

Percentage of two- and four-cell embryos in which mRNA is symmetrically localized

RNA	Strain	Embryonic stage	% with symmetry (n)
pos-1	Wild type	Two cell	16 (112)
		Four cell	0 (115)
	efl-1(se1)	Two cell	87 (31)
		Four cell	88 (32)
	mex-5(zu199)	Two cell	94 (62)
		Four cell	88 (43)
mex-1	Wild type	Two cell	67 (21)
		Four cell	4 (24)
	mex-5(zu199)	Two cell	100 (12)
		Four cell	43 (14)
	mex-5(zu199);mex-6(pk440)	Two cell	100 (40)
		Four cell	100 (28)

efl-1(se1) hermaphrodites were incubated at 26°. All other hermaphrodites were incubated at 22°.

In contrast, in *efl-1* and *mex-5* mutant embryos, *pos-1* mRNA was symmetric at the two- and four-cell stages (Table 3; Figure 5). This result, combined with the staining for POS-1, demonstrates that the asymmetric accumulation of POS-1 is not completely regulated by the distribution of its mRNA and is consistent with experiments by DERENZO *et al.* (2003), showing that POS-1 asymmetry is controlled by protein stability. Although an even distribution of the *pos-1* message does not appear to eliminate POS-1 protein asymmetry, this disruption of message asymmetry could subtly affect POS-1 protein levels in the anterior blastomere(s) at the two- and four-cell stages.

The *pos-1* message is a member of the class II mRNAs, a group of mRNAs with a characteristic distribution in the embryo. These messages appear to be localized and/or stabilized in the germline lineage of the early embryo (SEYDOUX and FIRE 1994). The disruption of *pos-1* mRNA asymmetry in the *mex-5* mutant could be specific to the *pos-1* message or could be due to a general defect in the localization and/or stability of class II messages. Therefore, we tested whether another class II message lost asymmetry in the *mex-5* mutant background. In early wild-type embryos, *mex-1* mRNA is asymmetrically localized, similar to *pos-1* mRNA. However, while *pos-1* asymmetry is visible at the two-cell stage, *mex-1* mRNA asymmetry is not clearly discernible until the four-cell stage, when *mex-1* mRNA is at high levels in the daughters of the posterior cell and rarely detected in the daughters of the anterior cell (GUEDES and PRIESS 1997). In *mex-5* mutant embryos, *mex-1* mRNA was symmetric at the four-cell stage (Table 3). Thus, *mex-5* controls not only the asymmetric pattern of SKN-1 accumulation, but also the asymmetric distribution of two class II maternal messages.

POS-1 binds the 3′-UTR of *mex-6*: Since POS-1 has been demonstrated to be a translational repressor

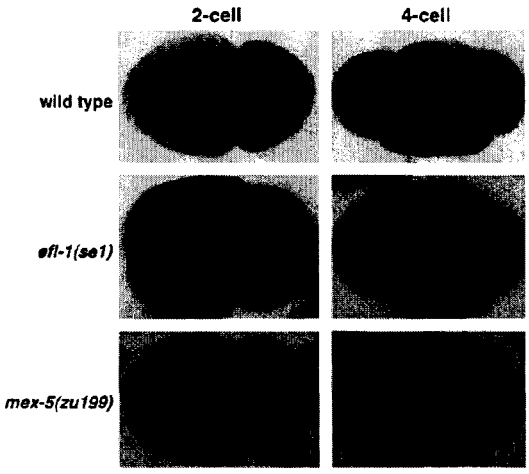

FIGURE 5.—*pos-1* mRNA is symmetrically localized in *efl-1* and *mex-5* mutant embryos. *In situ* hybridization was performed on two- and four-cell embryos with a probe for the *pos-1* mRNA. In wild-type embryos, *pos-1* mRNA has an asymmetric distribution, with a higher concentration in the posterior blastomeres; this asymmetry is absent in *efl-1* and *mex-5* mutant embryos.

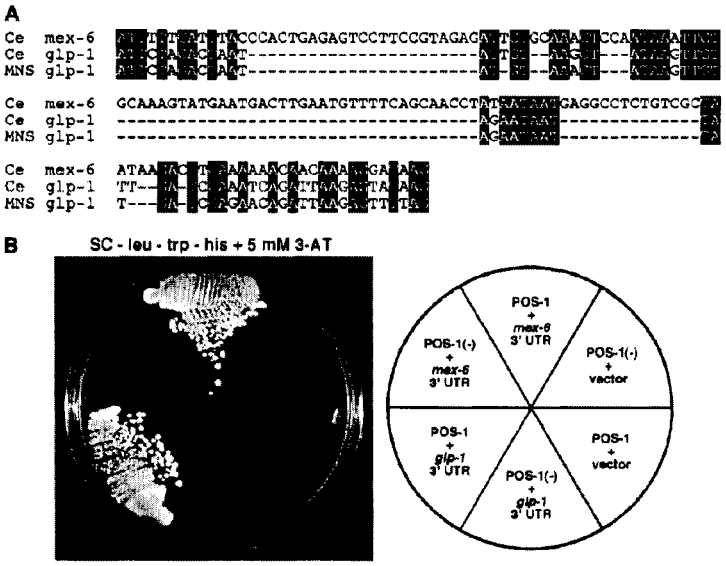

FIGURE 6.—POS-1 binds the SCR-like region of the *mex-6* 3′-UTR. (A) The *mex-6* 3′-UTR shares similarity with the conserved SCR of the *glp-1* 3′-UTR. The alignment shows the similarity between the *C. elegans* (Ce) *mex-6* 3′-UTR and the (Ce) *glp-1* 3′-UTR. In addition, the *mex-6* and *glp-1* 3′-UTRs are aligned with a conserved SCR that was derived from a comparison of *glp-1* 3′-UTRs from multiple nematode species (MNS) (RUDEL and KIMBLE 2001). Identical nucleotides are highlighted by a solid background. (B) POS-1 binds the *mex-6* 3′-UTR. (Left) The yeast trihybrid assay. (Right) A corresponding diagram indicating the various plasmid combinations tested. Growth on the selective medium is seen only when a plasmid containing functional *pos-1* is paired with a plasmid containing either the *mex-6* 3′-UTR or the *glp-1* 3′-UTR. The interaction between POS-1 and the *glp-1* 3′UTR was demonstrated by OGURA *et al.* (2003) and was used as a positive control in our experiment.

(OGURA *et al.* 2003), we reasoned that reduction of this function might explain the suppression of the Mex phenotype, *i.e.*, reduction in *pos-1(+)* levels leads to increased expression of its target. We would expect such a target to be more highly expressed in the anterior of the embryo, an expression pattern complementary to that of POS-1, and possibly to possess similarity to the *glp-1* spatial control region (SCR), a sequence within the *glp-1* 3′-UTR that POS-1 directly binds (EVANS *et al.* 1994; OGURA *et al.* 2003). An attractive candidate for such a target is *mex-6*. A MEX-6:GFP fusion protein is detected in the anterior blastomeres of the two-cell and the early four-cell embryo (CUENCA *et al.* 2003), and we identified a region in the *mex-6* 3′-UTR that is very similar to the conserved SCR of *glp-1* (Figure 6A). In this region of the *mex-6* 3′-UTR, 27 nucleotides are identical to the 34 nucleotides shown to be sufficient for *glp-1* repression in the embryo (MARIN and EVANS 2003). Additionally, *mex-5* and *mex-6* encode very similar proteins that function redundantly during early embryogenesis (SCHUBERT *et al.* 2000); thus, an increase in *mex-6* gene function might compensate for a loss of *mex-5*.

We tested whether POS-1 can bind the 3′-UTR of *mex-6* using the yeast trihybrid assay. The trihybrid assay is a modification of the two-hybrid assay; it uses two fusion proteins and a fusion RNA (PUTZ *et al.* 1996). The assayed protein, in this case POS-1, was fused to the GAL4 activation domain, and the GAL4 DNA-binding domain was fused to HIV-1 RevM1. The fusion RNA included RRE, a domain bound by HIV-1 RevM10, and the test RNA, in this case the 226 nucleotides of the *mex-6* 3′-UTR that contain similarity to the SCR of *glp-1* (Figure 6A). If POS-1 binds this region of the *mex-6* 3′-UTR, then the GAL4 DNA-binding domain and the GAL4 activation domain will be in close contact, activating transcription of genes under the control of the *gal4* promoter. In yeast, this interaction is detected as growth on a selective medium. Using this assay, we detected an interaction between POS-1 and the *mex-6* 3′-UTR, indicating that the similarity between the 3′-UTRs of *glp-1* and *mex-6* is functionally relevant (Figure 6B). We also retested the ability of POS-1 to bind the *glp-1* 3′-UTR, and as expected, detected an interaction. Conversely, no interactions were detected between a nonfunctional POS-1 protein, encoded by *pos-1(n51)*, and the *mex-6* 3′-UTR. Likewise, no interactions were detected between a functional POS-1 protein and RNA containing only the RRE domain. These results demonstrate the specificity of the interaction between functional POS-1 protein and the region of the *mex-6* 3′-UTR containing similarity to the *glp-1* SCR (Figure 6B).

mex-6 is required for the suppression of the Mex phenotype via reduction of *pos-1(+)*: If reducing the dosage of *pos-1(+)* relieves repression of MEX-6 translation, then the ability of *pos-1(−)* to dominantly suppress the Mex phenotype of *efl-1* should require *mex-6(+)*. To test this idea, we removed *mex-6* by RNAi in the *efl-1(se1) pos-1(−)/efl-1(se1) pos-1(+)* background. When *efl-1(se1) pos-1(zu148)/efl-1(se1) pos-1(+)* mothers were grown at 26°, 63% of their progeny appeared wild type (Table 1; Figure 1). In contrast, only 3% of the progeny from *efl-1(se1) pos-1(zu148)/efl-1(se1) pos-1(+); mex-6(RNAi)* mothers appeared wild type and 92% of the progeny were Mex ($n = 88$) (Figure 1). This result is consistent with the hypothesis that reducing *pos-1(+)*

dosage suppresses the Mex phenotype by increasing MEX-6 expression.

***pos-1* does not spatially restrict GFP:MEX-6 expression:** To examine MEX-6 expression in a *pos-1* mutant embryo, we generated a *C. elegans* strain that expressed a *gfp:mex-6* fusion containing the endogenous *mex-6* 3′-UTR (MATERIALS AND METHODS). In a wild-type background, the GFP:MEX-6 signal was enriched in the anterior blastomere of the two-cell embryo and in this blastomere's daughters at the early four-cell stage. We could not compare this pattern to that of endogenous MEX-6 because no antibodies presently exist that specifically recognize MEX-6. However, the GFP:MEX-6 expression pattern was very similar to that of MEX-5. When we removed *pos-1* by RNAi, we detected no difference in the GFP:MEX-6 expression pattern ($n = 13$ for *pos-1(−)* embryos and $n = 7$ for wild-type embryos).

DISCUSSION

Reducing the dosage of *pos-1(+)* indirectly suppresses the Mex phenotype: While screening for mutations that can dominantly suppress the Mex phenotype of *efl-1(se1)*, we isolated a loss-of-function mutation in the *pos-1* gene. We subsequently determined that a null mutation in *pos-1* can dominantly suppress two other Mex mutants, *dpl-1* and *mex-5*, but not *mex-1*. The *pos-1* gene was previously identified on the basis of loss-of-function mutations that cause a maternal-effect lethal phenotype. Embryos from *pos-1* mutant mothers are inviable and lack endoderm and a subset of mesodermal tissues (TABARA *et al.* 1999). This phenotype is similar to that of *skn-1* mutant embryos; thus, POS-1 previously was thought to be required for SKN-1 to specify mesoderm and endoderm (TABARA *et al.* 1999; MADURO *et al.* 2001).

In addition to showing that reduced dosage of *pos-1(+)* can suppress Mex mutants, we made three novel discoveries: (1) Although SKN-1 activity is exquisitely sensitive to the level of *pos-1(+)*, *pos-1* is not required for SKN-1 to specify mesodermal or endodermal tissues; (2) POS-1, a demonstrated translational repressor, can bind the 3′-UTR of the *mex-6* message; and (3) the asymmetry of two class II messages is disrupted in *mex-5* mutant embryos.

How does reducing *pos-1(+)* levels suppress Mex mutants? If *pos-1(+)* is not required for SKN-1 to specify mesoderm, then how does reduction of *pos-1(+)* suppress this SKN-1 ectopic activity? We propose that the low level of POS-1 detected in the anterior blastomere is functionally significant, and since POS-1 has been demonstrated to act as a translational repressor (OGURA *et al.* 2003), it is a decrease in this function that suppresses the Mex phenotype. Thus, we searched for a potential target of POS-1 with the expectations that such a target would have an accumulation pattern complementary to that of POS-1 and might have a 3′-UTR with similarity to the known POS-1 target, *glp-1* (OGURA *et al.* 2003). We determined that the 3′-UTR of *mex-6* contains similarity to the *glp-1* 3′-UTR and, using the yeast trihybrid assay, we showed that POS-1 binds this region of the *mex-6* message (Figure 6). Consistent with our hypothesis, suppression of the Mex phenotype by reduced *pos-1(+)* dosage requires *mex-6*. Together, these results suggest that reducing the level of *pos-1(+)* suppresses the Mex phenotype by decreasing repression of *mex-6* translation (Figure 7).

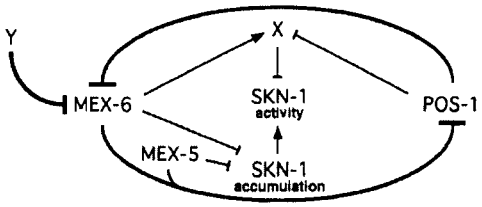

FIGURE 7.—This model depicts interactions between MEX-6, MEX-5, POS-1, and SKN-1 in the early embryo. The model incorporates previously demonstrated interactions and the genetic interactions implied by our analysis. SCHUBERT *et al.* (2000) showed that together MEX-5 and MEX-6 limit accumulation of POS-1. Our data suggest that POS-1 represses translation of MEX-6; however, an additional mechanism, denoted "Y," must exist to regulate MEX-6. It is the combined action of POS-1 and Y that restricts MEX-6 accumulation in the embryo. In addition to the effects of MEX-6, MEX-5, and POS-1 on each other, they each affect SKN-1. We argue that POS-1 affects SKN-1 indirectly by repressing translation of MEX-6 and/or an unknown SKN-1 inhibitor, denoted "X." MEX-6 affects SKN-1 activity by upregulating the accumulation of X and/or by inhibiting SKN-1 accumulation.

If MEX-5 and MEX-6 have identical functions and MEX-6 levels are increased by reducing *pos-1(+)*, then why is SKN-1 misexpression detected in the suppressed embryos? There are three possible explanations for this apparent inconsistency:

1. SKN-1 levels in the anterior blastomeres of suppressed Mex embryos are affected, but we cannot detect this reduction in SKN-1 accumulation. We believe that this is unlikely to be the only explanation, since reduction of Ras signaling restores a wild-type pattern of SKN-1 but only modestly suppresses the Mex phenotype (<40% of these double-mutant embryos are suppressed) (PAGE *et al.* 2001). In contrast, reducing *pos-1(+)* showed no detectable effect on SKN-1 misexpression, yet resulted in nearly 70% of double-mutant embryos being suppressed (Table 1).
2. MEX-6 is a target of POS-1, but another POS-1 target, either in combination with MEX-6 or independently, inhibits SKN-1 activity in the suppressed embryos. Our data do not rule out the existence of such an independent inhibitor; however, the Mex phenotype

of *efl-1(se1)pos-1(zu148)/efl-1(se1)pos-1(+);mex-6(RNAi)* embryos suggests that it is unlikely.

3. MEX-6 upregulates the expression of a SKN-1 inhibitor (Figure 7), and this regulation is more sensitive to MEX-6 levels than downregulation of SKN-1 accumulation.

POS-1 does not exclusively restrict MEX-6 expression: Although we have shown that POS-1 binds the 3′-UTR of *mex-6*, loss of *pos-1* function did not result in ectopic MEX-6 expression. The GLP-1 protein, a previously identified target of POS-1 repression, is ectopically expressed in the posterior blastomere of *pos-1(−)* mutant embryos (Ogura *et al.* 2003; B. D. Page, unpublished observation). If POS-1 also represses translation of *mex-6*, then why is MEX-6 not misexpressed in the posterior blastomere of *pos-1* mutant embryos? Two possibilities could explain this result. First, other CCCH proteins in the posterior blastomere may act redundantly with POS-1 to repress *mex-6* translation. Second, MEX-6 protein asymmetry may also be regulated posttranslationally. We favor the latter possibility since Cuenca *et al.* (2003) observed that after replacing the *mex-6* 3′-UTR with that of another gene, MEX-6 protein was still enriched in the anterior. The asymmetric distribution of several CCCH finger proteins is controlled by protein stability (Reese *et al.* 2000; Derenzo *et al.* 2003). In the cases where this has been demonstrated, these proteins are targeted for degradation in anterior blastomeres (Derenzo *et al.* 2003). If the MEX-6 protein is selectively degraded in the posterior blastomere, then POS-1 would function as an additional level of regulation in restricting MEX-6 accumulation, and MEX-6 misexpression might be detected only in an embryo defective in both MEX-6 degradation and POS-1 activity.

An example of a protein whose expression is under such dual regulation is the Drosophila transcription factor Tramtrack. Tramtrack is regulated both by its protein stability and by translational repression (Hirota *et al.* 1999; Okabe *et al.* 2001). Reduced function of the translational repressor alone has phenotypic consequences in the developing eye; however, under this circumstance, misexpression of Tramtrack is not detected. Extensive misexpression of Tramtrack is seen when the function of both pathways is reduced (Hirota *et al.* 1999). From our analysis, we suspect that MEX-6 accumulation is under similar dual regulation in the *C. elegans* embryo.

Mutations in *efl-1* and *mex-5* disrupt the asymmetric pattern of class II messages: Many markers that are asymmetrically expressed or localized in the two-cell embryo have been identified (Seydoux and Fire 1994; Rose and Kemphues 1998; Bowerman 2000; Pellettieri and Seydoux 2002). In previous studies of *efl-1* and *mex-5* mutant embryos, the only marker consistently detected as altered at the two-cell stage was the SKN-1 protein (Schubert *et al.* 2000; Page *et al.* 2001). In our current analysis of *mex-5* and *efl-1* single-mutant embryos, we observed that the asymmetry of two class II mRNAs is disrupted (Table 3). In the maternal germline of wild-type hermaphrodites, both *pos-1* and *mex-1* messages are detected on P granules and uniformly throughout the egg cytoplasm (Guedes and Priess 1997; Tabara *et al.* 1999; Schisa *et al.* 2001). Like other class II mRNAs in the early embryo, these messages become asymmetrically localized to the posterior cytoplasm and/or degraded from the anterior (Seydoux and Fire 1994; Guedes and Priess 1997; Tabara *et al.* 1999). In *mex-5* and *efl-1* mutant embryos, the mechanism(s) that control this asymmetry appear defective.

The idea that *mex-5* and *efl-1* influences more than SKN-1 asymmetry is not novel. Certain double-mutant combinations with *mex-5* or *efl-1* have extensive effects on embryonic polarity. In *efl-1;mex-5* and *mex-5;mex-6* double-mutant embryos, the normal asymmetric pattern of many markers is altered. In such double-mutant embryos, wild-type anterior markers are absent, and proteins that are normally restricted to the posterior and/or germline progenitor are expressed throughout the two-cell and four-cell embryo. Not surprisingly, we observed a symmetric distribution of a class II message in *mex-5;mex-6* double-mutant embryos (Table 3). This is consistent with the recent report that the class II message *nos-2* is symmetrically distributed in *mex-5(RNAi); mex-6 (RNAi)* embryos at the 16-cell stage (D'Agostino *et al.* 2006). Since many posterior proteins are misexpressed in these double-mutant embryos, the disruption of message asymmetry could be due to mislocalization of the posterior proteins. In early *mex-5* single-mutant embryos, the majority of posteriorly expressed proteins are properly localized (Schubert *et al.* 2000); yet, we still detected uniformly distributed messages in this mutant embryo. Thus, we propose that a primary function of *mex-5* involves message localization and/or stability. This function could be similar to that of the CCCH finger proteins TTP and Cth2. Each of these proteins targets mRNAs for destabilization, often by binding an AU-rich element (ARE) in the 3′-UTR of the mRNAs (Lai *et al.* 1999; Puig *et al.* 2005). Consistent with this idea, the 3′UTR of *mex-1*, contains an exact match to the ARE sequence 5′-UAUUUAUU-3′.

Interestingly, the dynamic pattern of MEX-5 expression is consistent with a function in mRNA degradation. At each early cell division of the germline lineage, a somatic sister cell and a germline progenitor are produced. At each of these divisions, MEX-5 becomes enriched in the somatic sister cell (Schubert *et al.* 2000), and maternal mRNAs disappear from this cell (Seydoux and Fire 1994).

Do the anterior and posterior CCCH proteins mutually restrict one another's expression? The anterior CCCH protein MEX-5 and the posterior CCCH protein POS-1 have complementary roles in regulating protein expression in the early embryo. MEX-5 limits

the expression of a posterior protein, whereas POS-1 restricts the expression of at least one anterior protein (SCHUBERT *et al.* 2000; OGURA *et al.* 2003). However, neither of these proteins exclusively restricts the expression of the other in the two-cell embryo. In *mex-5* mutant embryos, POS-1 was more highly enriched in the posterior, identical to its wild-type pattern, and in *pos-1* mutant embryos, MEX-5 was more concentrated in the anterior. Yet, our analyses of these two proteins suggest that they exert a subtle influence on one another. In *mex-5* mutant embryos, the asymmetry of the *pos-1* message was affected, such that *pos-1* mRNA was detected at high levels in both posterior and anterior cells. This disruption of *pos-1* message asymmetry did not affect POS-1 protein asymmetry, but it may affect the level of POS-1 present in the anterior. We have also demonstrated that POS-1 can bind the 3′-UTR of *mex-6*, a gene redundant in function to *mex-5*, and provided genetic data suggesting that POS-1 influences the amount of MEX-6 in the anterior blastomere. This intricate regulation between the MEX-5/6 and POS-1 proteins may be important for maintaining their strong complementary patterns. These complementary patterns not only are present at the two-cell stage but also are repeated at each subsequent asymmetric division of the germline lineage (TABARA *et al.* 1999; SCHUBERT *et al.* 2000). Although their asymmetric patterns were not altered at the two-cell stage in *pos-1* or *mex-5* mutant embryos, the expression of MEX-5 or POS-1 is more likely to become symmetric with each subsequent germline division in the respective mutant embryo (J. A. SCHISA and B. D. PAGE, unpublished observations). Thus, the interactions of these proteins may initiate a feedback loop that reestablishes and refines their expression in later asymmetric cell divisions.

We thank Edwin Ferguson and the Molecular Genetics and Cell Biology Department of the University of Chicago for giving B.D.P. a temporary home to do a few experiments and M. O. Casanueva and Y. C. Wang for making science in Chicago so enjoyable. We are grateful to J. R. Priess for his support and comments. We thank the editor for greatly improving the manuscript. This article could not have been completed without the caffeine and companionship provided by Cafe Dharwin. We also thank Yuji Kohara for cDNA clones and Kathryn Good for performing the fusion PCR for the *gfp:mex-6* gene construct. Part of this work was funded by a grant to B.D.P. from the Leukemia and Lymphoma Society (no. 3552-98). J.R.T. was supported by National Institutes of Health Training Grant 5T32 HDO7183.

LITERATURE CITED

ADERETH, Y., V. DAMMAI, N. KOSE, R. LI and T. HSU, 2005 RNA-dependent integrin alpha8 protein localization regulated by the Muscleblind-like protein MLP1. Nat. Cell Biol. **7:** 1140–1147.

BATCHELDER, C., M. A. DUNN, B. CHOY, Y. SUH, C. CASSIE *et al.*, 1999 Transcriptional repression by the Caenorhabditis elegans germ-line protein PIE-1. Genes Dev. **13:** 202–212.

BEGEMANN, G., N. PARICIO, R. ARTERO, I. KISS, M. PEREZ-ALONSO *et al.*, 1997 muscleblind, a gene required for photoreceptor differentiation in Drosophila, encodes novel nuclear Cys3His-type zinc-finger-containing proteins. Development **124:** 4321–4331.

BLACKSHEAR, P. J., 2002 Tristetraprolin and other CCCH tandem zinc-finger proteins in the regulation of mRNA turnover. Biochem. Soc. Trans. **30:** 945–952.

BOWERMAN, B., 2000 Embryonic polarity: protein stability in asymmetric cell division. Curr. Biol. **10:** R637–R641.

BOWERMAN, B., B. A. EATON and J. R. PRIESS, 1992 skn-1, a maternally expressed gene required to specify the fate of ventral blastomeres in the early C. elegans embryo. Cell **68:** 1061–1075.

BOWERMAN, B., B. W. DRAPER, C. C. MELLO and J. R. PRIESS, 1993 The maternal gene skn-1 encodes a protein that is distributed unequally in early C. elegans embryos. Cell **74:** 443–452.

BOWERMAN, B., M. INGRAM and C. HUNTER, 1997 The maternal par genes and the segregation of cell fate specification activities in early Caenorhabditis elegans embryos. Development **124:** 3815–3826.

BRENNER, S., 1974 The genetics of *Caenorhabditis elegans*. Genetics **77:** 71–94.

CHI, W., and V. REINKE, 2006 Promotion of oogenesis and embryogenesis in the *C. elegans* gonad by EFL-1/DPL-1 (E2F) does not require LIN-35 (pRB). Development **133:** 3147–3157.

CUENCA, A. A., A. SCHETTER, D. ACETO, K. KEMPHUES and G. SEYDOUX, 2003 Polarization of the C. elegans zygote proceeds via distinct establishment and maintenance phases. Development **130:** 1255–1265.

D'AGOSTINO, I., C. MERRITT, P-L. CHEN, G. SEYDOUX and K. SUBRAMANIAM, 2006 Translational repression restricts expression of the C. elegans Nanos homolog NOS-2 to the embryonic germline. Dev. Biol. **292:** 244–252.

DERENZO, C., K. J. REESE and G. SEYDOUX, 2003 Exclusion of germ plasm proteins from somatic lineages by cullin-dependent degradation. Nature **424:** 685–689.

EVANS, T. C., S. L. CRITTENDEN, V. KODOYIANNI and J. KIMBLE, 1994 Translational control of maternal glp-1 mRNA establishes an asymmetry in the C. elegans embryo. Cell **77:** 183–194.

GOLDSTEIN, B., and S. N. HIRD, 1996 Specification of the anteroposterior axis in Caenorhabditis elegans. Development **122:** 1467–1474.

GUEDES, S., and J. R. PRIESS, 1997 The C. elegans MEX-1 protein is present in germline blastomeres and is a P granule component. Development **124:** 731–739.

HIROTA, Y., M. OKABE, T. IMAI, M. KURUSU, A. YAMAMOTO *et al.*, 1999 Musashi and seven in absentia downregulate Tramtrack through distinct mechanisms in Drosophila eye development. Mech. Dev. **87:** 93–101.

HOBERT, O., 2002 PCR fusion-based approach to create reporter gene constructs for expression analysis in transgenic C. elegans. Biotechniques **32:** 728–730.

HUANG, N. N., D. E. MOOTZ, A. J. WALHOUT, M. VIDAL and C. P. HUNTER, 2002 MEX-3 interacting proteins link cell polarity to asymmetric gene expression in Caenorhabditis elegans. Development **129:** 747–759.

LADD, A. N., M. G. STENBERG, M. S. SWANSON and T. A. COOPER, 2005 Dynamic balance between activation and repression regulates pre-mRNA alternative splicing during heart development. Dev. Dyn. **233:** 783–793.

LAI, W. S., E. CARBALLO, J. R. STRUM, E. A. KENNINGTON, R. S. PHILLIPS *et al.*, 1999 Evidence that tristetraprolin binds to AU-rich elements and promotes the deadenylation and destabilization of tumor necrosis factor alpha mRNA. Mol. Cell. Biol. **19:** 4311–4323.

MADURO, M., and D. PILGRIM, 1995 Identification and cloning of *unc-119*, a gene expressed in the *Caenorhabditis elegans* nervous system. Genetics **141:** 977–988.

MADURO, M. F., M. D. MENEGHINI, B. BOWERMAN, G. BROITMAN-MADURO and J. H. ROTHMAN, 2001 Restriction of mesendoderm to a single blastomere by the combined action of SKN-1 and a GSK-3beta homolog is mediated by MED-1 and -2 in C. elegans. Mol. Cell **7:** 475–485.

MARIN, V. A., and T. C. EVANS, 2003 Translational repression of a C. elegans Notch mRNA by the STAR/KH domain protein GLD-1. Development **130:** 2623–2632.

MELLO, C. C., B. W. DRAPER, M. KRAUSE, H. WEINTRAUB and J. R. PRIESS, 1992 The pie-1 and mex-1 genes and maternal control of blastomere identity in early C. elegans embryos. Cell **70:** 163–176.

MELLO, C. C., C. SCHUBERT, B. DRAPER, W. ZHANG, R. LOBEL *et al.*, 1996 The PIE-1 protein and germline specification in C. elegans embryos. Nature **382:** 710–712.

Ogura, K., N. Kishimoto, S. Mitani, K. Gengyo-Ando and Y. Kohara, 2003 Translational control of maternal glp-1 mRNA by POS-1 and its interacting protein SPN-4 in Caenorhabditis elegans. Development **130:** 2495–2503.

Okabe, M, T. Imai, M. Kurusu, Y. Hiromi and H. Okano, 2001 Translational repression determines a neuronal potential in Drosophila asymmetric cell division. Nature **411:** 94–98.

Page, B. D., S. Guedes, D. Waring and J. R. Priess, 2001 The C. elegans E2F- and DP-related proteins are required for embryonic asymmetry and negatively regulate Ras/MAPK signaling. Mol. Cell **7:** 451–460.

Pellettieri, J., and G. Seydoux, 2002 Anterior-posterior polarity in C. elegans and Drosophila: PARallels and differences. Science **298:** 1946–1950.

Praitis, V., E. Casey, D. Collar and J. Austin, 2001 Creation of low-copy integrated transgenic lines in *Caenorhabditis elegans*. Genetics **157:** 1217–1226.

Priess, J. R., and J. N. Thomson, 1987 Cellular interactions in early C. elegans embryos. Cell **48:** 241–250.

Puig, S., E. Askeland and D. J. Thiele, 2005 Coordinated remodeling of cellular metabolism during iron deficiency through targeted mRNA degradation. Cell **120:** 99–110.

Putz, U., P. Skehel and D. Kuhl, 1996 A tri-hybrid system for the analysis and detection of RNA–protein interactions. Nucleic Acids Res. **24:** 4838–4840.

Reese, K. J., M. A. Dunn, J. A. Waddle and G. Seydoux, 2000 Asymmetric segregation of PIE-1 in C. elegans is mediated by two complementary mechanisms that act through separate PIE-1 protein domains. Mol. Cell **6:** 445–455.

Rose, L. S., and K. J. Kemphues, 1998 Early patterning of the C. elegans embryo. Annu. Rev. Genet. **32:** 521–545.

Rudel, D., and J. Kimble, 2001 Conservation of glp-1 regulation and function in nematodes. Genetics **157:** 639–654.

Sadler, P. L., and D. C. Shakes, 2000 Anucleate Caenorhabditis elegans sperm can crawl, fertilize oocytes and direct anterior-posterior polarization of the 1-cell embryo. Development **127:** 355–366.

Schisa, J. A., J. N. Pitt and J. R. Priess, 2001 Analysis of RNA associated with P granules in germ cells of C. elegans adults. Development **128:** 1287–1298.

Schubert, C. M., R. Lin, C. J. De Vries, R. H. Plasterk and J. R. Priess, 2000 MEX-5 and MEX-6 function to establish soma/germline asymmetry in early C. elegans embryos. Mol. Cell **5:** 671–682.

Seydoux, G., and A. Fire, 1994 Soma-germline asymmetry in the distributions of embryonic RNAs in Caenorhabditis elegans. Development **120:** 2823–2834.

Seydoux, G., C. C. Mello, J. Pettitt, W. B. Wood, J. R. Priess *et al.*, 1996 Repression of gene expression in the embryonic germ lineage of C. elegans. Nature **382:** 713–716.

Strome, S., J. Powers, M. Dunn, K. Reese, C. J. Malone *et al.*, 2001 Spindle dynamics and the role of gamma-tubulin in early Caenorhabditis elegans embryos. Mol. Biol. Cell **12:** 1751–1764.

Tabara, H., R. J. Hill, C. C. Mello, J. R. Priess and Y. Kohara, 1999 pos-1 encodes a cytoplasmic zinc-finger protein essential for germline specification in C. elegans. Development **126:** 1–11.

Tenenhaus, C., K. Subramaniam, M. A. Dunn and G. Seydoux, 2001 PIE-1 is a bifunctional protein that regulates maternal and zygotic gene expression in the embryonic germ line of Caenorhabditis elegans. Genes Dev. **15:** 1031–1040.

Wallenfang, M. R., and G. Seydoux, 2000 Polarization of the anterior-posterior axis of C. elegans is a microtubule-directed process. Nature **408:** 89–92.

Communicating editor: K. Kemphues

Curriculum Vitae

Jennifer R. Tenlen

EDUCATION

2007	Doctor of Philosophy, Molecular and Cellular Biology Program, University of Washington and Fred Hutchinson Cancer Research Center, Seattle, WA
1998	Master in Teaching (Secondary Education), Seattle University, Seattle, WA
1996	Honours student, Monash University, Melbourne, Australia
1995	B. S. in Biology with Honors, *cum laude*, University of Puget Sound, Tacoma, WA

RESEARCH EXPERIENCE

2001 – 2007	Doctoral student, Molecular and Cellular Biology Program, University of Washington and Fred Hutchinson Cancer Research Center, Seattle, WA, (dissertation adviser: James R. Priess)
1997	Research Technician I, Molecular Cytogenetics, Fred Hutchinson Cancer Research Center (principal investigator: Eileen Bryant)
1996	Postgraduate Honours Research, Department of Genetics and Development, Monash University, Melbourne, Australia (thesis adviser: John D. Hamill)
1994 – 1995	Undergraduate Honors Research, Department of Biology, University of Puget Sound, Tacoma, WA (thesis adviser: Elizabeth Kirkpatrick)

HONORS AND AWARDS

2006	Best Student Oral Presentation, Northwest Developmental Biology Meeting
2003 – 2006	Developmental Biology Training Grant, University of Washington
1995 – 1996	Rotary Foundation Ambassadorial Scholar to Australia
1995	Coolidge Otis Chapman Honors Scholar, University of Puget Sound
1995	Outstanding Honors Thesis award, University of Puget Sound
1994	Phi Beta Kappa Honor Society
1994	Phi Kappa Phi Honor Society

PUBLICATIONS

Le, T.N., Blomstedt, C.K. Kuang, J., **Tenlen, J.**, Gaff, D.F., Hamill, J.D. and Neale, A.D. (2007). Desiccation-tolerance specific gene expression in leaf tissue of the resurrection plant *Sporobolus stapfianus*. Functional Plant Biology *in press*.

Page, B.D., Diede, S.J., **Tenlen, J.R.**, and Ferguson, E.L. (2007). EEL-1, a Hect E3 ubiquitin ligase, controls asymmetry and persistence of the SKN-1 transcription factor in the early *C. elegans* embryo. Development *in press*.

Tenlen, J.R.*, Schisa, J.A.*, Diede, S.J. and Page, B.D. (2006). Reduced dosage of *pos-1* suppresses Mex mutants and reveals complex interactions among CCCH zinc-finger proteins during *Caenorhabditis elegans* embryogenesis. Genetics 174, 1933-1945. * These authors contributed equally to this work.

Park, F.D., **Tenlen, J.R.** and Priess, J.R. (2004). *C. elegans* MOM-5/Frizzled functions in MOM-2/Wnt-independent cell polarity and is localized asymmetrically prior to cell division. Current Biology 14, 2252-2258.

SEMINARS

Tenlen, J.R. "A place for everything and everything in its place: localization of the cell-fate regulator MEX-5 in nematode embryos." Thompson Hall Science and Mathematics Seminar Series, University of Puget Sound, Tacoma, WA, March 2007. (Invited speaker)

Tenlen, J.R. and Priess, J.R. "*C. elegans* Ser/Thr kinases PAR-1 and PAR-4 have multiple roles in MEX-5 asymmetry." 2006 Northwest Developmental Biology Meeting, Friday Harbor, WA, March 2006.

Tenlen, J.R. "Teaching Bioethics in the Science Classroom." Workshop presentation at the Western Washington Catholic Educators Conference, Seattle, WA, September 2000. (Invited speaker)

POSTERS

Tenlen, J.R. and Priess, J. R. "Linking PAR polarity proteins to cell fate determination: analysis of MEX-5 localization in C. elegans embryos." 15th International Developmental Biology Society Congress, Sydney, Australia, September 2005.

Tenlen, J., Munro, E., and Priess, J. " A C-terminal Ser residue is necessary for MEX-5 localization in early *C. elegans* embryos." 15th International *C. elegans* Meeting, UCLA, Los Angeles, CA, June 2005.